WYDZIAŁ BIOLOGII
i OCHRONY ŚRODOWISKA
Uniwersytet Łódzki

Interdyscyplinarne Studia Doktoranckie
InterDOC-STARt

Edyta Janik-Karpińska

Ocena mechanizmów cytotoksycznego i genotoksycznego działania toksyny T-2 produkowanej przez grzyby z rodzaju *Fusarium*

Evaluation of the mechanisms of cytotoxic and genotoxic effects of T-2 toxin produced by *Fusarium* fungi

Praca doktorska wykonana

w Centrum Zapobiegania Zagrożeniom Biologicznym

Promotor:

- dr hab. Michał Bijak prof. UŁ

Promotor pomocniczy:

- płk dr inż. Michał Ceremuga

Łódź, 2023

Spis treści

Załączniki:

- Publikacje będące podstawą rozprawy doktorskiej
- Oświadczenia współautorów

Projekt InterDOC-STARt

Praca doktorska została przygotowana w ramach projektu „InterDOC-STARt – Interdyscyplinarne Studia Doktoranckie na Wydziale BiOŚ UŁ” – Program Operacyjny Wiedza Edukacja Rozwój 2014-2020, Oś Priorytetowa III. Szkolnictwo wyższe dla gospodarki i rozwoju, Działanie 3.2 Studia Doktoranckie. Nr projektu: POWR.03.02.00-IP.08-00-DOK/16. Realizowany w latach 2018-2022; Kierownik projektu: prof. dr hab. Agnieszka Marczak.

Źródła finansowania

Część badań przeprowadzonych w ramach niniejszej rozprawy doktorskiej zostało sfinansowanych w ramach projektu PRELUDIUM 19 nr 2020/37/N/NZ9/01678 „Poznanie molekularnego mechanizmu toksycznego działania najgroźniejszego przedstawiciela trichotecenów - toksyny T-2” przyznanego przez Narodowe Centrum Nauki; Kierownik projektu: mgr Edyta Janik-Karpińska.

NARODOWE CENTRUM NAUKI

Dorobek naukowy

Publikacje będące podstawą rozprawy doktorskiej

W skład rozprawy doktorskiej wchodzą cztery publikacje: jedna przeglądowa i trzy doświadczalne.

Praca przeglądowa:

- **Janik E**, Niemcewicz M, Podogrocki M, Ceremuga M, Stela M, Bijak M. *T-2 Toxin-The Most Toxic Trichothecene Mycotoxin: Metabolism, Toxicity, and Decontamination Strategies.* Molecules 2021, 26(22), 6868; doi:10.3390/molecules26226868 [IF = 4.927 (2021); 5-letni IF = 5.110 (2021); liczba punktów MEiN = 140 (2021)] **(Praca nr 1)**

Prace doświadczalne:

- **Janik-Karpińska E**, Ceremuga M, Wieckowska M, Szyposzynska M, Niemcewicz M, Synowiec E, Sliwinski T, Bijak M. *Direct T-2 Toxicity on Human Skin-Fibroblast Hs68 Cell Line-In Vitro Study*. International Journal of Molecular Sciences 2022, 23(9), 4929; doi:10.3390/ijms23094929 [IF = 6.208 (2021); 5-letni IF = 6.628 (2021); liczba punktów MEiN = 140 (2021)] **(Praca nr 2)**
- **Janik-Karpińska E**, Ceremuga M, Niemcewicz M, Synowiec E, Sliwinski T, Bijak M. *Mitochondrial Damage Induced by T-2 Mycotoxin on Human Skin- Fibroblast Hs68 Cell Line*. Molecules 2023, 28(5), 2408; doi.org/10.3390/molecules28052408 [IF = 4.927 (2021); 5-letni IF = 5.110 (2021); liczba punktów MEiN = 140 (2021)] **(Praca nr 3)**
- **Janik-Karpińska E**, Ceremuga M, Niemcewicz M, Synowiec E, Sliwinski T, Bijak M. *DNA damage induced by T-2 Mycotoxin in Human Skin Fibroblast Cell Line – Hs68*. Toxins (praca w recenzji) [IF = 5.075 (2021); 5-letni IF = 5.305 (2021); liczba punktów MEiN = 100 (2021)] **(Praca nr 4)**

Sumaryczny dorobek naukowy prac wchodzących w skład rozprawy doktorskiej: 520 pkt MEiN według punktacji MEiN z dnia 01.12.2021 r. oraz IF = 21.137; IF 5-letni = 22.153.

Pozostały dorobek naukowy

Publikacje:

1. **Janik-Karpinska E**, Brancaleoni R, Niemcewicz M, Wojtas W, Foco M, Podogrocki M, Bijak M. *Healthcare Waste-A Serious Problem for Global Health.* Healthcare 2023, 11(2), 242; doi: 10.3390/healthcare11020242; [IF = 3.160 (2021); 5-letni IF = 3.460 (2021); liczba punktów MEiN = 40 (2021)].

2. **Janik-Karpinska E**, Ceremuga M, Niemcewicz M, Podogrocki M, Stela M, Cichon N, Bijak M. *Immunosensors-The Future of Pathogen Real-Time Detection.* Sensors 2022, 22(24), 9757; doi: 10.3390/s22249757; [IF = 3.847 (2021); 5-letni IF = 4.050 (2021); liczba punktów MEiN = 100 (2021)].

3. **Janik E**, Niemcewicz M, Podogrocki M, Ceremuga M, Gorniak L, Stela M, Bijak M. *The Existing Methods and Novel Approaches in Mycotoxins' Detection.* Molecules 2021, 26(13), 3981; doi: 10.3390/molecules26133981; [IF = 4.927 (2021); 5-letni IF = 5.110 (2021); liczba punktów MEiN = 140 (2021)].

4. **Janik E**, Niemcewicz M, Podogrocki M, Saluk-Bijak J, Bijak M. *Existing Drugs Considered as Promising in COVID-19 Therapy.* International Journal of Molecular Sciences 2021, 22(11), 5434; doi: 10.3390/ijms22115434; [IF = 6.208 (2021); 5-letni IF = 6.628 (2021); liczba punktów MEiN = 140 (2021)].

5. **Janik E**, Niemcewicz M, Podogrocki M, Majsterek I, Bijak M. *The Emerging Concern and Interest SARS-CoV-2 Variants.* Pathogens 2021, 10(6), 633; doi: 10.3390/pathogens10060633; [IF = 4.531 (2021); 5-letni IF = 4.580 (2021); liczba punktów MEiN = 100 (2021)].

6. **Janik E,** Bartos M, Niemcewicz M, Gorniak L, Bijak M. *SARS-CoV-2: Outline, Prevention, and Decontamination.* Pathogens 2021, 23;10(2):114. doi: 10.3390/pathogens10020114; [IF = 4.531 (2021); 5-letni IF = 4.580 (2021); liczba punktów MEiN = 100 (2021)].

7. **Janik E**, Niemcewicz M, Ceremuga M, Krzowski L, Saluk-Bijak J, Bijak M. *Various Aspects of a Gene Editing System—CRISPR–Cas9Various Aspects of a Gene Editing System—CRISPR–Cas9*. International Journal of Molecular Sciences 2020, 16;21(24):9604; doi: 10.3390/ijms21249604; [IF = 6.208 (2021); 5-letni IF = 6.628 (2021); liczba punktów MEiN = 140 (2021)].

8. **Janik E**, Niemcewicz M, Ceremuga M, Stela M, Saluk-Bijak J, Siadkowski A, Bijak M. *Molecular Aspects of Mycotoxins – A Serious Problem for Human Health.* International Journal of Molecular Sciences 2020, 31;21(21):8187. doi:10.3390/ijms21218187 [IF = 6.208 (2021); 5-letni IF = 6.628 (2021); liczba punktów MEiN = 140 (2021)].

9. **Janik E**, Ceremuga M, Niemcewicz M, Bijak M. *Dangerous Pathogens as a Potential Problem for Public Health.* Medicina (Kaunas) 2020, 6;56(11):591; doi: 10.3390/medicina56110591; [IF = 2.948 (2021); 5-letni IF = 2.985 (2021); liczba punktów MEiN = 40 (2021)].

10. Ceremuga M, Stela M, **Janik E**, Górniak L, Synowiec E, Sliwinski T, Sitarek P, Saluk-Bijak J, Bijak M. *Melittin-A Natural Peptide from Bee Venom Which Induces Apoptosis in Human Laukaemia Cells*. Biomolecules 2020, 6;10(2):247. doi: 10.3390/biom10020247; [IF = 6.064 (2021); 5-letni IF = 6.191 (2021); liczba punktów MEiN = 100 (2021)].

11. **Janik E**, Ceremuga M, Saluk-Bijak J, Bijak M. *Biological Toxins as the Potential Tools for Bioterrorism.* International Journal of Molecular Sciences 2019, 8;20(5):1181; doi: 10.3390/ijms20051181; [IF = 6.208 (2021); 5-letni IF = 6.628 (2021); liczba punktów MEiN = 140 (2021)].

Sumaryczny pozostały dorobek naukowy: 1180 pkt MEiN według punktacji MEiN z dnia 01.12.2021 r. oraz IF = 54.84; IF 5-letni = 57.468.

Podsumowanie całkowitego dorobku naukowego: 1700 pkt MEiN według punktacji MEiN z dnia 01.12.2021 r. oraz IF = 75,977; IF 5-letni = 79.621, liczba cytowań bez autocytowań – 292, indeks Hirsha – 9.

Komunikaty zjazdowe:

1. **Janik-Karpińska E**, Bijak M. *T-2 mycotoxin and its impact on mitochondria – in vitro study*. XVIth International Congress of Toxicology (ICT 2022). 18-21.09.2022, Maastricht, Holandia (Wystąpienie posterowe).
2. **Janik-Karpińska E**, Bijak M. *Effects of T-2 toxin on the skin – in vitro study.* 35th International Conference on Innovations in "Chemical, Biological and Environmental Sciences". 12-14.09.2022, Budapeszt, Węgry **(Wystąpienie posterowe - wyróżnienie za najlepsze wystąpienie posterowe).**
3. **Janik-Karpińska E**, Bijak M. *Analiza uszkodzeń DNA wywołanych działaniem mykotoksyny T-2 – badania in vitro.* III Ogólnopolska Konferencja Naukowa Toksyny – przegląd i badania. 04.03.2022, ONLINE (Wystąpienie ustne).
4. **Janik E**, Bijak M. *Impact of mycotoxins in food on human health*. National Scientific Conference Knowledge – Key to Success V edition. 23.01.2021, ONLINE (Wystąpienie ustne).
5. **Janik E**, Bijak M. *Charakterystyka trichotecenów ze szczególnym uwzględnieniem właściwości toksycznych toksyny T-2*. III Ogólnopolska Konferencja Naukowa Pierwotne i wtórne metabolity roślin i grzybów. 12.12. 2020, ONLINE (Wystąpienie ustne).
6. **Janik E**, Bijak M, Ceremuga M. *Toksyna T-2 – Broń biologiczna czy chemiczna?* Ogólnopolska Konferencja Naukowa Badania Młodych Naukowców Część V, Nauki Interdyscyplinarne. 13.12.2019, Kraków (Wystąpienie ustne).
7. **Janik E**, Bijak M, Ceremuga M. *Aktywność cytotoksyczna ochratoksyny A względem komórek prawidłowych ludzkich fibroblastów.* X Ogólnokrajowa Konferencja Naukowa Młodzi Naukowcy w Polsce – Badania i Rozwój. 20.11.2019, Wrocław (Wystąpienie ustne).
8. **Janik E**, Ceremuga M, Bijak M. *Study on the Apoptosis and Necrosis of Human Normal Fibroblast Induced by T-2 Toxin.* National Scientific Conference Understand the Science – 3rd Edition. 28.09.2019, Łódź (Wystąpienie ustne).
9. **Janik E**, Ceremuga M, Bijak M. *Ocena wpływu toksyny T-2 na generowanie wolnych rodników przez komórki ludzkich fibroblastów linii Hs68*. II Konferencja Doktorantów Nauk Przyrodniczych. 26.06.2019, Gdańsk (Wystąpienie ustne).

10. **Janik E**, Ceremuga M, Bijak M. *Ocena potencjału błony mitochondrialnej komórek ludzkich fibroblastów linii Hs68 traktowanych toksyną T-2.* XII Międzyuczelniane Seminarium Kół Naukowych. 04.06.2019, Warszawa (Wystąpienie ustne).
11. **Janik E**, Ceremuga M, Bijak M. *Ocena żywotności komórek ludzkich fibroblastów linii Hs68 traktowanych toksyną T-2.* V Ogólnopolska Konferencja Doktorantów Nauk o Życiu BIOOPEN. 31.05.2019, Łódź (Wystąpienie posterowe).

Wstęp

Mykotoksyny to wtórne metabolity syntetyzowane przez różne gatunki grzybów strzępkowych m.in. z rodzaju *Penicillium, Aspergillus, Fusarium, Trichoderma, Trichothecium* czy *Alternaria*. W produkcji mykotoksyn dominują głównie trzy rodzaje grzybów: *Aspergillus, Fusarium* i *Penicillium* (Tabela 1). Grzyby te zanieczyszczają produkty rolne i wytwarzają toksyny przed, w trakcie lub po zbiorach – w czasie magazynowania żywności w niewłaściwych warunkach. Podczas gdy gatunki *Aspergillus* i *Penicillium* infekują żywność i pasze podczas ich magazynowania, gatunki *Fusarium* zanieczyszczają rosnące uprawy, takie jak pszenica, jęczmień i kukurydza jeszcze na polu. Kilka czynników przyczynia się do obecności mykotoksyn w zbożach i wśród nich wyróżnić można mechaniczne uszkodzenia ziaren, inwazja szkodników czy złe praktyki w zakresie zbiorów i przechowywania. Ponadto warunki środowiskowe takie jak temperatura i wilgotność powietrza wpływają na kolonizację grzybów syntetyzujących toksyny i samą produkcję mykotoksyn (Adeyeye 2016) **(Praca nr 1)**.

Tabela 1. Główne rodzaje grzybów strzępkowych i produkowane przez nie mykotoksyny.

Rodzaj	Gatunek	Mykotoksyny
Aspergillus	*A. flavus*	aflatoksyna B1, B2
	A. parasiticus	aflatoksyna B1, B2, G1, G2
	A. nomius	aflatoksyna B1, B2, G1, G2, kwas aspergilowy
	A. ochraceus	ochratoksyna A
Fusarium	*F. sporotrichioides*	toksyna T-2, toksyna HT-2, neosolaniol
	F. poae	toksyna T-2, toksyna HT-2, fusarenon
	F. graminearum	deoksyniwalenol, niwalenol, zearalenon
	F. culmorum	zearalenon, deoksyniwalenol, fusarenon
Penicillium	*P. citrinum*	cytrynina
	P. patulum, P. expansum	patulina
	P. verrucosum	ochratoksyna A

Mykotoksyny stanowią grupę zróżnicowanych strukturalnie toksycznych związków o niskiej masie cząsteczkowej, która wynosi poniżej 1000 Da. Zidentyfikowanych zostało około 400 mykotoksyn i uważa się, że największe obawy w kontekście zdrowia publicznego i agroekonomii wzbudzają trichoteceny, ochratoksyny, aflatoksyny, zearalenon, fumonizyny, patulina i cytrynina. Toksyczny wpływ mykotoksyn na zdrowie zwierząt i ludzi określany jest mianem mykotoksykozy, której nasilenie zależne jest od stopnia toksyczności mykotoksyn, drogi ekspozycji, wieku i ogólnego stanu organizmu (El-Sayed et al. 2022; Alshannaq and Yu 2017; Oana et al. 2015).

Organizacje takie jak Agencja ds. Żywności i Leków (ang. Food and Drug Administration, FDA), Komisja Europejska (ang. European Commission, EC), Organizacja Narodów Zjednoczonych ds. Wyżywienia i Rolnictwa (ang. Food and Agriculture Organization of the United Nations, FAO) oraz Światowa Organizacja Zdrowia (ang. World Health Organization, WHO) opracowały normy i limity regulacyjne dla głównych klas oraz wybranych mykotoksyn. Do identyfikacji i ilościowego oznaczania mykotoksyn w próbkach żywności wykorzystywane są różne metody analityczne takie jak techniki chromatograficzne a także metody oparte na testach immunologicznych (The European Commission. Commission Regulation (EC) No 1881/2006 of 19 December Setting Maximum Levels or Certain Contaminants in Foodstuff. (accessed on 1 February 2023); Food and Agriculture Organization of the United Nations. Worldwide Regulations for Mycotoxins in Food and Feed in 2003 (accessed on 1 February 2023); World Health Organization. Evaluation of Certain Contaminants in Food: Eighty-Third Report of the Joint FAO/WHO Expert Committee on Food Additives (accessed on 1 February 2023)). Dzięki zastosowaniu różnych rodzajów chromatografii tj. chromatografii cienkowarstwowej (ang. thin layer chromatography, TLC) i wysokosprawnej chromatografii cieczowej (ang. high performance liquid chromatography, HPLC) w połączeniu z różnymi detektorami, takimi jak matryca diodowa, fluorescencja i UV, chromatografii cieczowej z tandemową spektrometrią mas (ang. liquid chromatography-tandem mass spectrometry, LC-MS/MS) oraz chromatografii gazowej z tandemową spektrometrią mas (ang. gas chromatography-tandem mass spectrometry, GC-MS/MS) technika ta jest szeroko stosowana i dominuje w wykrywaniu mykotoksyn. W przypadku, gdy konieczna jest szybka analiza mykotoksyn wykorzystywane są testy immunologiczne, takie jak test immunoenzymatyczny ELISA (ang. enzyme-linked immunosorbent assay) czy test immunologiczny przepływu bocznego (ang. lateral flow immunoassay, LFIA) (Tabela 2) (Lattanzio et al. 2019).

Tabela 2. Techniki analityczne stosowane w wykrywaniu mykotoksyn w żywności.

Technika detekcji	**Wykrywana mykotoksyna**	**Próbka żywności**	**Granica wykrywalności** (ang. limit of detection, LOD)	**Granica oznaczalności** (ang. limit of quantification, LOQ)
TLC	Patulina	Sok jabłkowy	14 µg/L	-
	Aflatoksyny	Orzechy brazylijskie	-	2000 µg/kg
HPLC	Deoksyniwalenol	Otręby pszenne	12,58 µg/kg	-
	Ochratoksyna A	Wino	0,09 µg/L	-
LC-MS/MS	Fumonizyna B_1	Kukurydza	1 µg/kg	-

	Toksyna T-2	Piwo	0,001 µg/mL	-
GC-MS/MS	Zearalenon	Płatki kukurydziane	-	10 µg/kg
	Diacetoksyscipernol	Semolina pszenna	-	5 µg/kg
ELISA bezpośrednia	Aflatoksyna B_1	Pszenica	0,05 µg/kg	-
	Aflatoksyna B_2		0,04 µg/kg	
	Aflatoksyna G_1		0,06 µg/kg	
	Aflatoksyna G_2		0,07 µg/kg	
ELISA kompetycyjna	Fumonizyny	Kukurydza	30 µg/kg	-
	Deoksyniwalenol		70 µg/kg	
LFIA	Zearalenon	Kukurydza	1 µg/kg	-
	Diacetoksyscipernol	Ryż	50 µg/kg	

Trichoteceny to mykotoksyny wytwarzane przez gatunki grzybów takie jak *Fusarium, Myrothecium* i *Stachybotrys*. Są to cykliczne seskwiterpenoidy, których charakterystycznym elementem budowy jest pierścień 12,13-epoksydowy, który odpowiedzialny jest za toksyczne działanie tej grupy toksyn. W zależności od budowy pozostałej części cząsteczki, trichoteceny zostały podzielone na cztery typy: A, B, C i D. Trichoteceny występują powszechnie jako zanieczyszczenia ziaren zbóż takich jak pszenica, owies, jęczmień i kukurydza. Występują również w sianie, słomie i kiszonce z zanieczyszczonych zbóż. Co więcej, spożywanie produktów takich jak mięso, mleko oraz jaja od bydła i drobiu karmionych paszą skażoną trichotecenami może być przyczyną zatruć u ludzi. Trichoteceny charakteryzują się dużą stabilnością i są odporne na wysoką temperaturę czy światło UV. Uważa się, że trichoteceny typu A są najbardziej toksycznymi przedstawicielami tej grupy mykotoksyn (Pascari et al. 2020) **(Praca nr 1)**. Ze względu na powszechne występowanie trichotecenów w produktach będących źródłem pożywienia dla ludzi i zwierząt hodowlanych stanowią one istotny problem dla bezpieczeństwa żywności oraz zdrowia publicznego (Mahato et al. 2022).

Toksyna T-2 należy do trichotecenów typu A i zawiera podwójne wiązanie między C-9 i C-10 oraz grupę epoksydową między C-12 i C-13. Budowa chemiczna toksyny T-2 charakteryzuje się grupą hydroksylową (OH) w pozycji C-3, grupami acetyloksylowymi (-OCOCH3) w pozycjach C-4 i C-15, atomem wodoru w pozycji C-7 oraz grupą izowalerylową z wiązaniem estrowym [OCOCH2CH(CH3)2] w pozycji C-8 (Rycina 1).

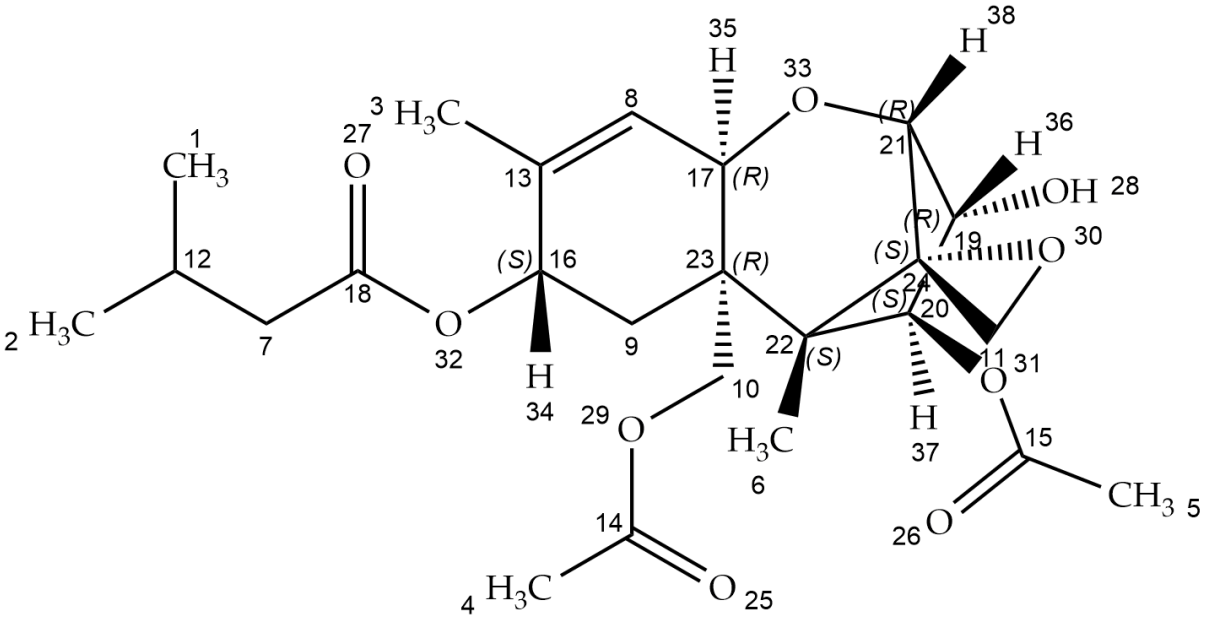

Rycina 1. Budowa chemiczna toksyny T-2.

Toksyna produkowana jest przez różne gatunki Fusarium, w tym *F. sporotrichioides, F. poae* i *F. acuminatum*. Najlepszymi warunkami do wzrostu *F. sporotrichioides*, który jest głównym producentem toksyny T-2 są: zakres temperatur od -2 do 35°C oraz aktywność wody powyżej 0,88. Dlatego też często można go znaleźć na ziarnach pochodzących z regionów o klimacie umiarkowanym. Aktywność wody i temperatura optymalne dla biosyntezy toksyny T-2 przez *F. sporotrichioides* wynoszą odpowiednio 0,980-0,995 oraz 20-30 °C (Kiš et al. 2021). Toksyna T-2 jest odporna na degradację pod wpływem wysokiej temperatury i światła UV. Pozostaje również aktywna podczas przetwarzania żywności i sterylizacji termicznej w autoklawie. Toksyna T-2 może być skutecznie dezaktywowana w silnie kwaśnym lub zasadowym środowisku, poprzez działanie temperatury 200-210 °C przez 30-40 min oraz metodą absorpcji podchlorynem sodu (NaClO) i wodorotlenkiem sodu (NaOH) przez minimum 4 godziny. Obecność współistniejących grzybów lub bakterii może również prowadzić do detoksykacji T-2 poprzez zmianę jej struktury chemicznej. Obecność toksyny T-2 wykrywano w ziarnach zbóż takich jak pszenica, jęczmień, owies, kukurydza czy ryż, ale także w produktach zbożowych m.in. mąka pszenna, płatkach śniadaniowych czy wyroby piekarnicze (Lavinia et al. 2011; European Food Safety et al. 2017) **(Praca nr 1)**.

Według przeprowadzonych badań naukowych toksyna T-2 ma najwyższą toksyczność spośród wszystkich mykotoksyn. Toksyna ta oddziałuje negatywnie na różne narządy i układy organizmu ludzi i zwierząt. Według badań toksyna T-2 wykazuje aktywność toksyczną względem układu immunologicznego, nerwowego, pokarmowego, moczowego i płciowego

(Li et al. 2011). Działa ona m.in. jako inhibitor syntezy białek poprzez wiązanie się z podjednostką 60S rybosomów eukariotycznych co prowadzi do zahamowania aktywności transferazy peptydylowej i zapobieganiu inicjacji łańcucha polipeptydowego (Adhikari et al. 2017). Dodatkowo wykazano, że toksyna T-2 niezależnie od hamowania syntezy białek oddziałuje na funkcje błony komórkowej i wpływa na transportery aminokwasów, nukleotydów i glukozy, a także na aktywność kanałów wapniowych (Bunner and Morris 1988). Toksyna T-2 ma charakter lipofilowy przez co może być łatwo wchłaniana z przewodu pokarmowego, przez błony śluzowe dróg oddechowych lub warstwy naskórka (Chaudhary and Lakshmana Rao 2010) **(Praca nr 1)**. Toksyczność ogólnoustrojowa toksyny T-2 może wynikać z głównych dróg narażenia: żołądkowo-jelitowej, wziewnej, kontaktowej i przezskórnej. Objawy mykotoksykozy spowodowanej przez toksynę T-2 są zwykle obserwowane w ciągu dwóch do czterech godzin, ale silna ekspozycja może spowodować wystąpienie objawów już w ciągu kilku minut. Objawy toksycznego działania T-2 będą się różnić w zależności od drogi ekspozycji jednak ogólnoustrojowe objawy u ludzi i zwierząt obejmują nudności, wymioty, biegunkę, utratę masy ciała, ataksję a także zawroty głowy. W ciężkich przypadkach może wystąpić tachykardia, hipotermia i niedociśnienie. Ekspozycja żołądkowo-jelitowa może powodować nudności, wymioty i wodnistą lub krwawą biegunkę ze skurczowym bólem brzucha. Uważa się, że mykotoksyna T-2 odpowiedzialna jest za rozwój klinicznego zespołu toksycznej aleukii pokarmowej (ATA); charakteryzującej się nudnościami, wymiotami, biegunką, leukopenią, krwotokiem, zapaleniem skóry a w ciężkich przypadkach śmiercią. Wziewna droga narażenia może powodować swędzenie nosa, ból, kichanie, krwawienie i wyciek z nosa. Toksyczność płucna i tchawiczo-oskrzelowa może powodować duszności, świszczący oddech, kaszel i zabarwioną krwią plwocinę. W przypadku kontaktu toksyny z ustami i gardłem występuje ból i zabarwienie śliny krwią. Narażenie oczu może wywoływać ból oka, łzawienie, zaczerwienienie, uczucie ciała obcego i niewyraźne widzenie. Przy ekspozycji przezskórnej zwykle obserwuje się objawy takie jak piekący ból, zaczerwienienie, tkliwość, pęcherze i progresja do martwicy skóry. Toksyna T-2 wykazuje również działanie radiomimetyczne (uszkodzenie dzielących się komórek) w szczególności na aktywnie dzielące się komórki szpiku kostnego, grasicy, śledziony czy węzłów chłonnych (Lavinia et al. 2011; Rahman et al. 2020; U.S. Army Medical Research Institute of Infectious Diseases (USAMRID). T-2 Mycotoxins. In: Medical Management of Biologic Causalities Handbook. 8th Edition. September 2014. Fort Detrick. Frederick, Maryland 21702-5001 (accessed on 19 October 2022)). Cechą charakterystyczną toksyny T-2, która wyróżnia ją na tle innych trichotecenów czy toksyn pochodzenia biologicznego jest działanie silnie drażniące na skórę. Uszkodzenia

skóry wywołane działaniem tej toksyny mogą być nawet 400-krotnie silniejsze niż przy wykorzystaniu iperytu siarkowego, który należy do grupy parzących bojowych środków trujących broni chemicznej. Ponadto aktywność toksyny T-2 po wniknięciu do organizmu przez drogi oddechowe jest porównywalna z aktywnością iperytu siarkowego, iperytów azotowych i luizytu. Dlatego też właściwości toksyny T-2 są bardziej zbliżone do środków chemicznych niż toksyn biologicznych **(Praca 2)**. Początkowe zmiany dotyczą przede wszystkim naskórka i górnej części skóry właściwej jednak w późniejszych etapach rozszerzają się na obszar skóry właściwej i tkankę podskórną (Pang et al. 1987). W badaniach na myszach wykazano, że w uszkodzeniu skóry wywołanym działaniem toksyny T-2 pośredniczy stres oksydacyjny, aktywacja mieloperoksydazy, aktywność metaloproteinaz macierzy pozakomórkowej, wzrost poziomu cytokin prozapalnych oraz apoptoza komórek naskórka. Zmiany histologiczne obejmowały wakuolizację, obrzęk i powiększenie keratynocytów oraz naciek komórek zapalnych w skórze właściwej. Zwiększenie dawki i czasu ekspozycji toksyny spowodowało hialinizację naskórka i ciężką martwicę skrzepową naskórka oraz skóry właściwej (Agrawal et al. 2012). Objawy takie jak rumień, intensywny obrzęk z rozszerzeniem naczyń w skórze właściwej, uszkodzenia fibroblastów i martwica są głównymi skutkami toksycznego miejscowego działania toksyny T-2 (Hemmati et al. 2012; Ueno 1984). Dodatkowo ekspozycja przezskórna na toksynę T-2 może początkowo wywołać silny obrzęk oraz zwiększoną grubość warstwy kolczystej i podstawnej (warstwa Malpighiego) naskórka a także pojawiają się pęcherze śródnaskórkowe. Następnie występuje ciężka i rozległa martwica skrzepowa i tworzenie się mikroropni śródnaskórkowych. Ponadto na powierzchni uszkodzonej skóry mogą wystąpić strupy z koloniami bakterii ziarniaków. Zmiany patologiczne skóry właściwej w początkowym etapie działania toksyny charakteryzują się łagodnym okołonaczyniowym naciekiem neutrofili, eozynofilii i makrofagów, obrzękiem łagodnym do umiarkowanego, odkładaniem fibryny oraz rozerwaniem kolagenu w warstwie brodawkowatej i okołonaczyniowych obszarach górnej warstwy siateczkowatej. W ciągu kilku dni zmiany te mogą stać się coraz bardziej rozległe i dotkliwe co prowadzi do martwicy i rozwoju stanu zapalnego. Fibroplazja górnej części skóry właściwej rozszerzyć się może do tkanki podskórnej. Zmiany skórne takie jak gąbczaste zapalenie skóry wraz z wysiękiem surowiczo-krwistym mogą się przekształcić w miejscowe rozległe martwicze zapalenie powięzi. Wynikać może to z immunosupresyjnego działania toksyny T-2 czego skutkiem jest zwiększona podatność na infekcje bakteryjne (Bhavanishankar, Ramesh, and Shantha 1988; Pang et al. 1987).

Cel pracy

Mykotoksyna T-2 charakteryzuje się szerokim spektrum toksycznego działania. Pomimo wielu lat badań nad jej toksycznością względem różnych komórek, organów oraz układów w organizmie ludzi i zwierząt, wpływ tej toksyny na skórę nadal nie został do końca poznany. Badania nad toksycznym działaniem toksyny T-2 względem skóry prowadzone do tej pory opierały się głównie o obserwacje makroskopowe, mikroskopowe oraz analizy histopatologiczne. Brak jest jednak informacji wskazujących na molekularne mechanizmy działania tej toksyny na komórki skóry. W związku z tym, celem niniejszej pracy było wyjaśnienie mechanizmów cytotoksycznego i genotoksycznego działania toksyny T-2 w warunkach *in vitro*, względem linii komórkowej prawidłowych ludzkich fibroblastów – Hs68. Postawiony w ten sposób cel ogólny został zrealizowany poprzez następujące cele szczegółowe:

1. Ocena bezpośredniego toksycznego działania toksyny T-2 względem ludzkich prawidłowych fibroblastów linii Hs68.
2. Analiza wpływu toksyny T-2 na uszkodzenia mitochondriów komórek linii Hs68.
3. Ocena wpływu toksyny T-2 na uszkodzenia genomu jądrowego komórek linii Hs68.

Hipoteza badawcza: Toksyna T-2 produkowana przez grzyby z rodzaju *Fusarium* w warunkach *in vitro* wykazuje właściwości cytotoksyczne oraz genotoksyczne względem komórek prawidłowych ludzkich fibroblastów linii Hs68.

Materiały i metody

Materiał badawczy

Materiał badań stanowiła linia komórkowa prawidłowych ludzkich fibroblastów – Hs68 pozyskana z American Type Culture Collection (ATCC^{TM}). Hodowlę komórek prowadzono z wykorzystaniem medium DMEM zawierającego dodatkowo 10% inaktywowaną bydlęcą surowicę płodową (FBS) oraz antybiotyki: 100 IU/ml penicyliny i 100 µg/ml streptomycyny. Hodowla prowadzona była w inkubatorze w środowisku 5% CO_2 oraz temperaturze 37ºC. Przed każdym eksperymentem komórki pasażowano przy użyciu TrypLe Express oraz hodowano minimum 12 godzin.

Toksyna

W badaniach wykorzystano komercyjnie dostępną toksynę T-2, którą traktowano komórki linii Hs68 w zakresie stężeń 0,001-100 µM oraz inkubowano przez 24 i 48 godzin. Toksyna T-2 produkowana przez grzyby *Fusarium* sp. zakupiona została w Sigma-Aldrich Chemical Co. (St. Louis, MO, USA) na licencji użytkownika końcowego.

Metody

Celem zbadania bezpośredniego toksycznego działania toksyny T-2 przeprowadzono następujące analizy:

- przeżywalność komórek z wykorzystaniem testu z błękitem trypanu
- przeżywalność komórek z wykorzystaniem testu MTT
- komórkowy poziom ATP metodą bioluminometrii
- aktywność kaspazy-3 oraz kaspazy-7 techniką cytometrii przepływowej
- zmiany apoptotyczne i nekrotyczne z wykorzystaniem wiązania aneksyny V i jodku propidyny metodą cytometrii przepływowej
- stężenie cytokeratyny 18 przy użyciu testu ELISA

W celu zbadania wpływu toksyny T-2 na uszkodzenia mitochondriów przeprowadzono następujące analizy

- zmiany potencjału błony mitochondrialnej przy użyciu sondy fluorescencyjnej JC-1
- generowanie reaktywnych form tlenu (reactive oxygen species – ROS) przy użyciu sondy fluorescencyjnej dioctanu 2′,7′-dichlorofluoresceiny (H2DCFDA)

- uszkodzenia mitochondrialnego DNA metodą Semi-Long Run qRT-PCR
- ilość kopii mitochondrialnego DNA metodą Real-Time-qPCR

W celu analizy wpływu toksyny T-2 na uszkodzenia genomu jądrowego przeprowadzono następujące analizy:

- uszkodzenia jądrowego DNA metodą kometową
- uszkodzenia jądrowego DNA metodą Semi-Long Run qRT-PCR
- zmiany ekspresji genów na poziomie mRNA dla genów odpowiedzialnych za naprawę DNA oraz genów związanych ze stanem zapalnym z wykorzystaniem Real-Time-qPCR
- Analiza *in silico* wiązania toksyny do DNA

Wyniki

Analiza bezpośredniego toksycznego działania toksyny T-2 względem ludzkich prawidłowych fibroblastów linii Hs68

Do oznaczenia bezpośredniego toksycznego działania toksyny wykorzystano szereg metod.

Przeżywalność komórek oceniono wykorzystując dwie niezależne metody (test z błękitem trypanu oraz MTT), które oparte są na różnych mechanizmach biochemicznych. Wyniki obu metod wykazały zależny od dawki i czasu efekt cytotoksyczny toksyny. Ponadto, na podstawie wyników obliczono wartości parametru EC_{50} (50% effective concentration), według którego określić można stężenie związku niezbędne do wywołania określonego efektu u 50% badanej populacji. Wartości dla metody z błękitem trypanu wynosiły 22,71 μM dla 24-godzinnej inkubacji komórek z toksyną oraz 7,81 μM po 48-godzinnej inkubacji z toksyną. Wartości dla testu MTT wyniosły 25,98 μM po 24-godzinnej inkubacji komórek z toksyną oraz 10,35 μM dla 48-godzinnej inkubacji z toksyną.

Metodą bioluminometrii określono względny poziom ATP w komórkach Hs68 w celu sprawdzenia aktywnego metabolizmu komórkowego. Ekspozycja komórek na toksynę T-2 spowodowała zależny od dawki i czasu spadek poziomu luminescencji, co bezpośrednio odpowiadało poziomowi ATP w próbce. Zmiany dla wszystkich stężeń toksyny i czasów ekspozycji z wyjątkiem najniższego stężenia tj. 0,001 μM dla 24- i 48-godzinnej ekspozycji są istotne statystycznie w stosunku do komórek kontrolnych.

Stosując metodę cytometrii przepływowej z podwójnym barwieniem (aneksyna V i jodek propidyny), zaobserwowano, że inkubacja komórek fibroblastów z toksyną T-2 spowodowała wzrost fluorescencji jodku propidyny. W najwyższym badanym stężeniu toksyny (100 μM) procent komórek barwionych jodkiem propidyny wynosił 79% po 24 godzinach od ekspozycji na toksynę oraz 93% po 48 godzinach od ekspozycji. Wzrost fluorescencji jodku propidyny, który wiąże się z DNA komórek z uszkodzoną błoną komórkową świadczy o występowaniu procesu nekrozy. W żadnej próbce nie zaobserwowano znaczącego wzrostu fluorescencji aneksyny V, która związana jest z procesem apoptozy w komórkach.

W kolejnym etapie badań przeprowadzono weryfikację zdolności toksyny T-2 do aktywacji szlaku kaspazy-3/7 w fibroblastach. Podczas oceny aktywności kaspaz na podstawie fluorescencji zaobserwowano, że traktowanie komórek fibroblastów toksyną nie indukowało żadnych zmian we fluorescencji, co wyraźnie wskazywało na brak aktywności proteolitycznej kaspaz 3/7 w tych komórkach.

Aby potwierdzić aktywację szlaku nekrotycznego wywoływanego działaniem toksyny T-2 w komórkach Hs68, przeprowadzono analizę stężenia ludzkiej cytokeratyny 18 (CK18) w supernatantach z hodowli komórkowych. Traktowanie komórek toksyną spowodowało zarówno dla 24- jak i 48-godzinnej ekspozycji zależny od dawki wzrost stężenia cytokeratyny 18. Zmiany dla wszystkich zastosowanych stężeń toksyny i czasów ekspozycji są istotne statystycznie w stosunku do komórek kontrolnych **(Praca nr 2)**.

Analiza wpływu toksyny T-2 na uszkodzenia mitochondriów komórek linii Hs68

Pierwszym etapem oceny wpływu toksyny na funkcjonowanie mitochondriów była analiza potencjału błony mitochondrialnej komórek Hs68, którą przeprowadzono z wykorzystaniem sondy fluorescencyjnej JC-1. Traktowanie linii komórkowej toksyną spowodowało zmiany stosunku fluorescencji agregatów do monomerów co wskazywało na spadek potencjału błonowego w komórkach inkubowanych z toksyną T-2. Ekspozycja komórek na toksynę T-2 spowodowała zaburzenia potencjału mitochondrialnego zarówno podczas 24- jak i 48-godzinnej inkubacji. Zaobserwowane zmiany dla wszystkich stężeń toksyny i czasów ekspozycji z wyjątkiem najniższego stężenia (0,001 μM) dla 48-godzinnej ekspozycji są istotne statystycznie w stosunku do komórek nietraktowanych toksyną.

Kolejnym etapem badań była ocena wpływu toksyny T-2 na mitochondria Hs68 poprzez analizę wewnątrzkomórkowego wytwarzania reaktywnych form tlenu. W tym celu przeprowadzono eksperyment z wykorzystaniem H2DCFDA. Inkubacja komórek Hs68 z toksyną T-2 we wszystkich badanych stężeniach (0,001-100 μM) zarówno przy 24- jak i 48-godzinnej ekspozycji na toksynę nie wykazała jej wpływu na wewnątrzkomórkowy poziom ROS.

Wykazano, że toksyna T-2 ma wpływ na genom mitochondrialny badanej linii komórkowej. Komórki traktowano toksyną w stężeniach 0,1, 1 oraz 10 μM i inkubowano 24 i 48 godzin. Genotoksyczność toksyny obserwowano jako zmianę liczby kopii mitochondrialnego DNA (mtDNA). Inkubacja z toksyną T-2 w sposób zależny od dawki i czasu powodowała zmniejszenie liczby kopii mtDNA w komórkach. W przypadku najwyższego badanego stężenia (10 μM) i 48-godzinnego okresu inkubacji poziom spadł ponad 100-krotnie. Uzyskane wyniki z wyjątkiem najniższego stężenia tj. 0,001 μM dla 24-godzinnej ekspozycji są istotne statystycznie w stosunku do komórek kontrolnych.

Określenie ilości uszkodzeń mtDNA wykonano za pomocą reakcji SLR-qRT-PCR, gdzie pomiar oparty jest na zależności, że wszelkie uszkodzenia na matrycy DNA będą

blokować polimerazę DNA, czego skutkiem jest z kolei zmniejszenie amplifikacji sekwencji docelowej. W tym celu zbadano uszkodzenia w dwóch regionach mtDNA: *ND1* oraz *ND5*. Reakcję SLR-qRT-PCR przeprowadzono z wykorzystaniem DNA wyizolowanego z komórek eksponowanych na toksynę T-2 w stężeniach 0,1; 1 i 10 μM przez 24 i 48 godzin. Analiza wykazała, że inkubacja komórek z toksyną T-2 w sposób zależny od dawki i czasu zwiększyła poziom uszkodzeń mtDNA w obu testowanych regionach mtDNA. Zaobserwowane zmiany dla wszystkich stężeń toksyny i czasów ekspozycji są istotne statystycznie w stosunku do komórek nietraktowanych toksyną **(Praca nr 3)**.

Ocena wpływu toksyny T-2 na uszkodzenia genomu jądrowego komórek linii Hs68

Poziom uszkodzeń DNA indukowanych przez toksynę T-2 w komórkach linii Hs68 analizowano za pomocą alkalicznej wersji testu kometowego. Metoda ta identyfikuje jedno- i dwuniciowe pęknięcia DNA oraz miejsca alkalicznie labilne na poziomie pojedynczej komórki. Miarą poziomu uszkodzeń DNA jest długość ogona i ilość zawartego w nim DNA, którą wykazano jako rosnący % DNA w ogonie komety. Wykazano, że wszystkie zastosowane stężenia toksyny zarówno po 24- jak i 48-godzinnej inkubacji indukują pęknięcia DNA oraz miejsca alkalicznie labilne. Stopień uszkodzenia DNA w komórkach jest skorelowany z dawką i czasem ekspozycji na toksynę T-2. Zaobserwowane zmiany dla wszystkich stężeń toksyny i czasów ekspozycji są istotne statystycznie w stosunku do komórek nietraktowanych toksyną.

Kolejną metodą wykorzystaną do określenia ilości uszkodzeń jądrowego DNA (nDNA) była reakcja SLR-qRT-PCR, gdzie pomiar uszkodzeń DNA oparty jest na zależności, że wszelkie zmiany (uszkodzenia/pęknięcia) na matrycy DNA będą blokować polimerazę DNA, a to następnie skutkować będzie zmniejszeniem amplifikacji sekwencji docelowej. Zbadano uszkodzenia w dwóch regionach nDNA, tj.: genach *HPRT1* i *TP53*. Uszkodzenia DNA określano jako poziom uszkodzeń nDNA na 10 kpz DNA badanego regionu genu. Analizowano uszkodzenia jądrowego DNA komórek eksponowanych na toksynę T-2 w stężeniach 0,1; 1 i 10 μM w dwóch okresach inkubacji – 24h i 48h. Zaobserwowano, że traktowanie komórek Hs68 toksyną T-2 w sposób zależny od dawki i czasu zwiększyło poziom uszkodzeń jądrowego DNA w obu testowanych regionach jądrowego DNA. Jednakże nie stwierdzono różnic istotnych statystycznie w poziomie uszkodzeń jądrowego DNA w porównaniu rejonów obu genów.

W celu oceny wpływu toksyny T-2 na ekspresję istotnych dla uszkodzeń DNA genów przeprowadzono analizę ekspresji genów na poziomie mRNA metodą Real-Time PCR. Oceny

zmian w ekspresji mRNA dokonano dla dwóch grup genów: genów związanych ze stanem zapalnym (*TNF, INFG, IL1A, IL1B*) oraz genów związanych z procesem naprawy DNA (*LIG1, LIG3, FEN, XRCC1, APEX*). Analiza wykazała, że toksyna T-2 w sposób zależny od dawki i czasu zwiększała poziom mRNA dla *TNF, INFG, IL1A* i *IL1B*. W grupie genów związanych w procesem naprawy DNA zaobserwowano zmiany ekspresji indukowane przez toksynę T-2 w dwóch z nich – *LIG3* i *APEX*. Poziom mRNA dla *LIG3* zmniejszał się w sposób zależny od dawki, podczas gdy dla *APEX* wykazano wzrost poziomu mRNA.

W celu określenia potencjalnego oddziaływania toksyny T-2 z dwuniciową strukturą DNA wykonano badania *in silico.* Ze względu na dostępność jedynie małych fragmentów DNA w bazach danych struktur 3D, wykorzystano 3 różne struktury pobrane z bazy RCSB PDB – 1BDZ, 3 AAF oraz 6O3T. Do każdej z tych struktur toksyna T-2 wykazała bardzo silne powinowactwo i posiadała termodynamicznie korzystnie przyłączony konformer strukturalny. Jako punkt odniesienia dla uzyskanych wartości powinowactwa dla T-2 przeprowadzono analizy związku referencyjnego jakim był iperyt siarkowy. Wartości powinowactwa toksyny T-2 były znacznie korzystniejsze (w zakresie -6.0 do -4.2 kcal/mol) niż otrzymane dla iperytu siarkowego (oscylują wokół -2 kcal/mol). Szczegółowa analiza miejsca wiązania toksyny T-2 do cząsteczki DNA wykazała, że związek ten ma silne powinowactwo do oddziaływania z dużym rowkiem podwójnej helisy DNA **(Praca nr 4).**

Omówienie wyników

Podczas prac badawczych zaplanowano szereg doświadczeń, których sekwencja miała na celu przedstawienie w ciągu logicznym molekularnego mechanizmu toksyczności toksyny T-2.

Testy MTT i z błękitem trypanu wykazały, że toksyna negatywnie wpływa na linię komórkową Hs68 i zmniejsza przeżywalność komórek. ATP to główny i uniwersalny nośnik energii w organizmie a energia uwalniana podczas hydrolizy ATP jest wykorzystywana przez komórkę do przemian wymagających nakładu energii np. aktywnego transportu błonowego czy reakcji syntez. Kiedy komórki przechodzą procesy takie jak apoptoza lub nekroza, poziom ATP ulega zmniejszeniu. Wykorzystanie bioluminometrii do oznaczenia względnego poziomu ATP dowiodło, że toksyna wywołuje spadek poziomu ATP w komórkach, a co za tym idzie spadek ich aktywnego metabolizmu. Dalsze analizy miały na celu sprawdzenie czy za toksyczne działanie toksyny T-2 odpowiedzialny jest proces apoptozy czy nekrozy. Podwójne barwienie komórek aneksyną V i jodkiem propidyny wykazało wzrost fluorescencji jodku propidyny, który wiąże się z DNA komórek z uszkodzoną błoną komórkową, czyli późnoapoptotycznych i nekrotycznych. Nie zaobserwowano natomiast znaczącego wzrostu fluorescencji aneksyny V, która wiąże się z eksponowaną na zewnętrznej błonie komórkowej fosfatydyloseryną w komórkach apoptotycznych. W kolejnym etapie badań przeprowadzono weryfikację zdolności toksyny T-2 do aktywacji kaspazy-3 i kaspazy-7 w komórkach apoptotycznych. Zgodnie z wynikami fluorescencji, toksyna T-2 nie aktywuje kaspazy-3 oraz kaspazy-7 w komórkach fibroblastów. Dodatkowo przeprowadzono analizę stężenia ludzkiej cytokeratyny 18, która obecna pozakomórkowo jest markerem martwicy komórek nabłonkowych. Wzrost stężenia cytokeratyny 18 potwierdziło nekrotyczne działanie badanej toksyny. Wyniki powyższych badań wskazują cytotoksyczne działanie toksyny T-2 względem komórek fibroblastów oparte na procesie nekrozy.

Następnym krokiem było określenie wpływu toksyny na funkcjonowanie mitochondriów. Pierwszym etapem badań była analiza potencjału błony mitochondrialnej (MMP) komórek. Jedna z teorii sugeruje że w przypadku, kiedy spadek MMP jest związany z dysfunkcją mitochondriów i wyczerpaniem ATP, może wystąpić śmierć komórek na drodze nekrozy (Lemasters et al. 1998). W tym kontekście, ekspozycja komórek na toksynę T-2 powodowała spadek MMP co wskazuje na zaburzenia funkcjonowania mitochondriów wywołane zaburzeniami procesu fosforylacji oksydacyjnej umożliwiającym powstanie ATP, co jest mechanizmem nekrotycznej śmierci komórki. Analiza wytwarzania reaktywnych form

tlenu nie wykazała natomiast wpływu toksyny na wewnątrzkomórkowy poziom ROS. Wynikać to może z braku działania stresu oksydacyjnego jako mechanizmu toksycznego działania toksyny T-2. Biorąc pod uwagę brak wpływu na poziom ROS oraz brak wpływu na aktywność kaspazy-3 i kaspazy-7, toksyna T-2 nie wywołuje procesu apoptozy w komórkach fibroblastów. Wykazano także, że toksyna T-2 ma wpływ na genom mitochondrialny badanej linii komórkowej a genotoksyczność toksyny obserwowano jako zmianę liczby kopii mitochondrialnego DNA (mtDNA). mtDNA człowieka zawiera 37 genów, które kodują m.in. 13 białek procesu fosforylacji oksydacyjnej odpowiadającego za produkcję energii. Przyczyną deplecji mtDNA w komórkach mogą być zaburzenia czynności mitochondriów w cyklu przemian energetycznych co potwierdza wcześniejsze wnioski dotyczące uszkodzeń mitochondriów i zaburzeń produkcji ATP indukowanych przez toksynę T-2. Ilość uszkodzeń mtDNA analizowano w dwóch regionach mtDNA: *ND1* oraz *ND5*. Geny te kodują odpowiednio podjednostkę 1 i 5 dehydrogenazy NADH, które jest białkiem I kompleksu łańcucha oddechowego znajdującego się w wewnętrznej błonie mitochondrialnej. Analiza wykazała, że inkubacja komórek z toksyną zwiększyła poziom uszkodzeń mtDNA w obu testowanych regionach mtDNA. Wyniki te potwierdzają negatywny wpływ toksyny T-2 na funkcjonowanie mitochondriów, co w konsekwencji może prowadzić do zahamowania produkcji ATP i procesu nekrozy komórek.

Jako podsumowanie badań określono genotoksyczne właściwości toksyny T-2 w stosunku do genomu jądrowego. Wpływ toksyny T-2 na uszkodzenia genomu jądrowego analizowano z wykorzystaniem testu kometowego w wersji alkalicznej, którego wyniki jasno wskazywały na występowanie jedno- i dwuniciowych pęknięć DNA oraz miejsc alkalicznie labilnych w komórkach. Następnie zbadano uszkodzenia w dwóch regionach nDNA, tj.: *HPRT1* i *TP53*. Oba geny odgrywają istotną rolę w funkcjonowaniu komórki. Białko kodowane przez gen *HPRT1* to transferaza enzymatyczna, która odgrywa kluczową rolę w wytwarzaniu nukleotydów purynowych poprzez szlak odzyskiwania puryn. Gen *TP53* natomiast koduje białko p53, które bierze udział w regulacji wielu procesów komórkowych np. aktywacji mechanizmów naprawy DNA czy indukcji apoptozy w odpowiedzi na uszkodzenia DNA. Zwiększenie poziomu uszkodzeń jądrowego DNA w obu testowanych regionach potwierdziło wyniki testu kometowego wskazując na wywoływanie uszkodzeń DNA przez toksynę T-2. Analiza ekspresji istotnych dla uszkodzeń DNA genów związanych ze stanem zapalnym oraz genów związanych z procesem naprawy DNA wskazuje na indukcję stanu zapalnego przez toksynę ze względu na istotny wzrost ekspresji genów *IL1A* oraz *IL1B*. W grupie genów związanych w procesem naprawy DNA zaobserwowano zmiany ekspresji

w dwóch z nich – *LIG3* i *APEX*. Wzrost ekspresji genu *APEX* wskazuje na wzrost uszkodzeń DNA komórki spowodowany pojawieniem się miejsc AP. Spadek ekspresji genu *LIG3* może być wynikiem znacznego uszkodzenia komórek, a w konsekwencji upośledzenia mechanizmów naprawy DNA. Wyniki analizy *in silico* jednoznacznie wykazały interakcję toksyny T-2 ze strukturą DNA. Wykonano dodatkowe dokowanie tych samych fragmentów struktury DNA do iperytu siarkowego, równie toksycznego dla DNA. Po przeanalizowaniu wyników powinowactwa związku referencyjnego do struktur DNA i porównaniu ich z energią wiązania badanej toksyny z DNA można wnioskować, że powinowactwo toksyny T-2 do łańcucha DNA jest co najmniej dwukrotnie większe niż powinowactwo iperytu siarkowego. Wyniki te jasno wskazują na silny potencjał genotoksyczny toksyny T-2, która wielokierunkowo oddziaływując na komórkę jest zdolna do wywołania procesu nekrotycznego poprzez uszkodzenia mitochondriów oraz cząsteczek DNA jądrowego.

Wnioski

1. Toksyna T-2 oddziałuje negatywnie na funkcjonowanie komórek prawidłowych ludzkich fibroblastów linii Hs68 wywołując śmierć komórek na drodze nekrozy.
2. Toksyna T-2 zaburza funkcjonowanie mitochondriów komórek oraz uszkadza strukturę ich DNA.
3. Toksyna T-2 posiada silne właściwości genotoksyczne w stosunku do genomu jądrowego i jest zdolna do bezpośredniego oddziaływania ze strukturą DNA.

Streszczenie

Mykotoksyna T-2 należy do trichotecenów typu A i swojej budowie zawiera podwójne wiązanie między C-9 i C-10 oraz grupę epoksydową między C-12 i C-13. Struktura chemiczna toksyny charakteryzuje się grupą hydroksylową (OH) w pozycji C-3, grupami acetyloksylowymi (-OCOCH3) w pozycjach C-4 i C-15, atomem wodoru w pozycji C-7 oraz grupą izowalerylową z wiązaniem estrowym [OCOCH2CH(CH3)2] w pozycji C-8. Toksyna T-2 produkowana jest przez różne gatunki grzybów strzępkowych z rodzaju *Fusarium* takie jak *F. sporotrichioides, F. poae* i *F. acuminatum*. Toksyna ta wykazuje odporność na degradację pod wpływem wysokiej temperatury i światła UV. Toksyna T-2 wywołuje skażenia wielu upraw a jej obecność wykrywano w ziarnach zbóż takich jak jęczmień, pszenica, owies, ryż i kukurydza, a także w produktach zbożowych m.in. mące pszennej, płatkach śniadaniowych czy wyrobach piekarniczych.

Wśród trichotecenów toksyna T-2 uważana jest za najbardziej toksycznego przedstawiciela. Dane literaturowe potwierdzają, że toksyna ta wykazuje toksyczność względem różnych układów organizmu ludzi i zwierząt tj. pokarmowego, immunologicznego, nerwowego, moczowego czy płciowego. Co więcej, toksyna T-2 oddziałuje silnie drażniąco na skórę i może być wchłaniana przez nienaruszoną powłoki skórne, powodując ogólnoustrojową toksyczność. Uważa się, że uszkodzenia skóry wywołane działaniem tej toksyny mogą być nawet 400-krotnie silniejsze niż przy zastosowaniu iperytu siarkowego, który należy do broni chemicznej. Ponadto aktywność toksyny T-2 po wniknięciu do organizmu przez drogi oddechowe jest porównywalna z aktywnością iperytu siarkowego, iperytów azotowych i luizytu. Dlatego też właściwości toksyny T-2 są bardziej zbliżone do środków chemicznych niż toksyn biologicznych. Dermatotoksyczne skutki działania toksyny charakteryzują się zaczerwienieniem, obrzękiem a w ciężkich przypadkach owrzodzeniem i martwicą skóry. Pomimo wielu lat badań nad toksycznym działaniem toksyny T-2 względem skóry brak jest informacji wskazujących na molekularne mechanizmy działania tej toksyny względem jej komórek.

Głównym celem pracy było wyjaśnienie mechanizmów cytotoksycznego i genotoksycznego działania toksyny T-2 w warunkach *in vitro*. Materiał do badań stanowiła linia komórkowa prawidłowych ludzkich fibroblastów – Hs68. Komórki traktowano mykotoksyną T-2 w zakresie stężeń 0,001-100 μM oraz inkubowano przez 24 i 48 godzin.

Oceny bezpośredniego toksycznego działania toksyny T-2 względem ludzkich prawidłowych fibroblastów linii Hs68 dokonano za pomocą analizy przeżywalności komórek

z wykorzystaniem testu z błękitem trypanu oraz testu MTT. Oznaczono także komórkowy poziom ATP metodą bioluminometrii oraz aktywność kaspazy-3 oraz kaspazy-7 techniką cytometrii przepływowej. Analizę zmian apoptotycznych i nekrotycznych przeprowadzono z wykorzystaniem wiązania aneksyny V i jodku propidyny metodą cytometrii przepływowej, natomiast stężenie cytokeratyny 18 oceniono przy użyciu testu ELISA. Analizę wpływu toksyny T-2 na uszkodzenia mitochondriów komórek linii Hs68 przeprowadzono oznaczając zmiany potencjału błony mitochondrialnej przy użyciu sondy fluorescencyjnej JC-1, generowanie reaktywnych form tlenu (reactive oxygen species – ROS) przy użyciu sondy fluorescencyjnej H2DCFDA, uszkodzenia mitochondrialnego DNA metodą Semi-Long Run qRT-PCR oraz ilość kopii mitochondrialnego DNA metodą Real-Time-qPCR. Analizę wpływu toksyny T-2 na uszkodzenia genomu jądrowego oparto na ocenie uszkodzeń jądrowego DNA metodą kometową, z wykorzystaniem reakcji Semi-Long Run qRT-PCR oraz ocenie zmian ekspresji genów na poziomie mRNA dla genów związanych z procesem stanu zapalnego i naprawy DNA. Dodatkowo przeprowadzono analizę *in silico* dotyczącą wiązania toksyny do DNA.

Przeprowadzone badania wykazują, że toksyna T-2 posiada toksyczne właściwości i negatywnie wpływa na funkcjonowanie komórek prawidłowych ludzkich fibroblastów linii Hs68. Analizy *in vitro* obejmujące traktowanie linii komórkowej toksyną w zakresie stężeń 0,001-100 μM przy 24- i 48-godzinnej inkubacji ukazują zarówno cytotoksyczny jak i genotoksyczny charakter toksyny T-2.

Summary

T-2 mycotoxin toxin belongs to type A trichothecenes and contains a double bond between C-9 and C-10 and an epoxy group between C-12 and C-13. The T-2 chemical structure is characterized by a hydroxyl (OH) group at the C-3 position, acetyloxy (-OCOCH3) groups at the C-4 and C-15 positions, an atom of hydrogen at the C-7 position and an ester-linked isovaleryl [OCOCH2CH(CH3)2] group at the C-8 position. T-2 toxin is produced by various species of filamentous fungi of the genus *Fusarium* such as *F. sporotrichioides*, *F. poae* and *F. acuminatum*. This toxin exhibits resistance to degradation under the influence of high temperature and UV light. T-2 toxin causes contamination of many crops, and its presence has been detected in grains of cereals such as barley, wheat, oats, rice and corn, as well as in cereal products such as wheat flour, breakfast cereals and bakery products.

Among the trichothecenes, the T-2 toxin is considered the most toxic representative. Literature data confirm that this toxin exhibits toxicity to various human and animal body systems, i.e., digestive, immunological, nervous, urinary and sexual. Moreover, T-2 toxin is a strong skin irritant and can be absorbed through intact skin, causing systemic toxicity. It is considered that skin damage caused by this toxin can be up to 400 times stronger than when using sulfur mustard, which belongs to chemical weapons. In addition, the activity of the T-2 toxin after entering the body through the respiratory tract is comparable to that of sulfur mustard, nitrogen mustard and lewisite. Therefore, the properties of the T-2 toxin are more similar to chemical agents than to biological toxins. Dermatotoxic effects of the toxin are characterized by redness, swelling and in severe cases ulceration and necrosis of the skin. Despite many years of studies on skin toxicity of T-2 toxin, there is no information indicating the molecular mechanisms of this toxin's action on this organ.

The main aim of the study was to elucidate the mechanisms of cytotoxic and genotoxic action of T-2 toxin under in vitro conditions. The study material was a cell line of normal human fibroblasts - Hs68. Cells were treated with mycotoxin T-2 at concentrations ranging from 0.001 to 100 μM and incubated for 24 and 48 hours.

The direct toxicity of T-2 toxin against human normal Hs68 fibroblasts was assessed by cell viability analysis using the trypan blue and the MTT assays. The cellular ATP level was also determined by bioluminometry and activity of caspase-3 and caspase-7 by flow cytometry. Analysis of apoptotic and necrotic lesions was performed using the binding of annexin V and propidine iodide by flow cytometry, while the concentration of cytokeratin 18 was assessed using the ELISA test. The analysis of the impact of T-2 toxin on mitochondrial damage of Hs68

cells was performed by determining changes of the mitochondrial membrane potential using the JC-1 fluorescent probe, generating reactive oxygen species (ROS) using the H2DCFDA fluorescent probe, determining mitochondrial DNA damage using the Semi-Long method Run qRT-PCR and the number of mitochondrial DNA copies by Real-Time-qPCR.

The analysis of the impact of T-2 toxin on nuclear genome damage was based on the assessment of nDNA damage using the comet method, Semi-Long Run qRT-PCR reaction and the evaluation of changes in gene expression at the mRNA level for genes related to inflammation and DNA repair. In addition, an *in silico* analysis of toxin binding to DNA was performed.

The studies show that T-2 toxin has toxic properties and negatively affects the functioning of normal human fibroblast cells of the Hs68 line. In vitro analyzes involving treatment of the cell line with toxin concentrations in the concentration range of 0.001-100 μM with 24- and 48-hour incubation show both the cytotoxic and genotoxic nature of the T-2 toxin.

Literatura

Adeyeye, Samuel A. O. 2016. "Fungal mycotoxins in foods: A review." *Cogent Food & Agriculture* 2 (1): 1213127. https://doi.org/10.1080/23311932.2016.1213127.

Adhikari, Manish, Bhawana Negi, Neha Kaushik, Anupriya Adhikari, Abdulaziz A. Al-Khedhairy, Nagendra Kumar Kaushik, and Eun Ha Choi. 2017. "T-2 mycotoxin: toxicological effects and decontamination strategies." *Oncotarget* 8 (20): 33933.

Agrawal, Mona, Preeti Yadav, Vinay Lomash, A. S. B. Bhaskar, and P. V. Lakshmana Rao. 2012. "T-2 toxin induced skin inflammation and cutaneous injury in mice." *Toxicology* 302 (2): 255-265. https://doi.org/https://doi.org/10.1016/j.tox.2012.08.007.

Alshannaq, Ahmad, and Jae-Hyuk Yu. 2017. Occurrence, Toxicity, and Analysis of Major Mycotoxins in Food. *International Journal of Environmental Research and Public Health* 14 (6). https://doi.org/10.3390/ijerph14060632.

Bhavanishankar, T. N., H. P. Ramesh, and T. Shantha. 1988. "Dermal toxicity of Fusarium toxins in combinations." *Archives of Toxicology* 61 (3): 241-244. https://doi.org/10.1007/BF00316641.

Bunner, David L., and Elena R. Morris. 1988. "Alteration of multiple cell membrane functions in L-6 myoblasts by T-2 toxin: An important mechanism of action." *Toxicology and Applied Pharmacology* 92 (1): 113-121. https://doi.org/https://doi.org/10.1016/0041-008X(88)90233-5.

Chaudhary, Manjari, and P. V. Lakshmana Rao. 2010. "Brain oxidative stress after dermal and subcutaneous exposure of T-2 toxin in mice." *Food and Chemical Toxicology* 48 (12): 3436-3442. https://doi.org/https://doi.org/10.1016/j.fct.2010.09.018.

El-Sayed, Raghda A., Ali B. Jebur, Wenyi Kang, and Fatma M. El-Demerdash. 2022. "An overview on the major mycotoxins in food products: characteristics, toxicity, and analysis." *Journal of Future Foods* 2 (2): 91-102. https://doi.org/https://doi.org/10.1016/j.jfutfo.2022.03.002.

European Food Safety, Authority, Davide Arcella, Petra Gergelova, Matteo Lorenzo Innocenti, and Hans Steinkellner. 2017. "Human and animal dietary exposure to T-2 and HT-2 toxin." *EFSA Journal* 15 (8): e04972. https://doi.org/https://doi.org/10.2903/j.efsa.2017.4972.

Food and Agriculture Organization of the United Nations. Worldwide Regulations for Mycotoxins in Food and Feed in 2003. Available online: http://www.fao.org/3/y5499e/y5499e00.html (accessed on 1 February 2023).

Hemmati, Ali Asghar, Hibatoallah Kalantari, Amir Jalali, Somie Rezai, and Hossein Haghighi Zadeh. 2012. "Healing effect of quince seed mucilage on T-2 toxin-induced dermal toxicity in rabbit." *Experimental and Toxicologic Pathology* 64 (3): 181-186. https://doi.org/https://doi.org/10.1016/j.etp.2010.08.004.

Kiš, Maja, Ana Vulić, Nina Kudumija, Bojan Šarkanj, Vesna Jaki Tkalec, Krunoslav Aladić, Mario Škrivanko, Sanja Furmeg, and Jelka Pleadin. 2021. "A Two-Year Occurrence of Fusarium T-2 and HT-2 Toxin in Croatian Cereals Relative of the Regional Weather." *Toxins* 13 (1). https://doi.org/10.3390/toxins13010039.

Lattanzio, Veronica M. T., Christoph von Holst, Vincenzo Lippolis, Annalisa De Girolamo, Antonio F. Logrieco, Hans G. J. Mol, and Michelangelo Pascale. 2019. Evaluation of Mycotoxin Screening Tests in a Verification Study Involving First Time Users. *Toxins* 11 (2). https://doi.org/10.3390/toxins11020129.

Lavinia, Petruta, Trif Alexandra, Lcrmiora Damiescu, and Gheorghita Simion. 2011. "T-2 Toxin Occurrence in Cereals and Cereal-Based Foods." *Bulletin of University of Agricultural Sciences and Veterinary Medicine Cluj-Napoca. Agriculture* 68: 1843-5386. https://doi.org/10.15835/buasvmcn-agr:6569.

Lemasters, John J., Anna-Liisa Nieminen, Ting Qian, Lawrence C. Trost, Steven P. Elmore, Yoshiya Nishimura, Ruth A. Crowe, Wayne E. Cascio, Cynthia A. Bradham, David A. Brenner, and Brian Herman. 1998. "The mitochondrial permeability transition in cell death: a common mechanism in necrosis, apoptosis and autophagy." *Biochimica et Biophysica Acta (BBA) - Bioenergetics* 1366 (1): 177-196. https://doi.org/https://doi.org/10.1016/S0005-2728(98)00112-1.

Li, Yanshen, Zhanhui Wang, Ross Beier, Jianzhong Shen, David Smet, Sarah Saeger, and Suxia Zhang. 2011. "T-2 Toxin, a Trichothecene Mycotoxin: Review of Toxicity, Metabolism, and Analytical Methods." *Journal of Agricultural and Food Chemistry* 59: 3441-53. https://doi.org/10.1021/jf200767q.

Mahato, Dipendra Kumar, Shikha Pandhi, Madhu Kamle, Akansha Gupta, Bharti Sharma, Brajesh Kumar Panda, Shubhangi Srivastava, Manoj Kumar, Raman Selvakumar, Arun Kumar Pandey, Priyanka Suthar, Shalini Arora, Arvind Kumar, Shirani Gamlath, Ajay Bharti, and Pradeep Kumar. 2022. "Trichothecenes in food and feed: Occurrence, impact on human health and their detection and management strategies." *Toxicon* 208: 62-77. https://doi.org/https://doi.org/10.1016/j.toxicon.2022.01.011.

Oana, Stanciu, Roxana Banc, Anamaria Cozma-Petruț, Filip Lorena, Miere Doina, Jordi Mañes, and Felicia Loghin. 2015. "Occurence of Fusarium Mycotoxins in Wheat from Europe – A Review." *Acta Universitatis Cibiniensis Series E: FOOD TECHNOLOGY* 19: 35-60. https://doi.org/10.1515/aucft-2015-0005.

Pang, Victor F., Steven P. Swanson, Val R. Beasley, William B. Buck, and Wanda M. Haschek. 1987. "The toxicity of T-2 toxin in swine following topical application: I. Clinical signs, pathology, and residue concentrations." *Fundamental and Applied Toxicology* 9 (1): 41-49. https://doi.org/https://doi.org/10.1016/0272-0590(87)90152-7.

Pascari, Xenia, Ronald Maul, Sabine Kemmlein, Sonia Marin, and Vicente Sanchis. 2020. "The fate of several trichothecenes and zearalenone during roasting and enzymatic treatment of cereal flour applied in cereal-based infant food production." *Food Control* 114: 107245. https://doi.org/https://doi.org/10.1016/j.foodcont.2020.107245.

Rahman, Shafiqur, Anil Kumar Sharma, Nittin Dev Singh, and Shahid Prawez. 2020. "Immunopathological effects of experimental T-2 mycotoxicosis in Wistar rats." *Human & Experimental Toxicology* 40 (5): 772-790. https://doi.org/10.1177/0960327120968852.

The European Commission. Commission Regulation (EC) No 1881/2006 of 19 December Setting Maximum Levels or Certain Contaminants in Foodstuff. Available online: https://eur-lex.europa.eu/legal-content/EN/TXT/PDF/?uri=CELEX:02006R1881- 20140701&from=EN (accessed on 1 February 2023).

U.S. Army Medical Research Institute of Infectious Diseases (USAMRID). T-2 Mycotoxins. In: Medical Management of Biologic Causalities Handbook. 8th Edition. September 2014. Fort Detrick. Frederick, Maryland 21702-5001 (accessed on 19 October 2022).

Ueno, Yoshio. 1984. "Toxicological features of T-2 toxin and related trichothecenes." *Fundamental and Applied Toxicology* 4 (2, Part 2): S124-S132. https://doi.org/https://doi.org/10.1016/0272-0590(84)90144-1.

World Health Organization. Evaluation of Certain Contaminants in Food: Eighty-Third Report of the Joint FAO/WHO Expert Committee on Food Additives. Available online: https://apps.who.int/iris/bitstream/handle/10665/254893/9789241210027-eng.pdf;jsessionid=4E6EBA0A0F5160EC5DC55868695CF4E1?sequence=1 (accessed on 1 February 2023).

molecules

MDPI

Review

T-2 Toxin—The Most Toxic Trichothecene Mycotoxin: Metabolism, Toxicity, and Decontamination Strategies

Edyta Janik [1], Marcin Niemcewicz [1], Marcin Podogrocki [1], Michal Ceremuga [2], Maksymilian Stela [3] and Michal Bijak [1,*]

[1] Biohazard Prevention Centre, Faculty of Biology and Environmental Protection, University of Lodz, Pomorska 141/143, 90-236 Lodz, Poland; edyta.janik@edu.uni.lodz.pl (E.J.); marcin.niemcewicz@biol.uni.lodz.pl (M.N.); marcin.podogrocki@biol.uni.lodz.pl (M.P.)
[2] Military Institute of Armament Technology, Prymasa Stefana Wyszyńskiego 7, 05-220 Zielonka, Poland; ceremugam@witu.mil.pl
[3] CBRN Reconnaissance and Decontamination Department, Military Institute of Chemistry and Radiometry, Antoniego Chrusciela "Montera" 105, 00-910 Warsaw, Poland; m.stela@wichir.waw.pl
* Correspondence: michal.bijak@biol.uni.lodz.pl; Tel./Fax: +48-42-635-43-36

Abstract: Among trichothecenes, T-2 toxin is the most toxic fungal secondary metabolite produced by different *Fusarium* species. Moreover, T-2 is the most common cause of poisoning that results from the consumption of contaminated cereal-based food and feed reported among humans and animals. The food and feed most contaminated with T-2 toxin is made from wheat, barley, rye, oats, and maize. After exposition or ingestion, T-2 is immediately absorbed from the alimentary tract or through the respiratory mucosal membranes and transported to the liver as a primary organ responsible for toxin's metabolism. Depending on the age, way of exposure, and dosage, intoxication manifests by vomiting, feed refusal, stomach necrosis, and skin irritation, which is rarely observed in case of mycotoxins intoxication. In order to eliminate T-2 toxin, various decontamination techniques have been found to mitigate the concentration of T-2 toxin in agricultural commodities. However, it is believed that 100% degradation of this toxin could be not possible. In this review, T-2 toxin toxicity, metabolism, and decontamination strategies are presented and discussed.

Keywords: trichothecenes; type A; T-2 toxin; toxicity; metabolism; decontamination

Citation: Janik, E.; Niemcewicz, M.; Podogrocki, M.; Ceremuga, M.; Stela, M.; Bijak, M. T-2 Toxin—The Most Toxic Trichothecene Mycotoxin: Metabolism, Toxicity, and Decontamination Strategies. *Molecules* **2021**, *26*, 6868. https://doi.org/10.3390/molecules26226868

Academic Editor: Terenzio Bertuzzi

Received: 17 October 2021
Accepted: 11 November 2021
Published: 14 November 2021

1. Introduction

Trichothecenes (TCT) are groups of chemically related mycotoxins compounds produced by diverse filamentous fungal species such as *Fusarium*, *Myrothecium*, *Stachybotrys*, *Trichoderma*, *Trichothecium*, and *Spicellum*, which pose a threat to human and animal health [1,2]. The fungi capable of producing TCT can be found throughout the world. They are able to grow under a variety of environmental conditions including the nutrient content, temperature, moisture content, and oxygen level in growth medium, which resulted in successful colonization [3,4]. TCT are non-volatile, low molecular weight (typically 200–500 Da) sesquiterpenoids synthesized by the terpenoid biosynthetic pathway [5,6]. They are slightly soluble in water but highly soluble in polar organic solvents such as ethyl acetate, chloroform, ethanol, methanol, and propylene glycol [7]. The TCT common structure consists of a three-ring molecule known as 12,13-epoxytrichothec-9-ene (EPT) (Figure 1) [8,9]. The cyclohexene (A-ring) is fused to the tetrahydropyran (B-ring), which is bridged by a two-carbon chain at C-2 and C-5, thus forming a cyclopentyl moiety (C-ring) [10]. TCT are divided based on the substitution pattern of EPT into four types (A–D) (Table 1) [11]. Type A TCT is distinguished by a hydroxyl (OH) group at C-8, an ester function at C-8, or no oxygen substitution at C-8 [12,13].

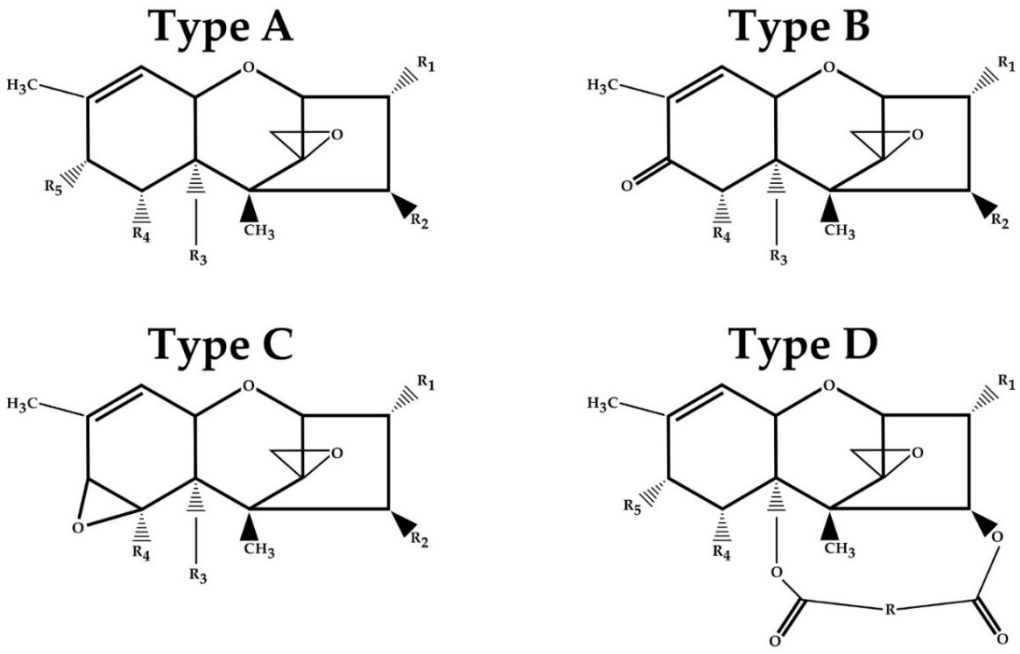

Figure 1. The core structures for A, B, C, and D trichothecenes (TCT) types.

Table 1. Substitution pattern of EPT of common trichothecenes (TCT).

Toxin	Type	R_1	R_2	R_3	R_4	R_5
T-2	A	OH	$OCOCH_3$	$OCOCH_3$	H	$OCOCH_2CH(CH_3)_2$
HT-2	A	OH	OH	$OCOCH_3$	H	$OCOCH_2CH(CH_3)_2$
Neosolaniol (NEO)	A	OH	$OCOCH_3$	$OCOCH_3$	H	OH
Diacetoxyscirpenol (DAS)	A	OH	$OCOCH_3$	$OCOCH_3$	H	H
Nivalenol (NIV)	B	OH	OH	OH	OH	=O
Deoxynivalenol (DON)	B	OH	H	OH	OH	=O
3-Acetyldeoxynivalenol (3-ADON)	B	$OCOCH_3$	H	OH	OH	=O
15-Acetyldeoxynivalenol (15-AcDON)	B	OH	H	$OCOCH_3$	OH	=O
Crotocin	C	H	$OCOCH\text{-}CHCH_3$	H	Epoxide	
Roridin E	D	H	Macrocyclic ring		H	H
Verrucarin A	D	H	Macrocyclic ring		H	H

TCT are identified as a significant threat to human and animal health. The most toxic TCT include T-2, HT-2 toxin, deoxynivalenol (DON), nivalenol (NIV), and diacetoxyscirpenol (DAS) [14]. TCT toxicological activity is related to the presence of the epoxide at the C 12,13 position. Their mechanism of action is mainly based on the protein synthesis inhibition and oxidative cell damage, which is followed by the disruption of synthesis of nucleic acid and the resulting apoptosis [15]. The main sources of TCT in food and feed are wheat, barley, rye, oats, and maize [16–18]. They also occur in hay, straw, green feed, and silage from contaminated cereals [19]. What is more, *Myrothecium* species can contaminate various vegetables e.g., tomato [20]. TCT can also enter human food chains through breakfast cereals, bakery products, snack foods, and beer. Moreover, consumption of products such as meat, milk, and eggs from livestock and poultry that are fed with TCT-contaminated feed are the primary cause of human poisoning [21,22]. TCT are easily absorbed through the gastrointestinal membranes and distributed to different tissues and

organs due to their low molecular weight and amphipathic nature. The consumption of TCT contaminated products may cause variable adverse effects including emesis, anorexia, carcinogenicity, hematotoxicity, immunotoxicity, and neurotoxicity [23–26]. Moreover, it has been reported that T-2 is extremely toxic to the mucous membranes and skin [27]. These effects depend on various factors including mycotoxin's toxicity, time of exposure, or individual nutritional status [28].

T-2 toxin, which belongs to the A TCT type, has the highest toxicity of all TCTs [14,29,30]. T-2 is produced by different *Fusarium* species, including *F. sporotrichioides*, *F. poae*, and *F. acuminatum* [31,32]. Their presence in a variety of cereal grains has been documented in cold and moderate climate regions and during wet storage conditions [33,34]. *F. sporotrichioides*, as the main T-2 producer, grows in the temperature ranging from −2 to 35 °C, preferably with water activity (aw) above 0.88 [35]. The temperature and aw optimal for the T-2 biosynthesis are 20–30 °C and aw in the range of 0.980–0.995, respectively [36]. T-2 is resistant to degradation in different environmental conditions, such as high temperature and UV light. However, it is effectively deactivated in a strong acid or alkaline environment, and it can be affected by the presence of coexisting fungi or bacteria leading to detoxifying T-2 by altering its chemical structure [29].

T-2 poses a potential threat to humans and animals as a natural cereals contaminant and can induce a wide range of toxic effects due to its strong toxicity. T-2 has different toxic effects depending on the dosage, age, and ways of exposure (oral, dermal, and aerosol). Generally, observed acute toxicological effects are feed refusal, vomiting, hemorrhages, stomach necrosis, and dermatitis [37,38]. In addition, T-2 is considered to be a main cause of a gastrointestinal disorder called alimentary toxic aleukia disease (ATA) affecting in history soldiers in World War II and humans in certain world regions after eating molded food [39,40].

The aim of this study is to characterize the T-2 mycotoxin with special attention paid to the aspect of the multidirectional toxicity, metabolism, and decontamination strategies.

2. Structure and Physical and Chemical Properties of T-2 Toxin

The T-2 toxin belongs to type A trichothecenes. As a TCT, it contains a double bond between C-9 and C-10 and an epoxy group between C-12 and C-13 [12]. The T-2 chemical structure is characterized by a hydroxyl (OH) group at the C-3 position, acetyloxy (-$OCOCH_3$) groups at the C-4 and C-15 positions, an atom of hydrogen at the C-7 position and an ester-linked isovaleryl [$OCOCH_2CH(CH_3)_2$] group at the C-8 position (Figure 2) [41].

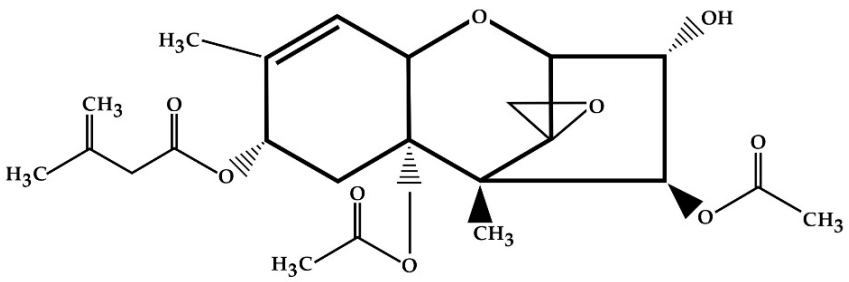

Figure 2. Chemical structure of T-2 toxin.

3. Metabolism of T-2 Toxin

T-2 toxin has a lipophilic character and can be immediately absorbed from the alimentary tract or through the respiratory mucosal membranes [42]. Liver is the primary organ of toxin's metabolism after its absorption [43]. After ingestion, toxin is rapidly absorbed and excreted in feces and urine. The half-life of T-2 in plasma is short, and elimination is usually completed within 48 h, depending on the administration mode, the consumed amount, and on species-specific differences [44]. In addition, toxin does not accumulate in significant quantity in various organs such as the kidneys, liver, or the

skeletal muscle [45,46]. The major metabolic pathways are usually hydrolysis, hydroxylation, conjugation, and de-epoxidation [45]. Typical metabolites of T-2 toxin are HT-2 toxin, T-2-triol, T-2-tetraol, neosolaniol (NEO), 3′-hydroxy-T-2 (3′-OH-T-2), 3′-hydroxyHT-2 toxin (3′-OH-HT-2), deepoxy-3′-hydroxy-T-2-triol, deepoxy-3′-hydroxy-HT-2, 3′-hydroxy-T-2-triol, dihydroxy-HT-2 toxin, 3′7-dihydroxy-T-2 (3′,7′-di-OH-T-2), and 3′,7-dihydroxy-HT-2 toxin (3′,7′-di-OH-HT-2) [29]. In recent years, some in vitro and in vivo studies of T-2 bioconversion have been conducted. The performed studies have led to characterization of the metabolic pathways and identification of the main T-2 metabolites in different species.

Yang et al. [47] performed in vitro study with animal and human liver microsomes that aimed to investigate the phase I and II metabolites. In this study, T-2 was incubated with chickens, swine, goats, cows, rats, or humans liver microsomes under identical experimental conditions. As a consequence, four phase I metabolites (HT-2, NEO, 3′-OH-T-2, and 3′-OH-HT-2) and three phase II glucuronide binding metabolites (T-2-3-glucuronide (T-2-3-GlcA), HT-2-3-glucuronide (HT-2-3-GlcA), HT-2-4-glucuronide (HT-2-4-GlcA)) of T-2 were discovered. The HT-2 toxin was the predominant metabolite in all species, suggesting that the HT-2 may serve as a biomarker allowing to assess the dietary exposure of animals and humans to T-2. The T-2 possible metabolic pathways mainly consist of hydrolysis (HT-2, NEO), hydroxylation (3′-OH-T-2 and 3′-OH-HT-2), and glucuronidation (T-2-3-GlcA, HT-2-3-GlcA, HT-2-4-GlcA). However, a significant metabolic difference was observed among species. Compared to other in vitro models, a large amount of unmetabolized T-2 remained after incubation with chicken liver microsomes, especially in the phase II incubation system. It suggests that the chickens have a lower ability to metabolize and conjugate T-2. Moreover, a significant difference was observed on the hydroxylated products. 3′-OH-T-2, 3 was the main hydroxylated product observed in chickens, cows, and rats, while for goats, swine, and humans, it was 3′-OH-HT-2. In addition, species-specific patterns of T-2 glucuronidation were also noticed. The major glucuronidation product in cows and goats was T-2-3-GlcA, while for the other animal species and human, it was HT-2-3-GlcA [47]. In vitro studies with rat liver microsomes and liver S9 fraction were used. The results showed that hydrolysis was the main metabolic pathway of T-2 toxin, followed by hydroxylation. The HT-2, NEO, 9′-hydroxy-T-2 (9-OH-T-2), and 4-deacetylneosolaniol were the main metabolites in liver microsomes systems, whereas HT-2, 4-deacetylneosolaniol (4-deAc-NEO), NEO, 9-OH-T-2, and 3′-OH-T-2 had high contents in liver S9 fraction systems [43].

An in vivo study was performed by Yang and colleagues [47], which aimed to investigate the metabolism of T-2 in chickens after oral administration. As a result, 18 metabolites (Table 2) were detected and identified in the chickens bile and feces. Some of these metabolites such as 3′-Hydroxy-T-2-3-sulfate (3′-OH-T-2 3-SO3H), 3′-Hydroxy-HT-2-3-sulfate (3′-OH-HT-2 3-SO3H), 4′-Hydroxy-HT-2 (4′-OH-HT-2), 3′,4′-Dihydroxy-T-2 (3′,4′-di-OH-T-2), 4′-Carboxyl-T-2 (4′-COOH-T-2), 4′-Carboxyl-HT-2 (4′-COOH-HT-2), 4′-Carboxyl-3′-hydroxy-T-2 (4′-COOH-3′-OH-T-2), and their isomers were discovered. T-2 was extensively metabolized in chickens demonstrated by the recovery of only traces of unmetabolized toxin in chicken excreta. This study showed that 3′-OH-HT-2 was the main metabolite of T-2 [47].

What is more, the same results were obtained in a study with rats [43]. These results suggested that in rats and chickens, T-2 was hydrolyzed to HT-2, and it could undergo hydroxylation at the isovaleryl group and produce 3′-OH-HT-2. Therefore, this metabolite may serve as a T-2 biomarker of exposure. What is more, two novel metabolites (3′-OH-T-2 3-SO3H, 3′-OH-HT-2 3-SO3H) indicate that the sulfonation may be a T-2 specific metabolic pathway in chickens [47].

In vivo studies in rats as an animal model revealed a significant difference between male and female rats concerning the type of T-2 toxin metabolites. For male rats, the main metabolite of T-2 toxin was 3′-OH-HT-2 followed by de-epoxy-3′-OH-HT-2, 3′,7′-di-OH-T-2, HT-2, 3′-OH-T-2, 4-deAc-NEO, and 7′-hydroxy-HT-2 (7′-OH-HT-2). In comparison,

for the female rats, the main metabolites were HT-2, 3′-OH-HT-2, de-epoxy-3′-OH-HT-2, 3′-OH-T-2, 9-OH-T-2, and 4-deAc-NEO, sequentially [43].

Table 2. Summary of T-2 toxin metabolites in in vivo study in chickens.

Number of Metabolite	Metabolite	Metabolic Pathway
1	HT-2 toxin (HT-2)	Hydrolysis
2	Neosolaniol (NEO)	
3	4-deacetylneosolaniol (4-deAc-NEO)	
4	3′-hydroxy-T-2 (3′-OH-T-2)	Hydroxylation
5	3′-hydroxy-HT-2 (3′-OH-HT-2)	
6	3′-Hydroxy-T-2-3-sulfate (3′-OH-T-2 3-SO3H)	Sulfonation
7	3′-Hydroxy-HT-2-3-sulfate (3′-OH-HT-2 3-SO3H)	
8	4′-Hydroxy-HT-2 (4′-OH-HT-2)	Hydroxylation
9	4′-OH-HT-2 isomer	
10	4′-Carboxyl-T-2 (4′-COOH-T-2)	Carboxylation
11	4′-COOH-T-2 isomer	
12	4′-Carboxyl-HT-2 (4′-COOH-HT-2)	
13	4′-COOH-HT-2 isomer	
14	4′-Carboxyl-3′-hydroxy-T-2 (4′-COOH-3′-OH-T-2)	
15	4′-COOH-3′-OH-T-2 isomer	
16	3′,4′-Dihydroxy-T-2 (3′,4′-di-OH-T-2)	Hydroxylation
17	3′,4′-di-OH-T-2 isomer	
18	4′,4′-Dihydroxy-T-2 (4′,4′-di-OH-T-2)	

4. T-2 Toxicity

Many studies have been performed in the last few decades focusing on the cytotoxic and genotoxic effects of T-2 toxin. At a cellular level, the major effect of T-2 is inhibition of protein synthesis, which leads to secondary DNA disruption and RNA synthesis [48]. T-2 is hypothesized to bind and inactivate peptidyl-transferase activity at the transcription site, resulting in the inhibition of protein synthesis. The most important molecular target of TCT is the 60S ribosomal unit, where it prevents polypeptide chain initiation. This inhibitory effect is most visible in actively proliferating cells such as the gastrointestinal tract, skin, thyroid, bone marrow, and erythroid cells [49,50]. The oxidative stress associated with detrimental effects, such as elevated lipid peroxidation, nuclear and mitochondrial DNA damage, disturbances in the cell signaling, and inflammatory pathways are also the effects of T-2 toxin intoxication. What is more, toxin affects the cell cycle and induces apoptosis [51–53]. Both in vitro and in vivo studies confirmed the toxic properties of this mycotoxin (Figure 3), and the results of some of them are presented below.

4.1. Hepatotoxicity

Ihara and colleagues [54] investigated whether T-2 possesses an ability to induce apoptosis in a mice model. The analysis revealed that the DNA fragmentation in liver happened shortly after exposition to the toxin. The induction of apoptotic cellular lesions and phagocytosis of apoptotic bodies by Kupffer cells was observed 2 hours after toxin administration. These lesions were not observed 12 hours after receiving T-2 [54]. In an in vivo study, Yin et al. [55] assessed the toxicological effect of T-2 on apoptosis and autophagy in chicken hepatocytes. The apoptosis rate and pathological changes degree hepatocytes increased in a dose-dependent manner. Histopathological analysis showed that the toxin caused pathological changes in liver tissue, including hepatocyte edema, increased volume,

and more granules in the cytoplasm. It suggests that the exposition to the T-2 leads to hepatocyte apoptosis. At the molecular level, T-2-induced mitochondria-mediated apoptosis was caused by producing reactive oxygen species (ROS) and promoting cytochrome c (cyt c) translocation between mitochondria and cytoplasm. What is more, the expression of the autophagy-related proteins such as Beclin-1, ATG5, and ATG7 and the LC3-II/LC3-I ratio were increased. It suggests that T-2 caused autophagy. Further experiments showed that the phosphoinositide 3-kinase (PI3K)/protein kinase B (AKT)/mammalian target of rapamycin (mTOR) signal may be involved in autophagy induced by T-2 in chicken hepatocytes [55]. An in vivo study with mice revealed the up-regulated expression of oxidative stress and apoptosis-related genes and the down-regulated expression of glycogen metabolism-, lipid metabolism-, drug metabolism- and blood coagulation-related genes. In particular, c-fos and c-jun expression was notably elevated immediately after T-2 toxin administration and remained at a high level up to 24 hours after. Moreover, T-2 induced death in a small number of hepatocytes 3 hours after administration, and dead hepatocytes at the early stage corresponded to necrosis, while at the late stage they corresponded to apoptosis, respectively [56].

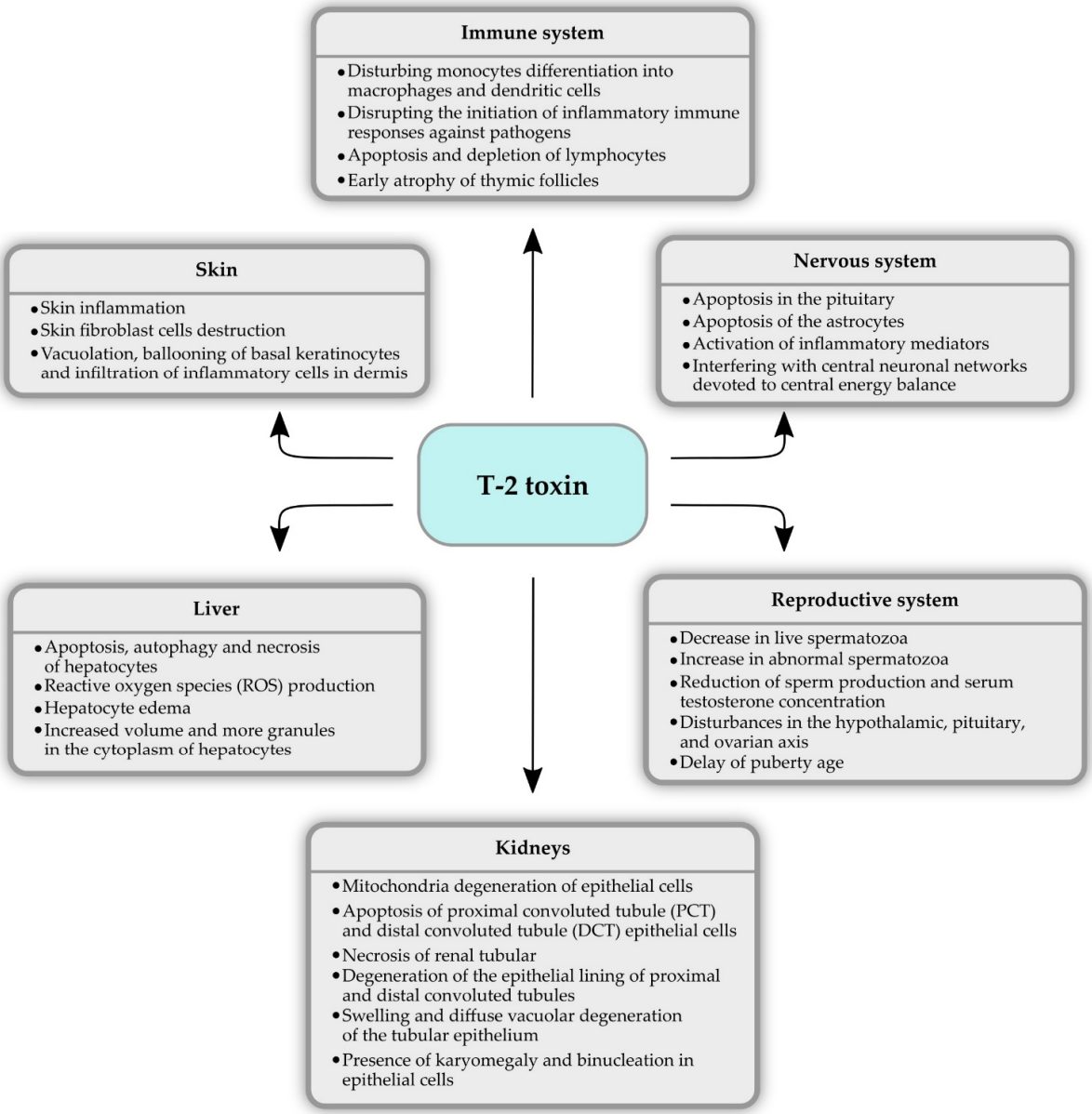

Figure 3. The main toxic effects of T-2 toxin in the organism.

4.2. Nephrotoxicity

A toxicopathological study of T-2 effects on the kidneys in juvenile goats was conducted. The histological analysis revealed the changes in the kidneys after 30 days of T-2 toxin-contaminated diet. The nucleus and mitochondria showed extensive degeneration, and the mitochondria were the most affected organelles. Affected epithelial cells had a loss of cristae, leading to the creation of empty space and rendering the mitochondria to pleomorphic forms (variable sizes and shapes—rounded, dumb bell, curved). Heterochromatin condensation and margination with an indistinct nuclear membrane were also noticed. Within the kidney tissues, proximal convoluted tubule (PCT) and distal convoluted tubule (DCT) epithelial cells exhibited apoptotic changes. In general, the findings showed dose and duration-dependent modifications. Pathomorphological alterations included interstitial engorgement, degeneration of the epithelial lining of proximal and distal convoluted tubules, and renal tubular necrosis. All of these alterations in the renal tissues indicate the toxin's harmful effect on kidneys [14]. A similar study with rats also showed that T-2 induced nephrotoxicity. Biochemical analysis showed increased levels of blood urea nitrogen (BUN) and serum creatinine. A significant increase in oxidative stress enzymes such as malondialdehyde (MDA) and decrease in superoxide dismutase (SOD), catalase, and glutathione (GSH) in kidneys enhanced the role of free radicals in causing kidney damage. The main renal histological changes were the swelling and diffuse vacuolar degeneration of the tubular epithelium. After 12 weeks of toxin-contaminated diet, almost all animals showed severe degenerated PCT epithelial cells, obliterating the lumen with the presence of denuded cells and protein aceous material in their lumina. What is more, the presence of karyomegaly and binucleation in epithelial cells was observed. The mononuclear cell infiltration around glomeruli and in the interstitium was also recorded in rats [57].

4.3. Immunotoxicity

Minervini et al. [58] conducted an in vitro study to investigate T-2 immunotoxicity effects on two lymphoid human cell lines, MOLT-4 (T lineage) and IM-9 (B lineage). As a result, cytotoxicity appeared to be due to early apoptosis in MOLT-4 cells, as indicated by the activation of caspase-3, and to direct cell membrane damage in IM-9 cells. Reduced viability (58%) was observed on the IM-9 line after 8 h of toxin administration. MOLT-4 showed a membrane damage (41% of cell viability) only after 24 h incubation at the higher than IM-9 line toxin concentration [58]. In a different in vitro study [59], the effect of T-2 toxin on human monocyte differentiation into macrophages and dendritic cells was shown. According to the results, T-2 is cytotoxic on monocytes during the differentiation process (in dendritic cells or macrophages, the results are similar). After 24 hours of incubation, only 32% of cells survived after 24 of incubation. What is more, 2% of immature dendritic cells and 9% of macrophages were viable after 24 h of incubation with toxin. CD71 (specific phenotypic macrophages cells marker) expression was downregulated to 40% after 6 days of culture in the condition, inducing monocyte differentiation into macrophages in the presence of toxin, whereas 91% of cells cultured without toxin expressed CD71. In addition, the expression of CD1a (specific dendritic cells marker) was downregulated, while the CD14 (specific monocyte marker) was upregulated. These results showed that the T-2 disturbs the human monocytes' differentiation process into macrophages and dendritic cells. In another study [60], the evaluation of the effects of T-2 on the activation of macrophages by various agonists of Toll-like receptors (TLR) using an in vitro model of primary porcine alveolar macrophages (PAM) was performed. It was established that the ingestion of low concentrations of T-2 can alter TLR activation by decreasing the pattern recognition of pathogens, thereby disrupting the initiation of inflammatory immune responses against viruses and bacteria. Based on this finding, it could be hypothesized that the exposure to low concentrations of T-2 can increase the animals' and humans' susceptibility to opportunistic infections.

Rahman and colleagues [57] showed the immunopathological effects of T-2 mycotoxicosis in rats. T-2 toxicity caused the suppression of both humoral and cellular immune

responses in a dose and duration-dependent manner. Suppression was followed by decreased serum immunoglobulin G (IgG), immunoglobulin M (IgM), immunoglobulin A (IgA) levels, hemagglutination (HA) titers, delayed type hypersensitivity (DTH) response to ovalbumin, CD4+:CD8+ ratios, and the number of CD4+ and CD8+ lymphocytes in peripheral blood and mRNA expression levels of cytokines such as interleukin 2 (IL-2), interferon gamma (IFN-γ), interleukin 4 (IL-4), and interleukin 10 (IL-10) in toxin-fed animals. In addition, lymphoid organs (spleen, thymus, and Peyer's patches) changes were observed. Changes in all organs were of a similar nature but were more severe in thymus than in spleen and Peyer's patches. The depletion of lymphocytes started as single-cell apoptosis, then forming large foci of lymphocytolysis, especially in the thymus. Changes in thymus also included inter and intrafollicular hemorrhage and increased interfollicular connective tissue, resulting in early atrophy of thymic follicles [57].

4.4. Neurotoxicity

Agrawal et al. [61] investigated the mechanism of T-2 toxin-induced apoptosis in a human neuroblastoma (IMR-32) cell line. A study showed that the apoptosis is induced through multiple signal transduction pathways. The exposition on IMR-32 cells to T-2 toxin is characterized by the generation of ROS and then loss of mitochondrial membrane permeability, caspase-3 activation, nuclear fragmentation, oligonucleosomal DNA fragmentation, poly (ADP-ribose) polymerase (PARP) cleavage, and apoptosis. Additionally, ROS can directly activate the Ras–Raf–MEK–extracellular signal-regulated kinase (ERK)–mitogen-activated protein kinase (MAPK) signal transduction pathway, leading to cell cycle arrest and apoptosis [61]. A different in vitro study showed that T-2 induces neurotoxicity in a mouse neuroblastoma2a (N2a) cell line in both a dose and time-dependent manner. A study revealed that toxin exposure inhibits the Nrf2/heme oxygenase-1 (HO-1) pathway and p53 activation, which leads to abnormal mitochondrial function and oxidative stress, which together contribute to caspase-dependent apoptotic cell death [62]. In another study, normal human astrocytes (NHA) in primary culture were used to investigate the apoptotic effects and accumulation of T-2 toxin. According to the results, human astrocytes were highly sensitive to the T-2 properties at low concentration. An increase in caspase-3-activity was reported 6 h after exposure to T-2, increasing up to 24 h. What is more, a strong accumulation of toxin was detected, and a study revealed a fast cellular uptake and high accumulation in NHA cells, leading to a 15- to 30-fold increased concentration in the intracellular compartment [63].

A study with rats showed pathological lesions in the brain three days after exposure to the T-2 toxin and damage in the pituitary seven days after exposure. Autophagy in the brain and apoptosis in the pituitary suggest that this toxin can induce various acute reactions in different tissues. Additionally, toxin was detected in the brain with low concentrations in rat, suggesting that T-2 may cross the blood–brain barrier (BBB). It is also possible that the detection of the toxin in the rat brain can be explained by individual differences in T-2 absorption and metabolism in different experimental animals [64]. Gaige et al. [65] provided that the T-2 toxin modifies feeding behavior by interfering with central neuronal networks devoted to central energy balance in a mice animal model. The results also suggest that inflammatory mediators partake in the toxin-induced anorexia and other symptoms such as reduced water intake, energy expenditure, body temperature, glycaemia, and locomotor activity. T-2 toxin ingestion resulted in the activation of several brain nuclei such as nucleus tractus solitarus (NTS), dorsal motor nucleus of the vagus (DMV), arcuate nucleus (Arc), paraventricular nucleus (PVN), and central amygdala (CeA) involved in the autonomic and endocrine regulation of feeding behavior and physiology. The authors suggest that cytokines from peripheral organs may signal the brain via neuronal and humoral pathways to modify animal homeostasis [65].

4.5. Reproductive System

An in vivo study that aimed to evaluate the toxic effect of T-2 on a reproductive system revealed that this toxin affects male mice fertility [66]. The results showed that the number of live spermatozoa decreased significantly. Moreover, the number of abnormal spermatozoa increased notably, and a remarkable decrease in spermatozoa with integrated acrosome was observed in mice treated with T-2 at both low and high doses. The efficiency of sperm production and serum testosterone concentration, testicular, and cauda epididymal sperm counts were significantly reduced in a dose-dependent manner. In addition, a low pregnancy rate and high fetal resorption rate were noticed when female mice were mated with toxin-exposed males. In a different study, Yang et al. [67] investigated spermatogenesis disorders in male mice caused by T-2 toxin exposition. Their studies also showed that the T-2 hinders the spermatogenesis, which is reflected in the decreased spermatozoa count and increased spermatozoa deformity rate. T-2 toxin exposition increased the ROS and MDA level and decreased the total anti-oxidation capacity (T-AOC) and the SOD activity in performed testes. In addition, an increased expression of caspase-3, caspase-8, caspase-9 mRNA, and Bax and inhibition of Bcl-2 expression were demonstrated. It suggests that spermatogenesis disorders caused by T-2 are related with germ cell apoptosis and mediated by oxidative stress [67]. The effects of maternal T-2 exposure (during gestation and lactation) on the development of testis in the mice offspring were investigated. The results showed significant decreases in body weight and testicular weight at puberty in male offspring. Toxin exposition led to the inhibition of an antioxidant system in testis by oxidative stress and decreased testosterone synthesis, and it also led to a decrease of testosterone levels at pre-puberty. What is more, a significant reduction in the gene expression levels of StAR and 3β-HSD that are involved in testosterone synthesis were noticed. Additionally, results revealed that maternal exposure to the toxin had no notable effects on the expression of genes related to apoptosis. In pre-puberty, the offspring of mice maternally exposed to T-2 tended to decrease the expression of apoptosis-related genes. However, maternal exposure to toxin had no significant impact on the offspring testis after sexual maturity, suggesting a return to reproductive function [68]. A similar study conducted by Perveen and colleagues [69] was performed. They investigated the effect of gestational and lactational exposure to the T-2 and its effects on the puberty of female mice offspring. The findings reported that postnatal exposure to the toxin delayed puberty age, which appears to be influenced by the stage of the estrus cycle. The results also showed that lactational exposure to the toxin induced disturbances in the hypothalamic, pituitary, and ovarian axis and caused oxidative damage. The mechanisms of the toxic effect of T-2 toxin on the reproduction system could be resulted by down-regulation of the mRNA level of hypothalamic Gnrh, pituitary Gnrhr, Lhb, and Fshb, and ovarian Lhr and Fshr, causing the interference with the relative expression of steroidogenesis genes and disrupting the synthesis of estrogen and progesterone [69]. In an in vitro study, the impact of T-2 on reproductive activity in pigs was investigated in porcine granulosa cell [70]. It was found that T-2 toxin has potent dose-dependent inhibitory effects on granulosa cell proliferation and steroidogenesis. The toxin strongly inhibited follicle-stimulating hormone (FSH) and insulin-like growth factor 1 (IGF-I) and induced progesterone production as well as granulosa cell proliferation.

4.6. Dermal Toxicity

Compared to other representatives of the trichothecenes, T-2 toxin has a toxic effect on the skin. Skin inflammation, skin fibroblast cells destruction, and skin damages similar to injuries caused by radiation are major topical effects of T-2 toxin [71]. The toxicity of T-2 in swine following topical application was investigated. The results showed that skin at the site of application was swollen and initially red and progressively turned dark red and purple. By day seven, at the edge of the exposed area, clefts were formed and were covered with serosanguinous exudate. These lesions were characterized as a sponge-like inflammation and progressed to locally extensive necrotizing dermatitis.

After seven days, the skin was focally separated from the underlying tissue and covered with a thick scab. Morphological changes in the internal organs were minimal and were based on the necrosis of single cells in the follicles of lymphoid tissues and in the exocrine pancreas [72]. Agrawal et al. [73] investigated histological and biochemical alterations of inflammation and cutaneous injury caused by T-2 in mice. The histological changes included degenerative alterations such as vacuolation, ballooning of basal keratinocytes, and infiltration of inflammatory cells in dermis. Topical application of toxin resulted in skin oxidative stress in the form of increased ROS generation, lipid peroxidation, and neutrophil mediated myeloperoxidase activity. The analysis of matrix metalloproteinases (MMP)-9 and 2 showed MMP activation and their role in degenerative skin histological alterations. The results also revealed an increase in inflammatory cytokines, a significant increase in the levels of phosphorylated p38 MAPK, and an increase in the sub-G1 population at all toxin doses and time points indicating apoptosis. To summarize, T-2 induced skin injury was mediated by oxidative stress, MMP activity, the activation of myeloperoxidase, the activation of p38 MAPK and apoptosis of epidermal cells and consequently led to degenerative skin histological alterations [73].

5. T-2 Degradation and Mitigation Strategies

Integrated mycotoxin contamination preventive practices could minimize the presence of T-2 toxin in food. Operations including pre-harvest control (e.g., appropriate sowing dates, balanced fertilization, pest infestation management, and selection of resistant varieties), harvest control (e.g., proper timeliness of harvest, reduction of mechanical damages, effective cleaning), and post-harvest strategies (e.g., efficient drying and good storage practices) should mitigate mycotoxin production in agricultural commodities [74]. However, it may not be possible to completely prevent the formation of T-2 in agricultural products, and decontamination strategies involving physical, chemical, and biological techniques need to be used to decontaminate T-2 toxin [75].

5.1. Physical Methods

Segregation, cleaning, milling, boiling, roasting, irradiation, and microwave heating are reported as commonly used physical methods for various mycotoxin control [74]. However, because of T-2's heat-stable nature, cooking processing such as boiling, baking, and extrusion cannot provide a 100% degradation rate of toxin from products [76]. The use of color sorting in order to remove the discolored oat groats can reduce the mycotoxin's level in end products of oat flake. The results showed that more than 90% of T-2 toxin can be removed during industrial processing [1]. According to De Angelis et al. [77], during bread-baking, T2 mitigation up to 74% was observed in naturally contaminated wheat flour. In another study [78], flaked oats were artificially contaminated and processed at the laboratory scale. During biscuit making, up to 45% of T-2 toxin was thermally degraded at 200 °C for 30 min. Different feed adsorbents were developed as an effective strategy to reduce mycotoxins. They have specific structures that allow them to absorb and trap target mycotoxins in feed. Several types of montmorillonite (MMT) clay were tested for their ability in binding T-2 in maize. Sodium montmorillonite (Na-MMT) was more effective than unmodified MMT because of the presence of Na+ ion, an alkali metal ion, which made the clay electrically neutral. As a consequence, the electrically neutral clay increased the binding of T-2 toxin. The Na-MMT is able to decontaminate 66% of T-2 in maize when applied at the level of 8%. Lemongrass powder mixed with MMT (LGP-MMT) was the second most efficient. LGP-MMT at 12% decontaminated 56% of toxin in maize. LGP-MMT contributed MMT clay that was more hydrophobic than the unmodified MMT. T-2 toxin, being a non-polar mycotoxin, attracts hydrophobic compounds and hence binds to the surface of the LGP-MMT [75]. Wei et al. [79] evaluated the ability of modified hydrated sodium calcium aluminosilicate (HSCAS) adsorbent to reduce the toxicity of T-2 in broilers. It was found that T-2 induced growth performance reduction, hepatic and small

intestinal injuries in the group that was fed with a basal diet containing T-2 toxin. Dietary supplementation of the modified HSCAS adsorbent mitigated these injuries.

5.2. Chemical Methods

Some chemical agents have been indicated as decontaminants dedicated for mycotoxins. Chemicals used nowadays for the decontamination of mycotoxins could be divided into the following categories: alkaline (ammonia gas, sodium hydroxide, calcium hydroxide); acids (acetic acid, phosphoric acid, formic acid, propionic acid); reducing agents (sodium bisulfite, sugars: D-glucose or D-fructose); oxidizing agents (ozone, hydrogen peroxide); other (chlorinating agents, salts, and other miscellaneous reagents). All of them have efficiency related to particular mycotoxin [80]. However, there are not many publications related to efficiency versus T-2 toxin. There are data demonstrating that bases, oxidizing agents, and organic acids are suitable for A type trichothecenes decontamination, but they are insufficient for T-2 toxin decontamination [23,81].

The treatment of 0.25% NaClO in 0.25 M NaOH for four hours is able to inhibit the biological activity of T-2 toxin and other trichothecenes. NaClO has also been acclaimed as a decontamination agent for the T-2 toxin. However, these methods cannot be applicable for all food staff [50]. Typical food processing could also reduce mycotoxins concentration; for instance, water-soluble toxins could be washed out partially from the surface of grains. Washing barley and corn three times reduces DON (deoxynivalenol) content by 65 to 69%, while ZEN (zearalenone) reduces it by 2 to 61%. Since T-2 solubility in water is closer to ZEN (T-2 347 mg/L, ZEN 117 mg/L while DON—36,000 mg/L), a rather smaller reduction should be expected [23]. Reinholds et. al. [82] investigated the influence of ozone gas in reduction of the T-2 toxin contamination in malting wheat grains. When the processing time reached 130 min and the ozone concentration was 20 mg/L, the degradation rate of T-2 in malting grain extended up to 65%.

Probably the most efficient approach to reduce mycotoxins concentration is the use of adsorption powders. Olopade et al. [75] used differently modified montmorillonite clays as an adsorption agent mixed with T-2 contaminated maize, showing even six times T-2 concentration reduction within 4 weeks of storage at 30 °C. Similar results were achieved by Carson et. al. [83] with bentonite, but to efficiently reduce the T-2 toxin level, much more than 10 g/kg of bentonite must be used. New adsorbents based on tri-octahedral bentonites are very promising, absorbing a variety of mycotoxins reaching even 75% absorption rate versus ochratoxin A, but these have not yet been tested against T-2 toxin [84].

5.3. Biological Methods

The effect of treatment with lactic acid bacteria (LAB) on various mycotoxins contained in malting wheat grains was studied [85]. Analyses revealed that the presence of *Pediococcus pentosaceus* strains resulted in the greatest reduction of T-2. The concentration of T-2 toxin in malting wheat was decreased by 58%. The inhibition of T-2 and other mycotoxins probably resulted from toxins binding with LAB or from the detoxification of toxin with LAB. Nathanail et al. [76] showed that *Saccharomyces pastorianus* A15 lager yeast were able to reduce the mycotoxins levels in wort or to mitigate their effects by physical binding and/or conjugation. T-2 toxin reduction up to 31% was observed during the 96 h fermentation time. In different study [86], the detoxification properties of probiotic *Lactobacillus* sp. bacteria and *Saccharomyces cerevisiae* yeast toward various mycotoxins were investigated. After 24 h of incubation in the presence of *Lactobacillus* sp. strains, T-2 toxin concentration was reduced by 61% in relation to the initial quantity of toxin. Similarly, the concentration of the toxin after 24 h of incubation with *S. cerevisiae* strains was reduced by 61% of the initial concentration. Hassan and colleagues demonstrated that Bacillus spp. has significant T-2 toxin biodegrading capacity, leading to an 88% decontamination rate in substrates artificially contaminated with mycotoxin [87].

6. Conclusions

T-2 toxin is found in various regions worldwide and has adverse effects on both human and animal health. T-2 affects many organs and systems and exhibits the following characteristics: immunotoxicity, neurotoxicity, hepatotoxicity, nephrotoxicity, dermal toxicity, as well as disruption of the reproductive system. Currently, there is no specific therapy for T-2 toxin intoxication. Supportive measures such as superactivated charcoal administration if toxin was ingested is suggested. Different decontamination strategies have been found to mitigate the presence of T-2 toxin in agricultural products. There are physical, chemical, and biological methods, and depending on the technique used, the concentration of the toxin can be reduced by up to 90%. However, it may not be possible to completely prevent the formation of T-2 in agricultural commodities. Therefore, it is important to constantly monitor the level of contamination. Control and good agricultural practices in the pre-harvest, during, and post-harvest stages can significantly reduce T-2 contamination of agricultural commodities and cereal-based products. In the future, new or improved techniques of decontamination and degradation should be used to mitigate the concentration of T-2 in various agricultural commodities.

Author Contributions: Conceptualization, M.B., M.S., M.C. and M.N.; supervision, M.B.; writing—original draft preparation E.J., M.N. and M.P.; writing—review and editing, M.B., M.N. and M.S. All authors have read and agreed to the published version of the manuscript.

Funding: This paper has been supported by Polish Ministry of Science and Higher Education—593/STYP/13/2018.

Institutional Review Board Statement: Not applicable.

Informed Consent Statement: Not applicable.

Data Availability Statement: Not applicable.

Conflicts of Interest: The authors declare no conflict of interest.

References

1. Chen, P.; Xiang, B.; Shi, H.; Yu, P.; Song, Y.; Li, S. Recent advances on type A trichothecenes in food and feed: Analysis, prevalence, toxicity, and decontamination techniques. *Food Control* **2020**, *118*, 107371. [CrossRef]
2. Milićević, D.R.; Škrinjar, M.; Baltić, T. Real and Perceived Risks for Mycotoxin Contamination in Foods and Feeds: Challenges for Food Safety Control. *Toxins* **2010**, *2*, 572. [CrossRef] [PubMed]
3. McCormick, S.P.; Stanley, A.M.; Stover, N.A.; Alexander, N.J. Trichothecenes: From simple to complex mycotoxins. *Toxins* **2011**, *3*, 802–814. [CrossRef] [PubMed]
4. Foroud, N.A.; Baines, D.; Gagkaeva, T.Y.; Thakor, N.; Badea, A.; Steiner, B.; Bürstmayr, M.; Bürstmayr, H. Trichothecenes in Cereal Grains—An Update. *Toxins* **2019**, *11*, 634. [CrossRef]
5. Arunachalam, C.; Doohan, F.M. Trichothecene toxicity in eukaryotes: Cellular and molecular mechanisms in plants and animals. *Toxicol. Lett.* **2013**, *217*, 149–158. [CrossRef]
6. Nielsen, C.; Casteel, M.; Didier, A.; Dietrich, R.; Märtlbauer, E. Trichothecene-induced cytotoxicity on human cell lines. *Mycotoxin Res.* **2009**, *25*, 77–84. [CrossRef]
7. Polak-Śliwińska, M.; Paszczyk, B. Trichothecenes in Food and Feed, Relevance to Human and Animal Health and Methods of Detection: A Systematic Review. *Molecules* **2021**, *26*, 454. [CrossRef] [PubMed]
8. Cardoza, R.E.; Malmierca, M.G.; Hermosa, M.R.; Alexander, N.J.; McCormick, S.P.; Proctor, R.H.; Tijerino, A.M.; Rumbero, A.; Monte, E.; Gutiérrez, S. Identification of Loci and Functional Characterization of Trichothecene Biosynthesis Genes in Filamentous Fungi of the Genus *Trichoderma*. *Appl. Environ. Microbiol.* **2011**, *77*, 4867–4877. [CrossRef]
9. Proctor, R.H.; McCormick, S.P.; Kim, H.-S.; Cardoza, R.E.; Stanley, A.M.; Lindo, L.; Kelly, A.; Brown, D.W.; Lee, T.; Vaughan, M.M. Evolution of structural diversity of trichothecenes, a family of toxins produced by plant pathogenic and entomopathogenic fungi. *PLoS Pathog.* **2018**, *14*, e1006946. [CrossRef]
10. Foroud, N.A.; Shank, R.A.; Kiss, D.; Eudes, F.; Hazendonk, P. Solvent and Water Mediated Structural Variations in Deoxynivalenol and Their Potential Implications on the Disruption of Ribosomal Function. *Front. Microbiol.* **2016**, *7*, 1239. [CrossRef]
11. Garvey, G.S.; McCormick, S.P.; Rayment, I. Structural and Functional Characterization of the TRI101 Trichothecene 3-O-Acetyltransferase from *Fusarium sporotrichioides* and *Fusarium graminearum*: *Kinetic insights to combating fusarium head blight*. *J. Biol. Chem.* **2008**, *283*, 1660–1669. [CrossRef] [PubMed]
12. Pestka, J.J. Deoxynivalenol: Toxicity, mechanisms and animal health risks. *Anim. Feed. Sci. Technol.* **2007**, *137*, 283–298. [CrossRef]

13. Wan, Q.; Wu, G.; He, Q.; Tang, H.; Wang, Y. The toxicity of acute exposure to T-2 toxin evaluated by the metabonomics technique. *Mol. BioSystems* **2015**, *11*, 882–891. [CrossRef] [PubMed]
14. Nayakwadi, S.; Ramu, R.; Kumar Sharma, A.; Kumar Gupta, V.; Rajukumar, K.; Kumar, V.; Shirahatti, P.S.; Rashmi, L.; Basalingappa, K.M. Toxicopathological studies on the effects of T-2 mycotoxin and their interaction in juvenile goats. *PLoS ONE* **2020**, *15*, e0229463. [CrossRef]
15. Pinton, P.; Oswald, I.P. Effect of deoxynivalenol and other Type B trichothecenes on the intestine: A review. *Toxins* **2014**, *6*, 1615–1643. [CrossRef]
16. Lancova, K.; Hajslova, J.; Poustka, J.; Krplova, A.; Zachariasova, M.; Dostalek, P.; Sachambula, L. Transfer of Fusarium mycotoxins and 'masked' deoxynivalenol (deoxynivalenol-3-glucoside) from field barley through malt to beer. *Food Addit. Contam. Part A* **2008**, *25*, 732–744. [CrossRef] [PubMed]
17. Male, D.; Wu, W.; Mitchell, N.J.; Bursian, S.; Pestka, J.J.; Wu, F. Modeling the emetic potencies of food-borne trichothecenes by benchmark dose methodology. *Food Chem. Toxicol.* **2016**, *94*, 178–185. [CrossRef]
18. Pascari, X.; Maul, R.; Kemmlein, S.; Marin, S.; Sanchis, V. The fate of several trichothecenes and zearalenone during roasting and enzymatic treatment of cereal flour applied in cereal-based infant food production. *Food Control* **2020**, *114*, 107245. [CrossRef]
19. Cope, R.B. Chapter 75—Trichothecenes. In *Veterinary Toxicology*, 3rd ed.; Gupta, R.C., Ed.; Academic Press: Cambridge, MA, USA, 2018; pp. 1043–1053.
20. Rameshkumar, G.; Sikha, M.; Ponlakshmi, M.; Selva pandiyan, A.; Lalitha, P. A rare case of Myrothecium species causing mycotic keratitis: Diagnosis and management. *Med. Mycol. Case Rep.* **2019**, *25*, 53–55. [CrossRef]
21. He, J.; Zhou, T.; Young, J.C.; Boland, G.J.; Scott, P.M. Chemical and biological transformations for detoxification of trichothecene mycotoxins in human and animal food chains: A review. *Trends Food Sci. Technol.* **2010**, *21*, 67–76. [CrossRef]
22. Meneely, J.P.; Ricci, F.; van Egmond, H.P.; Elliott, C.T. Current methods of analysis for the determination of trichothecene mycotoxins in food. *TrAC Trends Anal. Chem.* **2011**, *30*, 192–203. [CrossRef]
23. Karlovsky, P.; Suman, M.; Berthiller, F.; De Meester, J.; Eisenbrand, G.; Perrin, I.; Oswald, I.P.; Speijers, G.; Chiodini, A.; Recker, T.; et al. Impact of food processing and detoxification treatments on mycotoxin contamination. *Mycotoxin Res.* **2016**, *32*, 179–205. [CrossRef]
24. Zhang, J.; You, L.; Wu, W.; Wang, X.; Chrienova, Z.; Nepovimova, E.; Wu, Q.; Kuca, K. The neurotoxicity of trichothecenes T-2 toxin and deoxynivalenol (DON): Current status and future perspectives. *Food Chem. Toxicol.* **2020**, *145*, 111676. [CrossRef] [PubMed]
25. European Food Safety Authority (EFSA); Arcella, D.; Gergelova, P.; Innocenti, M.L.; Steinkellner, H. Human and animal dietary exposure to T-2 and HT-2 toxin. *EFSA J.* **2017**, *15*, e04972. [PubMed]
26. Zouagui, Z.; Asrar, M.; Lakhdissi, H.; Abdennebi, E.H. Prevention of mycotoxin effects in dairy cows by adding an anti-mycotoxin product in feed. *J. Mater. Environ. Sci.* **2017**, *8*, 3766–3770.
27. Cano-Sancho, G.; Valle-Algarra, F.M.; Jiménez, M.; Burdaspal, P.; Legarda, T.M.; Ramos, A.J.; Sanchis, V.; Marín, S. Presence of trichothecenes and co-occurrence in cereal-based food from Catalonia (Spain). *Food Control* **2011**, *22*, 490–495. [CrossRef]
28. Rosa Seus Arraché, E.; Fontes, M.R.V.; Garda Buffon, J.; Badiale-Furlong, E. Trichothecenes in wheat: Methodology, occurrence and human exposure risk. *J. Cereal Sci.* **2018**, *82*, 129–137. [CrossRef]
29. Li, Y.; Wang, Z.; Beier, R.C.; Shen, J.; Smet, D.D.; De Saeger, S.; Zhang, S. T-2 Toxin, a Trichothecene Mycotoxin: Review of Toxicity, Metabolism, and Analytical Methods. *J. Agric. Food Chem.* **2011**, *59*, 3441–3453. [CrossRef]
30. Moss, M.O. Mycotoxin review–2. Fusarium. *Mycologist* **2002**, *16*, 158–161. [CrossRef]
31. Nazari, L.; Pattori, E.; Terzi, V.; Morcia, C.; Rossi, V. Influence of temperature on infection, growth, and mycotoxin production by Fusarium langsethiae and F. sporotrichioides in durum wheat. *Food Microbiol.* **2014**, *39*, 19–26. [CrossRef]
32. Nathanail, A.V.; Varga, E.; Meng-Reiterer, J.; Bueschl, C.; Michlmayr, H.; Malachova, A.; Fruhmann, P.; Jestoi, M.; Peltonen, K.; Adam, G.; et al. Metabolism of the Fusarium Mycotoxins T-2 Toxin and HT-2 Toxin in Wheat. *J. Agric. Food Chem.* **2015**, *63*, 7862–7872. [CrossRef]
33. Edwards, S.G.; Imathiu, S.M.; Ray, R.V.; Back, M.; Hare, M.C. Molecular studies to identify the Fusarium species responsible for HT-2 and T-2 mycotoxins in UK oats. *Int. J. Food Microbiol.* **2012**, *156*, 168–175. [CrossRef]
34. Lippolis, V.; Pascale, M.; Maragos, C.M.; Visconti, A. Improvement of detection sensitivity of T-2 and HT-2 toxins using different fluorescent labeling reagents by high-performance liquid chromatography. *Talanta* **2008**, *74*, 1476–1483. [CrossRef] [PubMed]
35. Kiš, M.; Vulić, A.; Kudumija, N.; Šarkanj, B.; Jaki Tkalec, V.; Aladić, K.; Škrivanko, M.; Furmeg, S.; Pleadin, J. A Two-Year Occurrence of Fusarium T-2 and HT-2 Toxin in Croatian Cereals Relative of the Regional Weather. *Toxins* **2021**, *13*, 39. [CrossRef]
36. Medina, A.; Magan, N. Temperature and water activity effects on production of T-2 and HT-2 by Fusarium langsethiae strains from north European countries. *Food Microbiol.* **2011**, *28*, 392–398. [CrossRef]
37. Garai, E.; Risa, A.; Varga, E.; Cserháti, M.; Kriszt, B.; Urbányi, B.; Csenki, Z. Qualifying the T-2 Toxin-Degrading Properties of Seven Microbes with Zebrafish Embryo Microinjection Method. *Toxins* **2020**, *12*, 460. [CrossRef]
38. Makowska, K.; Obremski, K.; Gonkowski, S. The Impact of T-2 Toxin on Vasoactive Intestinal Polypeptide-Like Immunoreactive (VIP-LI) Nerve Structures in the Wall of the Porcine Stomach and Duodenum. *Toxins* **2018**, *10*, 138. [CrossRef]
39. Königs, M.; Mulac, D.; Schwerdt, G.; Gekle, M.; Humpf, H.-U. Metabolism and cytotoxic effects of T-2 toxin and its metabolites on human cells in primary culture. *Toxicology* **2009**, *258*, 106–115. [CrossRef] [PubMed]

40. Yagen, B.; Joffe, A.Z. Screeing of toxic isolates of Fusarium poae and Fusarium sporotrichiodes involved in causing alimentary toxic aleukia. *Appl. Environ. Microbiol.* **1976**, *32*, 423–427. [CrossRef] [PubMed]
41. Sokolović, M.; Garaj-Vrhovac, V.; Šimpraga, B. T-2 toxin: Incidence and toxicity in poultry. *Arhiv za Higijenu Rada i Toksikologiju* **2008**, *59*, 43–52. [CrossRef]
42. Wannemacher, R.W.; Wiener, S.L.; Sidell, F.R.; Takafuji, E.T.; Franz, D.R. Trichothecene mycotoxins. *Med. Asp. Chem. Biol. Warf.* **1997**, *6*, 655–676.
43. Yang, S.; Li, Y.; Cao, X.; Hu, D.; Wang, Z.; Wang, Y.; Shen, J.; Zhang, S. Metabolic Pathways of T-2 Toxin in in Vivo and in Vitro Systems of Wistar Rats. *J. Agric. Food Chem.* **2013**, *61*, 9734–9743. [CrossRef] [PubMed]
44. Kuca, K.; Dohnal, V.; Jezkova, A.; Jun, D. Metabolic pathways of T-2 toxin. *Curr. Drug Metab.* **2008**, *9*, 77–82. [CrossRef] [PubMed]
45. Mackei, M.; Orbán, K.; Molnár, A.; Pál, L.; Dublecz, K.; Husvéth, F.; Neogrády, Z.; Mátis, G. Cellular Effects of T-2 Toxin on Primary Hepatic Cell Culture Models of Chickens. *Toxins* **2020**, *12*, 46. [CrossRef]
46. EFSA Panel on Contaminants in the Food Chain (CONTAM). Scientific Opinion on the risks for animal and public health related to the presence of T-2 and HT-2 toxin in food and feed. *EFSA J.* **2011**, *9*, 2481. [CrossRef]
47. Yang, S.; De Boevre, M.; Zhang, H.; De Ruyck, K.; Sun, F.; Zhang, J.; Jin, Y.; Li, Y.; Wang, Z.; Zhang, S.; et al. Metabolism of T-2 Toxin in Farm Animals and Human In Vitro and in Chickens In Vivo Using Ultra High-Performance Liquid Chromatography-Quadrupole/Time-of-Flight Hybrid Mass Spectrometry Along with Online Hydrogen/Deuterium Exchange Technique. *J. Agric. Food Chem.* **2017**, *65*, 7217–7227. [CrossRef]
48. Escrivá, L.; Font, G.; Manyes, L. In vivo toxicity studies of fusarium mycotoxins in the last decade: A review. *Food Chem. Toxicol.* **2015**, *78*, 185–206. [CrossRef]
49. Rai, R.B.; Rahman, S.; Dixit, H.; Rai, S.; Singh, B.; Kumar, H.; Damodaran, T.; Dhama, K. Analysis of feed ingredients for Afla and T-2 mycotoxins by ELISA in rural areas of Uttar Pradesh. *Indian J. Vet. Pathol.* **2011**, *35*, 238–240.
50. Adhikari, M.; Negi, B.; Kaushik, N.; Adhikari, A.; Al-Khedhairy, A.A.; Kaushik, N.K.; Choi, E.H. T-2 mycotoxin: Toxicological effects and decontamination strategies. *Oncotarget* **2017**, *8*, 33933–33952. [CrossRef]
51. Sudakin, D.L. Trichothecenes in the environment: Relevance to human health. *Toxicol. Lett.* **2003**, *143*, 97–107. [CrossRef]
52. Ueno, Y. Toxicological features of T-2 toxin and related trichothecenes. *Fundam. Appl. Toxicol.* **1984**, *4*, S124–S132. [CrossRef]
53. Wu, Q.-H.; Wang, X.; Yang, W.; Nüssler, A.K.; Xiong, L.-Y.; Kuča, K.; Dohnal, V.; Zhang, X.-J.; Yuan, Z.-H. Oxidative stress-mediated cytotoxicity and metabolism of T-2 toxin and deoxynivalenol in animals and humans: An update. *Arch. Toxicol.* **2014**, *88*, 1309–1326. [CrossRef] [PubMed]
54. Ihara, T.; Sugamata, M.; Sekijima, M.; Okumura, H.; Yoshino, N.; Ueno, Y. Apoptotic cellular damage in mice after T-2 toxin-induced acute toxicosis. *Nat. Toxins* **1997**, *5*, 141–145. [CrossRef] [PubMed]
55. Yin, H.; Han, S.; Chen, Y.; Wang, Y.; Li, D.; Zhu, Q. T-2 Toxin Induces Oxidative Stress, Apoptosis and Cytoprotective Autophagy in Chicken Hepatocytes. *Toxins* **2020**, *12*, 90. [CrossRef]
56. Shinozuka, J.; Miwa, S.; Fujimura, H.; Toriumi, W.; Doi, K. Hepatotoxicity of T-2 toxin, trichothecene mycotoxin. *Mycotoxins* **2006**, *2006*, 62–66. [CrossRef]
57. Rahman, S.; Sharma, A.K.; Singh, N.D.; Prawez, S. Immunopathological effects of experimental T-2 mycotoxicosis in Wistar rats. *Hum. Exp. Toxicol.* **2020**, *40*, 772–790. [CrossRef]
58. Minervini, F.; Fornelli, F.; Lucivero, G.; Romano, C.; Visconti, A. T-2 toxin immunotoxicity on human B and T lymphoid cell lines. *Toxicology* **2005**, *210*, 81–91. [CrossRef] [PubMed]
59. Hymery, N.; Léon, K.; Carpentier, F.G.; Jung, J.L.; Parent-Massin, D. T-2 toxin inhibits the differentiation of human monocytes into dendritic cells and macrophages. *Toxicol. In Vitro* **2009**, *23*, 509–519. [CrossRef]
60. Seeboth, J.; Solinhac, R.; Oswald, I.P.; Guzylack-Piriou, L. The fungal T-2 toxin alters the activation of primary macrophages induced by TLR-agonists resulting in a decrease of the inflammatory response in the pig. *Vet. Res.* **2012**, *43*, 35. [CrossRef]
61. Agrawal, M.; Bhaskar, A.S.B.; Rao, P.V.L. Involvement of Mitogen-Activated Protein Kinase Pathway in T-2 Toxin-Induced Cell Cycle Alteration and Apoptosis in Human Neuroblastoma Cells. *Mol. Neurobiol.* **2015**, *51*, 1379–1394. [CrossRef]
62. Zhang, X.; Wang, Y.; Velkov, T.; Tang, S.; Dai, C. T-2 toxin-induced toxicity in neuroblastoma-2a cells involves the generation of reactive oxygen, mitochondrial dysfunction and inhibition of Nrf2/HO-1 pathway. *Food Chem. Toxicol.* **2018**, *114*, 88–97. [CrossRef]
63. Weidner, M.; Lenczyk, M.; Schwerdt, G.; Gekle, M.; Humpf, H.-U. Neurotoxic Potential and Cellular Uptake of T-2 Toxin in Human Astrocytes in Primary Culture. *Chem. Res. Toxicol.* **2013**, *26*, 347–355. [CrossRef]
64. Guo, P.; Liu, A.; Huang, D.; Wu, Q.; Fatima, Z.; Tao, Y.; Cheng, G.; Wang, X.; Yuan, Z. Brain damage and neurological symptoms induced by T-2 toxin in rat brain. *Toxicol. Lett.* **2018**, *286*, 96–107. [CrossRef] [PubMed]
65. Gaigé, S.; Djelloul, M.; Tardivel, C.; Airault, C.; Félix, B.; Jean, A.; Lebrun, B.; Troadec, J.-D.; Dallaporta, M. Modification of energy balance induced by the food contaminant T-2 toxin: A multimodal gut-to-brain connection. *Brain Behav. Immun.* **2014**, *37*, 54–72. [CrossRef] [PubMed]
66. Yang, J.Y.; Zhang, Y.F.; Liang, A.M.; Kong, X.F.; Li, Y.X.; Ma, K.W.; Jing, A.H.; Feng, S.Y.; Qiao, X.L. Toxic effects of T-2 toxin on reproductive system in male mice. *Toxicol. Ind. Health* **2009**, *26*, 25–31. [CrossRef] [PubMed]
67. Yang, X.; Zhang, X.; Zhang, J.; Ji, Q.; Huang, W.; Zhang, X.; Li, Y. Spermatogenesis disorder caused by T-2 toxin is associated with germ cell apoptosis mediated by oxidative stress. *Environ. Pollut.* **2019**, *251*, 372–379. [CrossRef]

68. Shen, J.; Perveen, A.; Kaka, N.; Li, Z.; Dai, P.; Li, C. Maternal Exposure to T-2 Toxin Induces Changes in Antioxidant System and Testosterone Synthesis in the Testes of Mice Offspring. *Animals* **2019**, *10*, 74. [CrossRef]
69. Perveen, A.; Shen, J.; Ali Kaka, N.; Li, C. Maternal Exposure to T-2 Toxin Affects Puberty Genes and Delays Estrus Cycle in Mice Offspring. *Animals* **2020**, *10*, 471. [CrossRef] [PubMed]
70. Caloni, F.; Ranzenigo, G.; Cremonesi, F.; Spicer, L.J. Effects of a trichothecene, T-2 toxin, on proliferation and steroid production by porcine granulosa cells. *Toxicon* **2009**, *54*, 337–344. [CrossRef] [PubMed]
71. Hemmati, A.A.; Kalantari, H.; Jalali, A.; Rezai, S.; Zadeh, H.H. Healing effect of quince seed mucilage on T-2 toxin-induced dermal toxicity in rabbit. *Exp. Toxicol. Pathol.* **2012**, *64*, 181–186. [CrossRef] [PubMed]
72. Pang, V.F.; Swanson, S.P.; Beasley, V.R.; Buck, W.B.; Haschek, W.M. The toxicity of T-2 toxin in swine following topical application: I. Clinical signs, pathology, and residue concentrations. *Fundam. Appl. Toxicol.* **1987**, *9*, 41–49. [CrossRef]
73. Agrawal, M.; Yadav, P.; Lomash, V.; Bhaskar, A.S.B.; Lakshmana Rao, P.V. T-2 toxin induced skin inflammation and cutaneous injury in mice. *Toxicology* **2012**, *302*, 255–265. [CrossRef] [PubMed]
74. Shi, H.; Li, S.; Bai, Y.; Louzada Prates, L.; Lei, Y.; Yu, P. Mycotoxin contamination of food and feed in China: Occurrence, detection techniques, toxicological effects and advances in mitigation technologies. *Food Control* **2018**, *91*, 202–215. [CrossRef]
75. Olopade, B.K.; Oranusi, S.U.; Nwinyi, O.C.; Lawal, I.A.; Gbashi, S.; Njobeh, P.B. Decontamination of T-2 Toxin in Maize by Modified Montmorillonite Clay. *Toxins* **2019**, *11*, 616. [CrossRef]
76. Nathanail, A.V.; Gibson, B.; Han, L.; Peltonen, K.; Ollilainen, V.; Jestoi, M.; Laitila, A. The lager yeast Saccharomyces pastorianus removes and transforms Fusarium trichothecene mycotoxins during fermentation of brewer's wort. *Food Chem.* **2016**, *203*, 448–455. [CrossRef]
77. De Angelis, E.; Monaci, L.; Pascale, M.; Visconti, A. Fate of deoxynivalenol, T-2 and HT-2 toxins and their glucoside conjugates from flour to bread: An investigation by high-performance liquid chromatography high-resolution mass spectrometry. *Food Addit. Contam. Part A Chem. Anal. Control Expo. Risk Assess.* **2012**, *30*, 345–355. [CrossRef] [PubMed]
78. Kuchenbuch, H.; Becker, S.; Schulz, M.; Cramer, B.; Humpf, H.-U. Thermal stability of T-2 and HT-2 toxins during biscuit- and crunchy muesli-making and roasting. *Food Addit. Contam. Part A Chem. Anal. Control Expo. Risk Assess.* **2018**, *35*, 2158–2167. [CrossRef]
79. Wei, J.-T.; Wu, K.-T.; Sun, H.; Khalil, M.M.; Dai, J.-F.; Liu, Y.; Liu, Q.; Zhang, N.-Y.; Qi, D.-S.; Sun, L.-H. A Novel Modified Hydrated Sodium Calcium Aluminosilicate (HSCAS) Adsorbent Can Effectively Reduce T-2 Toxin-Induced Toxicity in Growth Performance, Nutrient Digestibility, Serum Biochemistry, and Small Intestinal Morphology in Chicks. *Toxins* **2019**, *11*, 199. [CrossRef]
80. Čolović, R.; Puvača, N.; Cheli, F.; Avantaggiato, G.; Greco, D.; Đuragić, O.; Kos, J.; Pinotti, L. Decontamination of Mycotoxin-Contaminated Feedstuffs and Compound Feed. *Toxins* **2019**, *11*, 617. [CrossRef]
81. Luo, Y.; Liu, X.; Li, J. Updating techniques on controlling mycotoxins—A review. *Food Control* **2018**, *89*, 123–132. [CrossRef]
82. Reinholds, I.; Gražina, J.; Bartkiene, E.; Zadeike, D.; Bartkevics, V.; Lele, V.; Cernauskas, D.; Cizeikiene, D. Evaluation of ozonation as a method for mycotoxins degradation in malting wheat grains. *World Mycotoxin J.* **2016**, *9*, 1–10. [CrossRef]
83. Carson, M.S.; Smith, T.K. Role of bentonite in prevention of T-2 toxicosis in rats. *J. Anim. Sci.* **1983**, *57*, 1498–1506. [CrossRef]
84. Vila-Donat, P.; Marín, S.; Sanchis, V.; Ramos, A.J. New mycotoxin adsorbents based on tri-octahedral bentonites for animal feed. *Anim. Feed Sci. Technol.* **2019**, *255*, 114228. [CrossRef]
85. Juodeikiene, G.; Bartkiene, E.; Cernauskas, D.; Cizeikiene, D.; Zadeike, D.; Lele, V.; Bartkevics, V. Antifungal activity of lactic acid bacteria and their application for Fusarium mycotoxin reduction in malting wheat grains. *LWT* **2018**, *89*, 307–314. [CrossRef]
86. Chlebicz, A.; Śliżewska, K. In Vitro Detoxification of Aflatoxin B(1), Deoxynivalenol, Fumonisins, T-2 Toxin and Zearalenone by Probiotic Bacteria from Genus *Lactobacillus* and *Saccharomyces cerevisiae* Yeast. *Probiotics Antimicrob. Proteins* **2020**, *12*, 289–301. [CrossRef] [PubMed]
87. Hassan, Z.U.; Al Thani, R.; Alsafran, M.; Migheli, Q.; Jaoua, S. Selection of *Bacillus* spp. with decontamination potential on multiple *Fusarium* mycotoxins. *Food Control* **2021**, *127*, 108119. [CrossRef]

International Journal of
Molecular Sciences

MDPI

Article

Direct T-2 Toxicity on Human Skin—Fibroblast Hs68 Cell Line—In Vitro Study

Edyta Janik-Karpinska [1], Michal Ceremuga [2], Magdalena Wieckowska [1], Monika Szyposzynska [3], Marcin Niemcewicz [1], Ewelina Synowiec [4], Tomasz Sliwinski [4] and Michal Bijak [1,*]

[1] Biohazard Prevention Centre, Faculty of Biology and Environmental Protection, University of Lodz, Pomorska 141/143, 90-236 Lodz, Poland; edyta.janik.karpinska@edu.uni.lodz.pl (E.J.-K.); magdalena.wieckowska@edu.uni.lodz.pl (M.W.); marcin.niemcewicz@biol.uni.lodz.pl (M.N.)
[2] Military Institute of Armament Technology, Prymasa Stefana Wyszyńskiego 7, 05-220 Zielonka, Poland; ceremugam@witu.mil.pl
[3] CBRN Reconnaissance and Decontamination Department, Military Institute of Chemistry and Radiometry, Antoniego Chrusciela "Montera" 105, 00-910 Warsaw, Poland; m.szyposzynska@wichir.waw.pl
[4] Laboratory of Medical Genetics, Faculty of Biology and Environmental Protection, University of Lodz, Pomorska 141/143, 90-236 Lodz, Poland; ewelina.synowiec@biol.uni.lodz.pl (E.S.); tomasz.sliwinski@biol.uni.lodz.pl (T.S.)
* Correspondence: michal.bijak@biol.uni.lodz.pl

Abstract: T-2 toxin is produced by different *Fusarium* species, and it can infect crops such as wheat, barley, and corn. It is known that the T-2 toxin induces various forms of toxicity such as hepatotoxicity, nephrotoxicity, immunotoxicity, and neurotoxicity. In addition, T-2 toxin possesses a strong dermal irritation effect and can be absorbed even through intact skin. As a dermal irritant agent, it is estimated to be 400 times more toxic than sulfur mustard. Toxic effects can include redness, blistering, and necrosis, but the molecular mechanism of these effects still remains unknown. This in vitro study focused on the direct toxicity of T-2 toxin on human skin—fibroblast Hs68 cell line. As a result, the level of toxicity of T-2 toxin and its cytotoxic mechanism of action was determined. In cytotoxicity assays, the dose and time-dependent cytotoxic effect of T-2 on a cell line was observed. Bioluminometry results showed that relative levels of ATP in treated cells were decreased. Further analysis of the toxin's impact on the induction of apoptosis and necrosis processes showed the significant predominance of PI-stained cells, lack of caspase 3/7 activity, and increased concentration of released Human Cytokeratin 18 in treated cells, which indicates the necrosis process. In conclusion, the results of an in vitro human skin fibroblast model revealed for the first time that the T-2 toxin induces necrosis as a toxicity effect. These results provide new insight into the toxic T-2 mechanism on the skin.

Keywords: T-2 toxin; skin; Hs68 cell line; cytotoxicity; necrosis

Citation: Janik-Karpinska, E.; Ceremuga, M.; Wieckowska, M.; Szyposzynska, M.; Niemcewicz, M.; Synowiec, E.; Sliwinski, T.; Bijak, M. Direct T-2 Toxicity on Human Skin—Fibroblast Hs68 Cell Line—In Vitro Study. *Int. J. Mol. Sci.* **2022**, *23*, 4929. https://doi.org/10.3390/ijms23094929

Academic Editor: Guido R.M.M. Haenen

Received: 31 March 2022
Accepted: 26 April 2022
Published: 29 April 2022

1. Introduction

T-2 toxin (Figure 1)—((1R,9R,10R,11S,12R)-11-acetyloxy-2-(acetyloxymethyl)-10-hydroxy-1,5-dimethylspiro(8-oxatricyclo(7.2.1.02,7])dodec-5-ene-12,2'-oxirane)-4-yl)-3-methylbutanoate (according the IUPAC nomenclature)—is the most toxic member of the fungal secondary metabolite belonging to the type A trichothecenes [1]. Trichothecenes are tetracyclic sesquiterpene compounds that consist of a trichothecene core with epoxy rings at the C-12 and -13 positions. This ring is responsible for toxicological activity. Trichothecenes are classified based on the carbonyl group at the 8-position, macrolide rings at the 4- and 5-positions, and the number of epoxy rings. Trichothecene-producing genera include *Fusarium*, *Myrothecium*, *Spicellum*, *Stachybotrys*, *Cephalosporium*, *Trichoderma*, and *Trichothecium* [2,3].

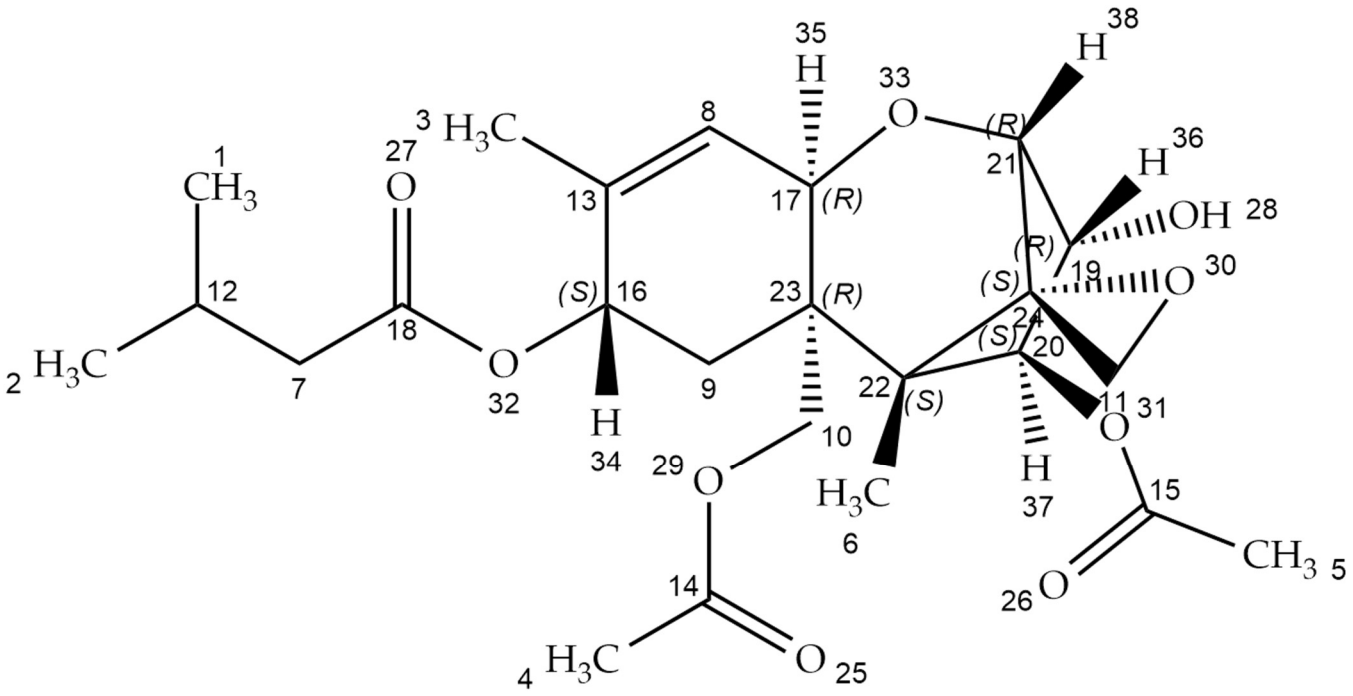

Figure 1. T-2 toxin chemical structure (structure generated from InChI code. Available online: https://pubchem.ncbi.nlm.nih.gov/ (accessed on 21 April 2022)).

The T-2 toxin is produced mainly by *Fusarium* species (*F. poae*, *F. sporotrichioides*, *F. tricinctum*) and is a major crop and fodder pollutant. It can infect corn, barley, and wheat, both in the field and in wet storage conditions. Consumption of mycotoxin-contaminated cereal-based food and feed is a potential hazard for human and animal health [4]. The conditions which are optimal for enhancing toxin production are: substrate humidity (10–20%), relative humidity (≥70%), temperature (0 to 50 °C, depending on the fungus species), and oxygen availability [5].

The T-2 toxin has a low molecular weight of about 466.51 Da. It is also nonvolatile, insoluble in water, and highly resistant to degradation in different environmental conditions such as heat and UV light. It generates problems with toxin deactivation, however, the decontamination process is effective in strong acid or alkaline conditions [6]. The chemical structure of T-2 is characterized by the hydroxyl (OH) group at the C-3 position, acetyloxy (-$OCOCH_3$) groups at the C-4 and C-15 positions, an atom of hydrogen at the C-7 position, and an ester-linked isovaleryl ($OCOCH_2CH(CH_3)_2$) group at the C-8 position. The presence of hydroxyl groups, the structure, and the side-chain position affect the T-2 toxin's biological activity [7,8].

The T-2 toxin is readily absorbed by various modes, including topical, oral, and inhalational routes. Unlike most typical biotoxins that do not affect the skin, T-2 is a potent, strong skin irritant and can be absorbed through intact skin causing systemic toxicity. As a blistering and dermal irritant agent, it is supposed to be 400 times more intoxicating than sulfur mustard (mustard gas, yperite), which is a chemical warfare agent [7]. In addition, the toxicity of the T-2 toxin by inhalation route is similar to that observed in mustards or lewisite. Therefore, the T-2 toxin's properties are more similar to chemical agents than biological toxins. Dermal irritating properties of the T-2 toxin have been studied in different experimental animal models, e.g., rats [9], rabbits [10], guinea pigs [11], and cynomolgus monkeys [12]. In the case of poultry, dermatoxic effects are characterized as fatal ulceration or necrohemorrhagic dermatitis. Some animals exhibit comb cyanosis and depigmentation of the leg skin [13]. Agrawal et al. showed that in the mice model, T-2-mycotoxin-induced skin inflammation and cutaneous injuries occur [14].

In the late 1940s, scientists in the Soviet Union coined the term stachybotryotoxicosis to characterize an acute syndrome involving pharyngitis, bloody rhinorrhea, dyspnea, tussis, and fever resulting from mycotoxin inhalation. Alimentary toxic aleukia (ATA), a disease responsible for the losses of thousands of Soviet Union civilians during World War II, was caused by consumption of wheat that was unintentionally contaminated with *Fusarium* fungi. The victims developed a protracted lethal illness with a disease pattern similar to ATA [15].

Based on extensive eyewitness and victim accounts, it had been established that the T-2 toxin was used during the military conflicts in Laos, Cambodia, and Afghanistan from 1975 to 1981. The aerosolized form of the T-2 toxin was delivered by low-flying aircraft in the form of yellow oily droplets. Witnesses called the event "yellow rain" due to sticky, yellow drops of liquid that sounded similar to rain as they fell to the ground. It is estimated that exposure to "yellow rain" caused more than 6300 death in Laos, 3000 in Afghanistan, and 1000 in Cambodia [16,17]. The first symptoms appeared after a few minutes to an hour and included skin burning pain, tenderness, redness, and blistering. In fatal cases, progression of skin necrosis with leathery blackening and sloughing of large areas of skin occurred. Nasal contact was manifested by sneezing, pain, epistaxis, and rhinorrhea. Nausea, vomiting, diarrhea, and abdominal pain occurred in gastrointestinal toxicity. Systemic toxicity was manifested by weakness, ataxia, and loss of coordination. Additionally, in lethal cases, hypothermia, tachycardia, and hypotension were reported. Death occurred after a few minutes, hours, or days [18].

For this reason, it was decided to perform a study aimed at the direct toxicity action of the T-2 toxin on a cellular model of human skin—fibroblast cell line Hs68. The level of toxicity of the T-2 toxin as well as its cytotoxic mechanism of action were determined.

2. Results

2.1. Cell Viability

The cytotoxic effect of the T-2 toxin was evaluated in a normal human fibroblast cell line (Hs68) by two independent methods (trypan blue and MTT) which are based on different biochemical mechanisms. During the cytotoxicity assays for both methods, the dose-dependent cytotoxic effect of the T-2 toxin in the tested cell line was observed. Additionally, the cytotoxic effect was higher after 48 h of exposure in comparison to 24 h of time. The results in the form of cytotoxicity curves are presented in Figure 1.

Using an online tool (https://www.aatbio.com/tools/ec50-calculator (accessed on 21 April 2022))—Quest Graph™ EC50 Calculator—AAT Bioquest (Sunnyvale, CA, USA)—the T-2 toxin effective concentration 50 (EC50) parameters for the Hs68 cell line were obtained. The calculated values for the trypan blue method (Figure 2A) were 22.71 µM for 24 h of treatment and 7.81 µM for 48 h of treatment. The calculated results for the MTT test (Figure 2B) were 25.98 µM for 24 h of treatment and 10.35 µM for 48 h of treatment.

2.2. Cellular ATP Level

Measurement of the level of ATP is the most sensitive, reliable, and convenient method for monitoring active cell metabolism. Using the bioluminometry method, the relative level of ATP in Hs68 cell suspension was determined. The treatment of the cell line resulted in a dose-dependent and time-dependent decrease in the level of luminescence, which directly corresponded to the ATP level in the sample (Figure 3).

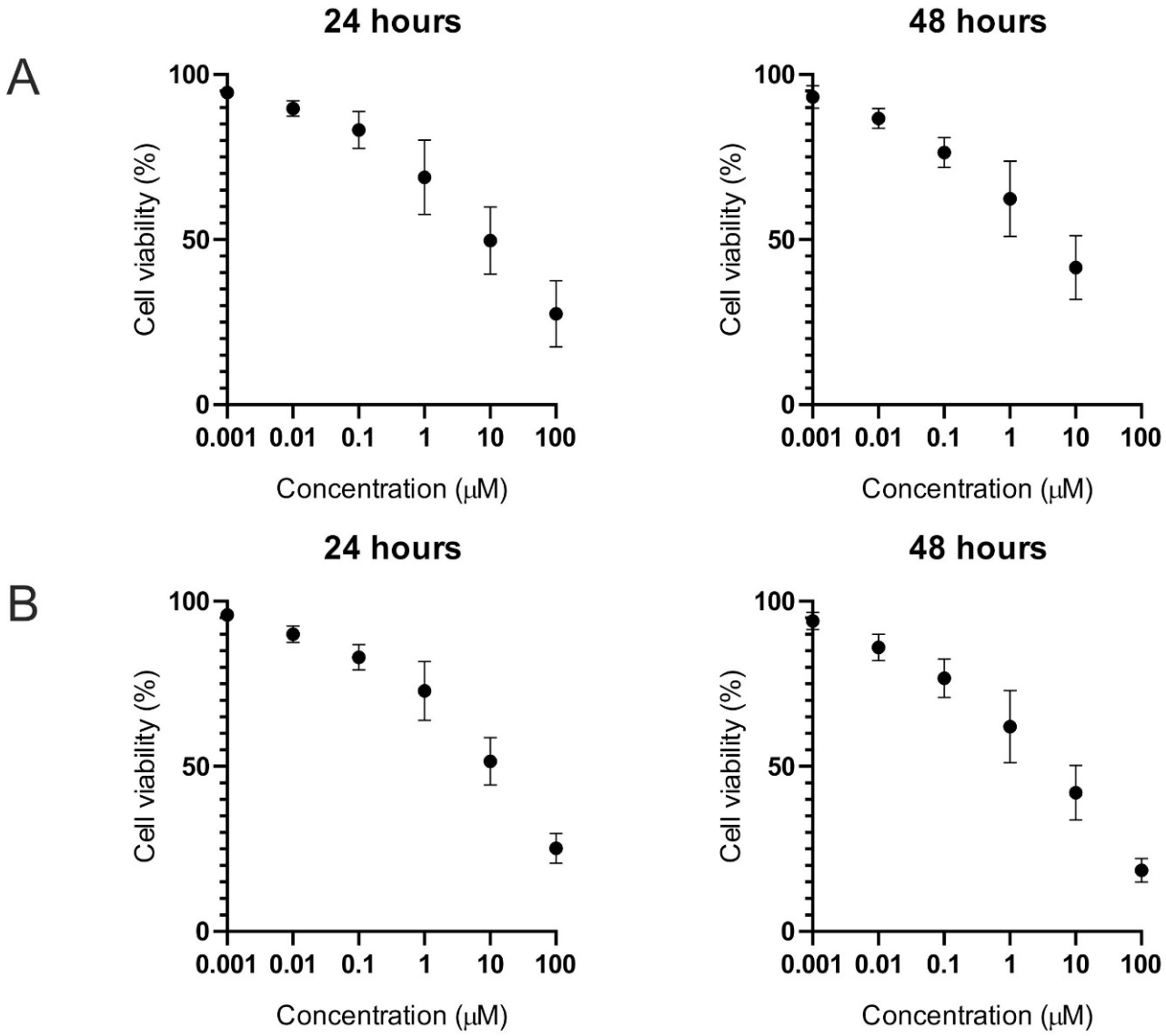

Figure 2. The T-2 toxin's effect (in a concentration range from 0.001 to 100 μM) on Hs68 cell viability. Cell viability was estimated by using trypan blue (**A**) and MTT (**B**) methods. The data represent cell viability curves obtained from six independent measurements (n = 6).

2.3. Apoptosis and Necrosis

2.3.1. Annexin V and Propidium Iodide Staining

It was observed, using the double-staining flow cytometry method, that incubation of a normal human fibroblast cell line (Hs68) with T-2 mycotoxin resulted in both a dose-and time-dependent increase in propidium iodide (PI) fluorescence. It was related to the cells' necrosis process. In Figure 3, the results obtained during this analysis are presented. In the highest tested concentration of toxin—100 μM—the % of PI-stained cells was 79% after 24 h of incubation and 93% after 48 h of incubation (Figure 4A). In all samples, any significant increase of annexin V fluorescence related to the apoptosis process in cells (Figure 4B) was not observed.

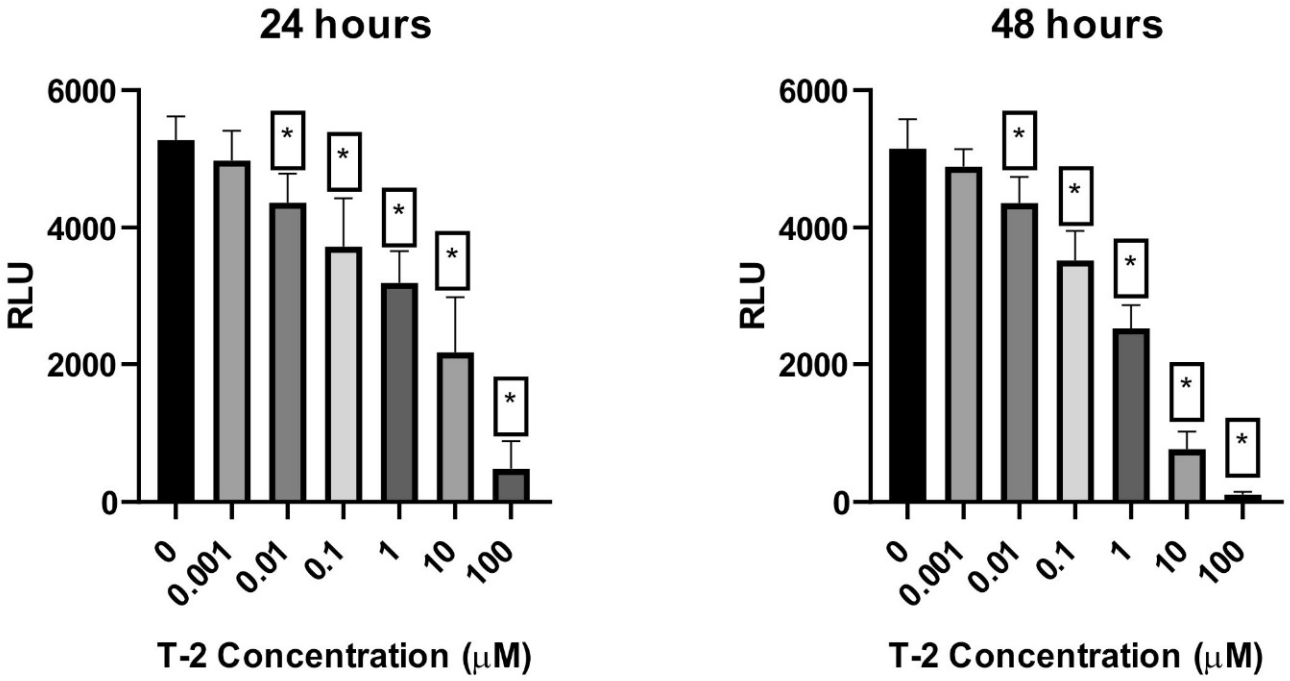

Figure 3. The T-2 toxin effect on the necrosis of ATP-level Hs68 cells estimated by the bioluminometry method. Values: means ± SD (n = 6). * $p < 0.001$. 0: untreated (control) cells; 0.001: concentration of toxin—0.001 μM; 0.01: concentration of toxin—0.01 μM; 0.1: concentration of toxin—0.1 μM; 1: concentration of toxin—1 μM; 10: concentration of toxin—10 μM; 100: concentration of toxin—100 μM.

2.3.2. Caspase-3/7 Pathway

In the next step of the study, the verification of the T-2 toxin's ability to activate the caspase-3/7 pathway in human fibroblast cells was performed. During the fluorescence-based caspase activity estimation, it was observed that T-2 treatment of human fibroblast cells did not induce any changes in 590 nm fluorescence (Figure 5), which clearly indicated the absence of caspase 3/7 proteolytic activity in these cells.

2.3.3. Cytokeratin 18 Concentration

To confirm the activation of the necrotic pathway by the T-2 toxin in Hs68 cells, the analysis focused on examining full-length Human Cytokeratin 18 (CK18) concentration in cell culture supernatants was performed. The cell line treatment resulted in dose and time-dependent increased concentration of released Human CK18 (Figure 6). Additionally, in all tested concentrations of T-2 toxin, statistical significance ($p < 0.001$) of differences in comparison to the control sample was observed.

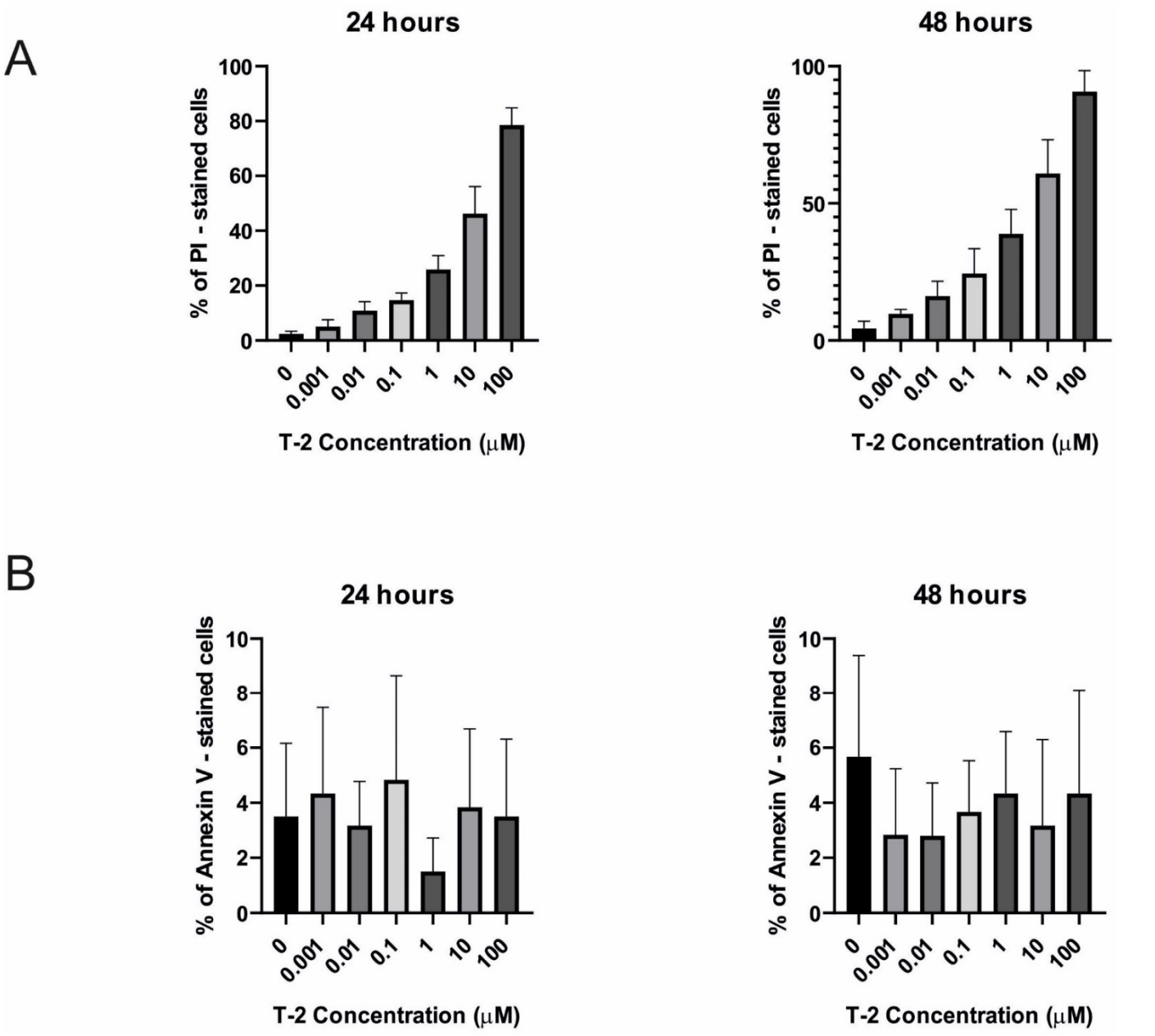

Figure 4. The T-2 effect on necrosis and apoptosis induction in Hs68 cells. The cell death pathway was assayed by flow cytometry with annexin V/propidium iodide staining after 24 h (**A**) and 48 h (**B**) of incubation with the toxin. Values: means ± SD (n = 6). 0: untreated (control) cells; 0.001: concentration of toxin—0.001 μM; 0.01: concentration of toxin—0.01 μM; 0.1: concentration of toxin—0.1 μM; 1: concentration of toxin—1 μM; 10: concentration of toxin—10 μM; 100: concentration of toxin—100 μM.

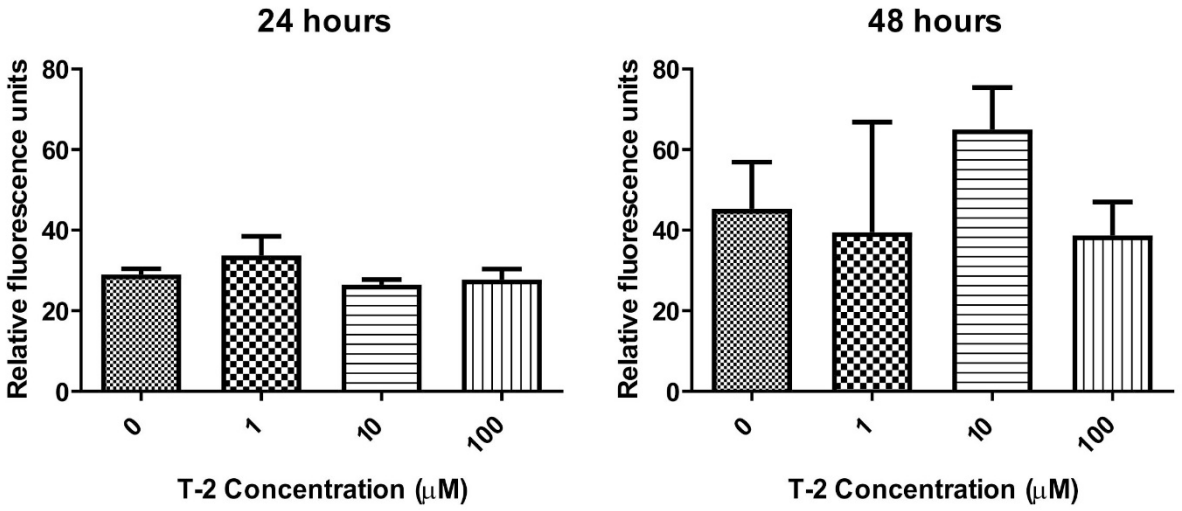

Figure 5. The T-2 effect on the caspase 3/7 pathway activation in Hs68 cells. Caspases' proteolytic activity was measured by fluorescence of 485 nm/538 nm after 24 h and 48 h incubation with the toxin, respectively. Values means ± SD (n = 6). 0: untreated (control) cells; 1: concentration of toxin—1 μM; 10: concentration of toxin—10 μM; 100: concentration of toxin—100 μM.

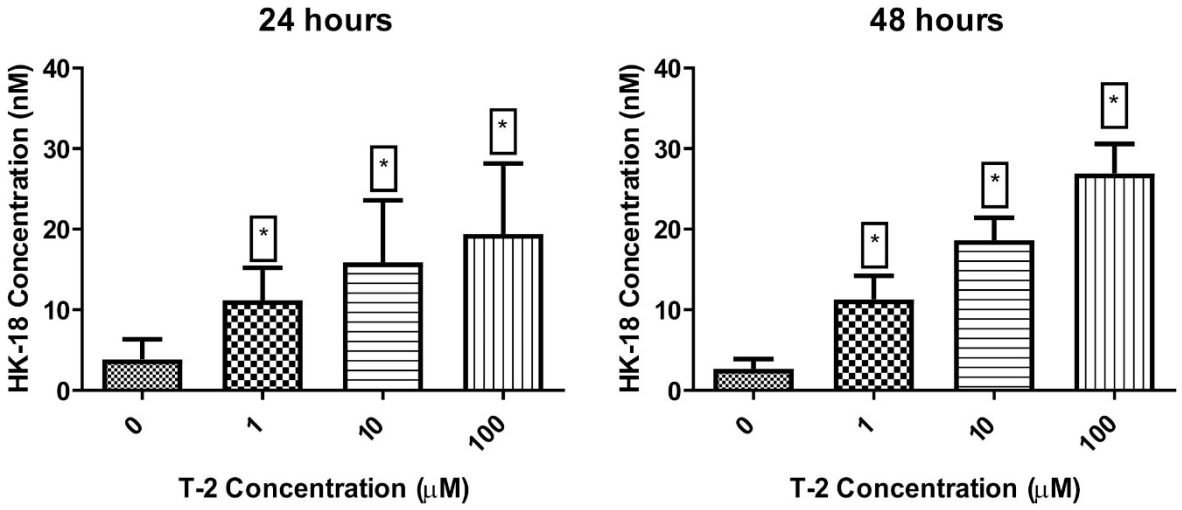

Figure 6. The T-2 effect on full-length Human Cytokeratin 18 concentration in Hs68 cells. Concentration was measured using ELISA method with absorbance measured at λ = 450 nm. Values: means ± SD (n = 6). * $p < 0.001$. 0: untreated (control) cells; 1: concentration of toxin—1 μM; 10: concentration of toxin—10 μM; 100: concentration of toxin—100 μM.

3. Discussion

Human skin consists of a few tissue layers: epidermis, dermis, and subcutaneous tissue. The first, the epidermis, is the outermost layer. It is composed of melanocytes responsible for pigment production, keratinocytes for protein secretion, and lipids forming the extracellular matrix (ECM), as well as Langerhans cells (LCs) involved the antigen (Ag) presentation. Below the epidermis is the dermis, consisting of connective tissue, which provides skin elasticity and tensile strength through the ECM. The skin's innermost layer is the subcutaneous tissue composed of macrophages that eliminate pathogens, fibroblasts producing ECM proteins, and adipocytes [19].

The T-2 mycotoxin, in contrast to most biological toxins, is a strong skin irritant, and it may cause toxicity through contact with intact skin [20]. Associated symptoms of transdermal exposure are burning pain, redness, tenderness, and blisters, leading to skin necrosis. In addition to the above-presented symptoms, the affected skin area is affected by

leathery blackening and sloughing off of exposed skin areas. The immediate toxic effect is characterized by the onset of symptoms seconds after exposure; however, lethal effects are only achieved with a high dose of toxin T-2 [7]. Moreover, T-2 toxic effects expressed by dystrophia in various organs (kidney, liver, heart, peripheral ganglia of the vegetative nervous system), digestive system ulceration and necrosis, hemorrhagic inflammation, diathesis, and injury of blood vessel walls have been observed [21].

Most of the information about T-2 blistering potential is based on observation, and there is no research data concerning in vitro studies aiming to establish the toxic effect of the T-2 toxin on human fibroblast cell line—Hs68.

The mechanism of the toxic effect of T-2 is based on the inhibition of protein synthesis, reduction of lymphocyte proliferation, immunosuppression by inhibiting the production of antibodies (Abs), and impaired development of dendritic cells (DCs) [22,23]. In vitro and animal models studies have suggested a pro-apoptotic effect of the toxin through oxidative damage of cellular components, mainly mitochondria and the rough endoplasmic reticulum. The T-2 toxin inhibited cellular energy by blocking the activity of metabolically important enzymes, leading to a reduction in protein synthesis in the mitochondria, and inhibiting the oxidation of malate, pyruvate, and succinate. It has been noted that certain antioxidants such as lycopene, vitamin E, and rutin counteracted the T-2 toxic effects by inhibiting lipid peroxidation, regulating glutathione metabolism, and enhancing antioxidant enzyme activity [7,24–26]. Thus, the cytotoxic activity of T-2 is associated with oxidative stress induction leading to damage of DNA and lipids, as well as protein synthesis inhibition [27].

For these reasons, this study focused on the evaluation of T-2 toxicity in in vitro conditions on human skin using an Hs68 human dermal fibroblast cell line. The evaluation of the cytotoxic effect demonstrated the high toxic properties of the T-2 toxin in two independent assays. The EC_{50} parameter is very often used as a compound toxicity indicator as well as in pharmacology, because it serves as an indication of drug potency. The calculated values of this parameter clearly demonstrate that T-2 as a dermal agent can be very effective.

ATP is an intracellular energy transfer molecule which has been found in all known forms of all living things. The properties of ATP are related to phosphate groups that link through phosphodiester bonds, which are associated with electronegative charges exerting a repelling force. The process of ATP hydrolysis to ADP is energetically favorable, yielding Gibbs-free energy of −7.3 cal/mol. In eukaryotic cells, the main place of ATP synthesis is the mitochondrial matrix, generating approximately thirty-two ATP molecules per one glucose molecule that is oxidized [28]. ATP is involved in a variety of enzymatic reactions to maintain normal life activities. When normal cells undergo apoptosis and necrosis, the content of ATP will be characteristically changed. Thus, ATP has been widely accepted as a valid marker of metabolically active cells [29]. One of the best measurement methods of intracellular ATP is using firefly luciferase, which takes part in the oxidation of D-luciferin to oxyluciferin [30]. In these experiments, it was confirmed that the T-2 decreases the level of intracellular ATP in a dose-dependent manner. In the probes with the maximum tested toxin concentration (100 μM), after 48 h, an almost total reduction in the ATP level was observed. These results confirmed cytotoxic analysis of the T-2 toxin's potential to damage the human skin fibroblast cell line—Hs68.

Necrosis is uncontrolled cell death induced by external injury, such as inflammation, ischemia, hypoxia, hypoglycemia, toxin exposure, extreme temperature changes, nutrient deprivation, or ROS-induced injury [31]. The other cell death form, apoptosis, takes place as the physiological state of the organism during development and ageing and is a homeostatic mechanism to maintain cell populations in different tissues. During the apoptotic process, there is no inflammatory reaction. This is related to three main characteristics of apoptosis: (i) apoptotic cells do not release their cellular ingredients into the extracellular matrix; (ii) the cell fragments are rapidly phagocytosed by neighboring cells and, (iii) the engulfing cells do not produce anti-inflammatory cytokines [32]. In contrast to apoptosis, necrosis is a passive process requiring only minimal energy. It does not require new protein synthesis and is not

regulated by any homeostatic mechanism [33]. This form of cell death is accompanied by extensive swelling of the cell (as it does not maintain homoeostasis with its environment), distension of different cellular organelles, clumping and random degradation of nuclear DNA, and extensive loss of the intracellular contents [34,35]. Necrosis is a consequence of extensive crosstalk among several biochemical and molecular events at different cellular levels. It often involves the upregulation of numerous pro-inflammatory proteins and compounds, such as nuclear factor-κB (NF-κB), resulting in a cascade of inflammation and tissue damage [36]. In addition, necrosis can be accompanied by ATP depletion [35]. Necrosis may be the result of the toxicity of other mycotoxins, as shown by the following studies. Dolensek et al. showed the effects of a diet contaminated with zearalenone (ZEN), deoxynivalenol (DON), and fusaric acid (FA) on gilts' liver and their suckling piglets. The experimental diet contained 0.09 mg ZEN, 5.08 mg DON, and 21.6 mg FA per kg of feed. The gilts were fed the experimental diet for 54 ± 1 day. The results showed histopathological liver changes and a significant increase in hepatocellular necrosis [37]. In a different study, piglets receiving a diet multi-contaminated with DON (3 mg per kg of feed), ZEN (1.5 mg per kg of feed), and nivalenol (NIV) (1.3 mg per kg of feed) for 28 days exhibited focal liver necrosis [38]. Antonissen and colleagues conducted a study aimed at examining the effect of DON on necrotic enteritis development in broiler chickens. Results demonstrated that the intake of DON-contaminated feed at concentrations below the EU maximum guidance level of 5.000 μg/kg feed significantly increased the number of broiler chickens affected with necrotic enteritis. It lead to an altered intestinal barrier function and resulted in an increased permeability of the intestinal wall [39]. A study with male rats as an animal model demonstrated the neurodegenerative properties of aflatoxin B1 (AFB1). AFB1 was orally administered to male rats at a dose of 0.025 mg/kg of body weight for 90 days. The oral intake of AFB1 caused a time-dependent severity of histopathological impairments in the brain tissue, including spongiform necrosis [40]. A different study concerned the effects of fumonisin B1 (FB1) on the BV-2 cell line and primary murine astrocytes. Cells were exposed to various concentrations of FB1 for 4 to 8 days. Results showed that FB1 induces necrotic cell death in both BV-2 and primary astrocytes [41]. Kupski et al. studied the toxic effects of ochratoxin A (OTA) in human neutrophils in vitro. The study showed that OTA activates neutrophils culminating in cell death by necrosis. According to the results, OTA induces the release of Ca^{2+} from internal stores, leading to an increase in intracellular Ca^{2+} and human neutrophils' oxidative burst followed by depletion of ATP levels and changes in mitochondrial potential, leading to cell death through necrosis [42].

The double-staining cytometry method was used to estimate which potential mechanism of cell death is induced by the T-2 toxin. An annexin V and PI staining kit has been specifically designed for the identification of apoptotic and necrotic cells. Annexin V is a member of the annexin family of intracellular proteins that binds to phosphatidylserine (PS) in a calcium-dependent manner. The surface expression of phosphatidylserine on the cellular membrane lipid is a characteristic event of the apoptotic process, which leads to the recognition of apoptotic cells for phagocytosis [43]. PI is a fluorescent dye that binds to DNA. Early apoptotic cells will exclude PI, while late-stage apoptotic cells and necrotic cells will stain positively due to the passage of these dyes into the nucleus, where they bind to DNA. The flow cytometry analysis clearly demonstrated the lack of presence of PS on cells treated by the T-2 toxin, simultaneously showing the binding of PI to the cells' genetic material (Figure 4), which suggests induction of necrosis by this compound. To verify the absence of induction of the apoptosis, another method—evaluation of activation caspases 3 and 7—was used. These protease enzymes cleave proteins at positions containing aspartic acid residues. The specificity of different caspases is dependent on the recognition of neighboring amino acids. Furthermore, activation of caspases appears to lead to an irreversible induction of programmed cell death [32]. This analysis confirmed the purposes concerning no signs of an apoptotic pathway in T-2-induced Hs-68 cell death (Figure 5). The increased cell permeability without significant increases in caspase 3/7 activation indicated that apoptosis is not involved in the death of these cells.

For final verification of observations, the quantitative analysis of the presence of full-length human cytokeratin was performed. CK18 is a cytoskeletal protein and the main intermediate filament family member expressed in the liver. The full-length form is liberated from necrotic cells, whereas a caspase-cleaved fragment is a product of the structural changes that occur during apoptosis [44]. It was observed that supernatant concentration of CK18 in cell samples increased in a dose-dependent and time-dependent manner (Figure 5). This observation confirmed hypotheses based on other analyses presented in the current study that the T-2 toxin has very strong toxic potential against human skin fibroblast cells and is also a necrosis-induced factor. Other studies have shown that the T-2 toxin activated p38MAPK (SAPK2) and/or Jun N-terminal kinase 1 (JNK1), which induced MAP kinases, including ERK 1/2 [24]. Moreover, it has also been shown that the T-2 toxin stimulates the caspase-3-dependent apoptotic pathway through the upregulation of Fas and p53, which leads to an enhancement of the Bax/Bcl-xL and Bax/Bcl2 ratios [45]. In turn, in this work, it was noted that the effect of T-2 on Hs68 cells was independent of the activation of caspase 3/7.

4. Materials and Methods

4.1. Reagents

Dimethyl sulfoxide (DMSO) and T-2 Toxin from Fusarium sp. (cat. No T4887) were obtained from Sigma-Aldrich Chemical Co. (St. Louis, MO, USA). Penicillin–streptomycin mixture, Dulbecco's Modified Eagle Medium (DMEM) with 4.5 g/L Glucose and with L-Glutamine, heat-inactivated fetal bovine serum (FBS), and PBS (1X) without calcium or magnesium were purchased from Lonza (Basel, Switzerland). A cell viability kit with trypan blue dye and cell counter slides was obtained from BIO-RAD (Hercules, CA, USA). A FITC Annexin V Apoptosis Detection Kit I was obtained from Becton Dickinson (Franklin Lakes, NJ, USA). The MTT (3-(4,5-Dimethylthiazol-2-yl)-2,5-Diphenyltetrazolium Bromide) and CellEvent™ Caspase-3/7 Green Flow Cytometry Assay Kit were obtained from Thermo Fisher Scientific (Waltham, MA, USA). All other chemicals were reagent-grade or the highest-quality available.

4.2. Cellular Material and Culturing Procedure

In this study, the human foreskin fibroblast line Hs68 (ATCC® CRL-1635™) obtained from the American Type Culture Collection (ATCC™, Manassas, VA, USA) was used. Hs68 cells were cultured in DMEM medium supplemented with 100 units of potassium penicillin and 100 µg of streptomycin sulphate per 1 mL of culture media and 10% (v/v) FBS. The cell growing process was performed in a humidified incubator at 37 °C and 5% CO_2. To perform the analysis, cells were seeded at 3×10^6 cells per well and were left in the incubator for 12 h before treatment procedures. Next, the cell samples were incubated with T-2 toxin with a concentration range of 0.001 to 100 µM for 24 h and 48 h.

4.3. Cell Viability Determination

The viability of T-2-treated cell samples was evaluated via two different methods. The first method was the trypan blue dye exclusion test. Analysis of viability via this method was performed using the BIO-RAD TC20 automated cell counter (Hercules, CA, USA), according to the manufacturer's protocol. Cell viability was expressed as a percentage relative to the untreated (control) cells, defined as 100%. The second test was based on measuring cell metabolic activity, which reduces the tetrazolium dye MTT to its insoluble formazan. During this assay, the MTT (0.5 mg/mL) was added to all cell samples and incubated for 4 h at 37 °C. Next, the MTT solution was discarded carefully, and the formed formazan crystals were dissolved in DMSO. The amount of formed formazan crystals was measured calorimetrically at a wavelength of 570 nm with background subtraction at 630 nm on Microplate Reader—BioTek Synergy HT (BioTek Instruments, Winooski, VT, USA). Cell viability was expressed as a percentage relative to the untreated (control) cells, defined as 100%. Half maximal effective concentration (EC_{50}) parameters were

calculated using "Quest Graph™ EC500 Calculator" (Bioquest Inc., San Francisco, CA, USA, https://www.aatbio.com/tools/ec50-calculator (accessed on 19 March 2022)).

4.4. Analysis of Cellular ATP Level Using the Bioluminometry Method

The ATP level in Hs68 cells was evaluated using the bioluminometry method. This method is based on the measurement of light emission that arises during enzymatic degradation of ATP. Luciferase (via oxidation of luciferin) decomposes ATP molecules into AMP. This reaction is accompanied by the emission of light photons with an electromagnetic wavelength of 562 nm. Analysis of cells' metabolic activity via this method was performed using the Hygiena SystemSURE Plus™ (Camarillo, CA, USA). The 100 µL of cell suspension (3×10^6 cells/mL) in sterile DMEM was inserted in the Hygiena AquaSnap™ Total tubes (Camarillo, CA, USA). After that, the tubes were activated by breaking a Hygiena Snap Valve™ (Camarillo, CA, USA) and bending the bulb forward and backward to expel all liquid reagent into the tube. The tube nest was shaken for 5 s to mix the sample. The measurements were performed according to the manufacturer's guidelines. The results were expressed as relative light units (RLU). The baseline was calibrated using the pure DMEM solution.

4.5. Apoptosis/Necrosis Assay—Annexin V Binding and Propidium Iodide Staining

The presence of apoptotic cells was evaluated based on the exposition of phosphatidylserine residues by flow cytometry method using FITC Annexin V Apoptosis Detection Kit I. After the culturing procedure, the cells were washed twice in cold PBS, then suspended in 100 µL 1× annexin-binding buffer (cell density: 1×10^5) and transferred to a standard cytometric tube. Next to the cell suspension, the mixture of 5 µL of FITC Annexin V and 5 µL of propidium iodide (PI) was added, and probes were incubated at 37 °C in an atmosphere of 5% CO_2. After 15 min of incubation, 400 µL of the 1× annexin-binding buffer was added, and samples were analyzed by flow cytometry with the PARTEC CUBE 6 (Görlitz, Germany) flow cytometer using 488 nm excitation. Gates for PI (630 nm Longpass filter) and FITC (536/40 nm filter) fluorescence were estimated based on the fluorescence of unstained probes. The apoptotic index was calculated as the mean percentage of apoptotic cells in 5×10^4 cells measured in each experiment. All data analysis was performed in CyFlow version 1.5.1.2—PARTEC (Görlitz, Germany).

4.6. Determination of Activity of Caspase-3/Caspase-7

Flow cytometric detection of activated caspase-3 and caspase-7 in apoptotic cells was performed using the CellEvent™ Caspase-3/-7 Green Flow Cytometry Assay Kit. For this analysis, cells treated with the T-2 toxin were washed twice in cold PBS and suspended (cell density: 1×10^5) in 1 mL PBS in an Eppendorf tube. In the next step, to each tube, 1 µL of CellEvent™ Caspase-3/-7 Green Detection Reagent was added and mixed gently and left at 37 °C in an atmosphere of 5% CO_2. After the incubation procedure (30 min), 1 µL of the 1 mM SYTOX™ AADvanced™ (prepared in DMSO) was added and left in the dark, RT for 5 min. The final step of the analysis was performed using 96-well black plates (Greiner Bio-One, Kremsmünster, Austria), where 50 µL of samples was transferred to each well. Fluorescence was measured using the Bio-Tek Synergy HT Microplate Reader (Bio-Tek Instruments, Winooski, VT, USA), with filter pairs of 530 nm/590 nm and 485 nm/538 nm.

4.7. Concentration of Cytokeratin 18 Analysis in Cell Culture Supernatants

Human Cytokeratin 18 (CK18) concentration in cell culture supernatants obtained from the Hs68 cell line during the culturing process (with T-2 toxin) was analyzed using a sandwich ELISA kit—Human Cytokeratin 18/KRT18 ELISA (RayBiotech, Peachtree Corners, GA, USA). The whole procedure was performed according to the manufacturer's protocol. Detection of absorbance measured at $\lambda = 450$ nm was performed using the SPECTROStar Nano Microplate Reader (BMG Labtech, Ortenberg, Germany). The concentration

of CK18 concentration in cell culture supernatants was determined based on a standard curve expressed as ng/mL.

4.8. Data Analysis

All obtained experimental values were elaborated using Microsoft Excel (Redmond, WA, USA) and expressed as means ± standard deviations (SDs). The statistical analysis was performed using StatsDirect statistical software V. 2.7.2.—StatsDirect Ltd (Cheshire, UK). In the first step, all results were analyzed according to the normality of the distribution by the Shapiro–Wilk test. Next, the results were analyzed according to equality of variance via Levene's test. The significance of the differences among the values was analyzed using ANOVA: Tukey's range test (for data with a normal distribution and equality of variance) or the Kruskal–Wallis test; $p < 0.05$ was accepted as statistically significant [46,47].

5. Conclusions

We have demonstrated for the first time using an in vitro human skin fibroblast model that the T-2 toxin is able to induce the necrosis process. This is a very important step for research concerning the prevention of damages induced by this toxin. Further analysis at the molecular level has been planned for the next research project, which will also focus on T-2 toxin toxicity.

Author Contributions: Conceptualization, M.B., M.C., M.N. and E.S.; experiments, E.J.-K., M.S., M.W. and E.S.; writing—original draft preparation, E.J.-K. and M.B.; writing—review and editing, M.B., M.N. and T.S.; supervision, M.C. and M.B. All authors have read and agreed to the published version of the manuscript.

Funding: The publication's printing cost was co-financed by the European Union, from the European Social Fund under the "InterDOC-STARt" project (POWR.03.02.00-00-I033/16-00).

Institutional Review Board Statement: Not applicable.

Informed Consent Statement: Not applicable.

Data Availability Statement: Not applicable.

Conflicts of Interest: The authors declare no conflict of interest.

References

1. Nesic, K.; Ivanovic, S.; Nesic, V. Fusarial toxins: Secondary metabolites of Fusarium fungi. *Rev. Environ. Contam. Toxicol.* **2014**, *228*, 101–120. [CrossRef] [PubMed]
2. McCormick, S.P.; Stanley, A.M.; Stover, N.A.; Alexander, N.J. Trichothecenes: From simple to complex mycotoxins. *Toxins* **2011**, *3*, 802–814. [CrossRef] [PubMed]
3. Foroud, N.A.; Eudes, F. Trichothecenes in cereal grains. *Int. J. Mol. Sci.* **2009**, *10*, 147–173. [CrossRef] [PubMed]
4. Janik, E.; Ceremuga, M.; Saluk-Bijak, J.; Bijak, M. Biological Toxins as the Potential Tools for Bioterrorism. *Int. J. Mol. Sci.* **2019**, *20*, 1181. [CrossRef]
5. Kanora, A.; Maes, D. The role of mycotoxins in pig reproduction: A review. *Vet. Med.* **2009**, *54*, 565–576. [CrossRef]
6. Zhang, M.; Huo, B.; Yuan, S.; Ning, B.; Bai, J.; Peng, Y.; Liu, B.; Gao, Z. Ultrasensitive detection of T-2 toxin in food based on bio-barcode and rolling circle amplification. *Anal. Chim. Acta* **2018**, *1043*, 98–106. [CrossRef]
7. Adhikari, M.; Negi, B.; Kaushik, N.; Adhikari, A.; Al-Khedhairy, A.A.; Kaushik, N.K.; Choi, E.H. T-2 mycotoxin: Toxicological effects and decontamination strategies. *Oncotarget* **2017**, *8*, 33933–33952. [CrossRef]
8. Fung, F. T-2 Toxin (Trichothecene Mycotoxins) Attack. In *Ciottone's Disaster Medicine*; Elsevier: Amsterdam, The Netherlands, 2016; Volume 157, pp. 801–803.
9. Albarenque, S.M.; Shinozuka, J.; Iwamoto, S.; Nakayama, H.; Doi, K. T-2 toxin-induced acute skin lesions in Wistar-derived hypotrichotic WBNIILA-Ht rats. *Histol. Histopathol.* **1999**, *14*, 337–342.
10. Hemmati, A.A.; Kalantari, H.; Jalali, A.; Rezai, S.; Zadeh, H.H. Healing effect of quince seed mucilage on T-2 toxin-induced dermal toxicity in rabbit. *Exp. Toxicol. Pathol.* **2012**, *64*, 181–186. [CrossRef]
11. Ueno, Y. Comparative study on skin-necrotizing effect of scirpene metabolites of Fusaria. *Jpn. J. Exp. Med.* **1970**, *40*, 33–38.
12. Bunner, D.; Wannemacher, R.; Neufeld, H.; Hassler, C.; Parker, G. Pathophysiology of Acute T-2 Intoxication in the Cynomolgus Monkey and Comparison to the Rat as a Model. *Toxicology* **1983**, *21*, 411–421.
13. Sokolović, M.; Garaj-Vrhovac, V.; Simpraga, B. T-2 toxin: Incidence and toxicity in poultry. *Arch. Ind. Hyg. Toxicol.* **2008**, *59*, 43–52. [CrossRef] [PubMed]

14. Agrawal, M.; Yadav, P.; Lomash, V.; Bhaskar, A.S.; Lakshmana Rao, P.V. T-2 toxin induced skin inflammation and cutaneous injury in mice. *Toxicology* **2012**, *302*, 255–265. [CrossRef] [PubMed]
15. Afsah-Hejri, L.; Jinap, S.; Hajeb, P.; Radu, S.; Shakibazadeh, S. A Review on Mycotoxins in Food and Feed: Malaysia Case Study. *Compr. Rev. Food Sci. Food Saf.* **2013**, *12*, 629–651. [CrossRef]
16. Haig, A. *Chemical Warfare in Southwest Asia and Afghanistan: Report to the Congress from Secretary of State*; Special Report No. 98; US Department of State, Bureau of Public Affairs, Office of Public Communication, Editorial Division: Washington, DC, USA, 1982.
17. Kalantari, H.; Moosavi, M. Review on T-2 Toxin. *Jundishapur J. Nat. Pharm. Prod.* **2010**, *5*, 26–38.
18. Venkataramana, M.; Chandranayaka, S.; Prakash, H.; Niranjana, S. Mycotoxins Relevant to Biowarfare and Their Detection. In *Biological Toxins and Bioterrorism*; Gopalakrishnakone, P., Balali-Mood, M., Llewellyn, L., Singh, B., Eds.; Springer: Dordrecht, The Netherlands, 2015; Volume 1, p. 295319.
19. Shin, J.W.; Kwon, S.H.; Choi, J.Y.; Na, J.I.; Huh, C.H.; Choi, H.R.; Park, K.C. Molecular Mechanisms of Dermal Aging and Antiaging Approaches. *Int. J. Mol. Sci.* **2019**, *20*, 2126. [CrossRef]
20. Ueno, Y. The toxicology of mycotoxins. *Crit. Rev. Toxicol.* **1985**, *14*, 99–132. [CrossRef]
21. Bertero, A.; Moretti, A.; Spicer, L.J.; Caloni, F. Molds and Mycotoxins: Potential Species-Specific Effects. *Toxins* **2018**, *10*, 244. [CrossRef]
22. Guilford, F.T.; Hope, J. Deficient glutathione in the pathophysiology of mycotoxin-related illness. *Toxins* **2014**, *6*, 608–623. [CrossRef]
23. Obremski, K.; Podlasz, P.; Zmigrodzka, M.; Winnicka, A.; Woźny, M.; Brzuzan, P.; Jakimiuk, E.; Wojtacha, P.; Gajecka, M.; Zielonka, Ł.; et al. The effect of T-2 toxin on percentages of $CD4^+$, $CD8^+$, $CD4^+$ $CD8^+$ and $CD21^+$ lymphocytes, and mRNA expression levels of selected cytokines in porcine ileal Peyer's patches. *Pol. J. Vet. Sci.* **2013**, *16*, 341–349. [CrossRef]
24. Li, M.; Pestka, J.J. Comparative induction of 28S ribosomal RNA cleavage by ricin and the trichothecenes deoxynivalenol and T-2 toxin in the macrophage. *Toxicol. Sci.* **2008**, *105*, 67–78. [CrossRef] [PubMed]
25. Hoehler, D.; Marquardt, R.R. Influence of vitamins E and C on the toxic effects of ochratoxin A and T-2 toxin in chicks. *Poult. Sci.* **1996**, *75*, 1508–1515. [CrossRef] [PubMed]
26. Leal, M.; Shimada, A.; Ruíz, F.; de Mejía, E.G. Effect of lycopene on lipid peroxidation and glutathione-dependent enzymes induced by T-2 toxin in vivo. *Toxicol. Lett.* **1999**, *109*, 1–10. [CrossRef]
27. Yang, L.; Yu, Z.; Hou, J.; Deng, Y.; Zhou, Z.; Zhao, Z.; Cui, J. Toxicity and oxidative stress induced by T-2 toxin and HT-2 toxin in broilers and broiler hepatocytes. *Food Chem. Toxicol.* **2016**, *87*, 128–137. [CrossRef] [PubMed]
28. Meurer, F.; Do, H.T.; Sadowski, G.; Held, C. Standard Gibbs energy of metabolic reactions: II. Glucose-6-phosphatase reaction and ATP hydrolysis. *Biophys. Chem.* **2017**, *223*, 30–38. [CrossRef]
29. Méry, B.; Guy, J.B.; Vallard, A.; Espenel, S.; Ardail, D.; Rodriguez-Lafrasse, C.; Rancoule, C.; Magné, N. In Vitro Cell Death Determination for Drug Discovery: A Landscape Review of Real Issues. *J. Cell Death* **2017**, *10*, 1179670717691251. [CrossRef]
30. Nguyen, L.T.; Zajíčková, M.; Mašátová, E.; Matoušková, P.; Skálová, L. The ATP bioluminescence assay: A new application and optimization for viability testing in the parasitic nematode Haemonchus contortus. *Vet. Res.* **2021**, *52*, 124. [CrossRef]
31. Moriwaki, K.; Chan, F. Necrosis-dependent and independent signaling of the RIP kinases in inflammation. *Cytokine Growth Factor Rev.* **2014**, *25*, 167–174. [CrossRef]
32. Elmore, S. Apoptosis: A review of programmed cell death. *Toxicol. Pathol.* **2007**, *35*, 495–516. [CrossRef]
33. Golstein, P.; Kroemer, G. Cell death by necrosis: Towards a molecular definition. *Trends Biochem. Sci.* **2007**, *32*, 37–43. [CrossRef]
34. Syntichaki, P.; Tavernarakis, N. Death by necrosis. Uncontrollable catastrophe, or is there order behind the chaos? *EMBO Rep.* **2002**, *3*, 604–609. [CrossRef] [PubMed]
35. Cullen, J.M. Histologic Patterns of Hepatotoxic Injury. In *Comprehensive Toxicology*, 2nd ed.; McQueen, C., Ed.; EPA: Washington, DC, USA, 2010; pp. 141–173.
36. D'Arcy, M.S. Cell death: A review of the major forms of apoptosis, necrosis and autophagy. *Cell Biol. Int.* **2019**, *43*, 582–592. [CrossRef] [PubMed]
37. Dolenšek, T.; Švara, T.; Knific, T.; Gombač, M.; Luzar, B.; Jakovac-Strajn, B. The Influence of Fusarium Mycotoxins on the Liver of Gilts and Their Suckling Piglets. *Animals* **2021**, *11*, 2534. [CrossRef] [PubMed]
38. Gerez, J.; Pinton, P.; Callu, P.; Grosjean, F.; Oswald, I.; Bracarensem, A. Deoxynivalenol alone or in combination with nivalenol and zearalenone induce systemic histological changes in pigs. *Exp. Toxicol. Pathol.* **2015**, *67*, 89–98. [CrossRef]
39. Antonissen, G.; Van Immerseel, F.; Pasmans, F.; Ducatelle, R.; Haesebrouck, F.; Timbermont, L.; Verlinden, M.; Janssens, G.; Eeckhaut, V.; Eeckhout, M.; et al. The mycotoxin deoxynivalenol predisposes for the development of Clostridium perfringens-induced necrotic enteritis in broiler chickens. *PLoS ONE* **2014**, *9*, e108775. [CrossRef]
40. Alsayyah, A.; ElMazoudy, R.; Al-Namshan, M.; Al-Jafary, M.; Alaqeel, N. Chronic neurodegeneration by aflatoxin B1 depends on alterations of brain enzyme activity and immunoexpression of astrocyte in male rats. *Ecotoxicol. Environ. Saf.* **2019**, *182*, 109407. [CrossRef]
41. Osuchowski, M.; Sharma, R. Fumonisin B1 Induces Necrotic Cell Death in BV-2 Cells and Murine Cultured Astrocytes and is Antiproliferative in BV-2 Cells While N2A Cells and Primary Cortical Neurons are Resistant. *NeuroToxicology* **2005**, *26*, 981–992. [CrossRef]
42. Kupski, L.; Freitas, M.; Ribeiro, D.; Furlong, E.; Fernandes, E. Ochratoxin A activates neutrophils and kills these cells through necrosis, an effect eliminated through its conversion into ochratoxin α. *Toxicology* **2016**, *368–369*, 91–102. [CrossRef]

43. Bratton, D.L.; Fadok, V.A.; Richter, D.A.; Kailey, J.M.; Guthrie, L.A.; Henson, P.M. Appearance of phosphatidylserine on apoptotic cells requires calcium-mediated nonspecific flip-flop and is enhanced by loss of the aminophospholipid translocase. *J. Biol. Chem.* **1997**, *272*, 26159–26165. [CrossRef]
44. Dive, C.; Smith, R.A.; Garner, E.; Ward, T.; George-Smith, S.S.; Campbell, F.; Greenhalf, W.; Ghaneh, P.; Neoptolemos, J.P. Considerations for the use of plasma cytokeratin 18 as a biomarker in pancreatic cancer. *Br. J. Cancer* **2010**, *102*, 577–582. [CrossRef]
45. Bouaziz, C.; El Dein, O.S.; El Golli, E.; Abid-Essefi, S.; Brenner, C.; Lemaire, C.; Bacha, H. Different apoptotic pathways induced by zearalenone, T-2 toxin and ochratoxin A in human hepatoma cells. *Toxicology* **2008**, *254*, 19–28. [CrossRef] [PubMed]
46. Zbikowska, H.M.; Antosik, A.; Szejk, M.; Bijak, M.; Olejnik, A.K.; Saluk, J.; Nowak, P. Does quercetin protect human red blood cell membranes against γ-irradiation? *Redox Rep.* **2014**, *19*, 65–71. [CrossRef] [PubMed]
47. Bijak, M.; Saluk, J.; Antosik, A.; Ponczek, M.B.; Zbikowska, H.M.; Borowiecka, M.; Nowak, P. Aronia melanocarpa as a protector against nitration of fibrinogen. *Int. J. Biol. Macromol.* **2013**, *55*, 264–268. [CrossRef] [PubMed]

molecules

MDPI

Article

Mitochondrial Damage Induced by T-2 Mycotoxin on Human Skin—Fibroblast Hs68 Cell Line

Edyta Janik-Karpinska [1], Michal Ceremuga [2], Marcin Niemcewicz [1], Ewelina Synowiec [3], Tomasz Sliwiński [3] and Michal Bijak [1,*]

[1] Biohazard Prevention Centre, Faculty of Biology and Environmental Protection, University of Lodz, Pomorska 141/143, 90-236 Lodz, Poland
[2] Military Institute of Armament Technology, Prymasa Stefana Wyszyńskiego 7, 05-220 Zielonka, Poland
[3] Laboratory of Medical Genetics, Faculty of Biology and Environmental Protection, University of Lodz, Pomorska 141/143, 90-236 Lodz, Poland
* Correspondence: michal.bijak@biol.uni.lodz.pl

Abstract: T-2 toxin is produced by different *Fusarium* species and belongs to the group of type A trichothecene mycotoxins. T-2 toxin contaminates various grains, such as wheat, barley, maize, or rice, thus posing a risk to human and animal health. The toxin has toxicological effects on human and animal digestive, immune, nervous and reproductive systems. In addition, the most significant toxic effect can be observed on the skin. This in vitro study focused on T-2 toxicity on human skin fibroblast Hs68 cell line mitochondria. In the first step of this study, T-2 toxin's effect on the cell mitochondrial membrane potential (MMP) was determined. The cells were exposed to T-2 toxin, which resulted in dose- and time-dependent changes and a decrease in MMP. The obtained results revealed that the changes of intracellular reactive oxygen species (ROS) in the Hs68 cells were not affected by T-2 toxin. A further mitochondrial genome analysis showed that T-2 toxin in a dose- and time-dependent manner decreased the number of mitochondrial DNA (mtDNA) copies in cells. In addition, T-2 toxin genotoxicity causing mtDNA damage was evaluated. It was found that incubation of Hs68 cells in the presence of T-2 toxin, in a dose- and time-dependent manner, increased the level of mtDNA damage in both tested mtDNA regions: NADH dehydrogenase subunit 1 (ND1) and NADH dehydrogenase subunit 5 (ND5). In conclusion, the results of the in vitro study revealed that T-2 toxin shows adverse effects on Hs68 cell mitochondria. T-2 toxin induces mitochondrial dysfunction and mtDNA damage, which may cause the disruption of adenosine triphosphate (ATP) synthesis and, in consequence, cell death.

Keywords: T-2 toxin; mitochondria; mtDNA damage; Hs68 cell line; skin

Citation: Janik-Karpinska, E.; Ceremuga, M.; Niemcewicz, M.; Synowiec, E.; Sliwiński, T.; Bijak, M. Mitochondrial Damage Induced by T-2 Mycotoxin on Human Skin—Fibroblast Hs68 Cell Line. *Molecules* **2023**, *28*, 2408. https://doi.org/10.3390/molecules28052408

Academic Editors: Adam Szewczyk and Andrea Salvo

Received: 16 January 2023
Revised: 20 February 2023
Accepted: 2 March 2023
Published: 6 March 2023

1. Introduction

Mitochondria are essential organelles playing a key role in various cell processes. They are frequently called the "powerhouses of the cell". This is mainly due to the fact that their primary and most well-described role is in adenosine triphosphate (ATP) production via oxidative phosphorylation (OXPHOS), which is executed by the mitochondrial electron transport chain (ETC) [1,2]. However, mitochondria are also responsible for iron–sulphur cluster formation, calcium handling, lipid metabolism, reactive oxygen species (ROS) generation, cell signaling, apoptotic activation, and mediation of cell growth and death [3,4]. The mitochondrial membrane potential (MMP) generated by proton pumps (complexes I, III, and IV) is a key indicator of mitochondrial activity. It reflects the process of electron transport and oxidative phosphorylation and provides the driving force for ATP synthesis in mitochondria [5]. Furthermore, MMP is required for mitochondrial protein import and for regulating metabolite transport [6]. A loss of MMP is a signal of bioenergetic stress and may cause the release of pro-apoptotic factors leading to cell death [7].

Mitochondria contain their own genome: mitochondrial DNA (mtDNA), housed in the mitochondrial matrix [8]. The mitochondrial genome is circular, double-stranded, and contains very few introns, and it is built of 16,569 base pairs. Mitochondrial DNA possesses a small number of genes, which encode 13 proteins, 22 transfer RNAs (tRNAs), and 2 ribosomal RNAs (rRNAs): 12S and 16S in humans. These proteins are important components of the mitochondrial respiratory chain (MRC) and of the ATP synthase complex, while tRNA and rRNA are required for translation [9]. One mitochondrion can contain 2–10 copies of mtDNA, and up to 1000 mitochondria are present per cell [10]. Transcription, translation, and replication of mtDNA, including the synthesis of ribosomal proteins, are under nuclear regulation. As a consequence, mitochondrial function depends on coordinated interaction between nuclear DNA (nDNA) and mtDNA-encoded proteins, protein assembly factors, and chaperone proteins, which are involved in protein folding and scaffolding and structural support [11]. mtDNA is inherited exclusively maternally, while the sperm-borne mitochondria are mostly degraded by autophagy after fertilization [12].

T-2 toxin belongs to the group of type A trichothecene mycotoxins and is produced by various *Fusarium* species, such as *F. sporotrichioides*, *F. poae*, and *F. tricinctum* [13]. T-2 mycotoxin contaminates a variety of grains, including wheat, barley, maize, rice, oat, and soybeans, and therefore poses a risk to human and animal health [14]. The European Food Safety Authority (EFSA) established new standards for T-2 toxin: a tolerable daily intake (TDI) of 0.02 µg/kg body weight (bw) per day and an acute reference dose (ARfD) of 0.3 µg/kg bw [15]. T-2 is considered one of the most toxic trichothecenes [16]. It is mainly harmful to human and animal digestive, reproductive, nervous, and immune systems. T-2 shows dermal toxicity, hematotoxicity, carcinogenic, and mutagenic effects [17]. T-2 toxin is a low molecular chemical compound with a weight of approximately 466.51 Da [18]. According to IUPAC nomenclature: 1R,9R,10R,11S,12R(-11-acetyloxy-2-(acetyloxymethyl)-10-hydroxy-1,5-dimethylspiro(8-oxatricyclo(7.2.1.02,7))dodec-5-ene-12,2′-oxirane)-4-yl)-3-methylbutanoate. The epoxy rings at the C-12 and -13 positions are responsible for toxicological activity [19]. This structure is responsible for T-2 toxin's lipophilic character and the fact that it can be immediately absorbed by exposed cells [20]. The main effect of T-2 toxin is protein synthesis inhibition, which leads to the secondary disruption of DNA and RNA synthesis. Toxin also causes lipid peroxidation and reactive oxygen species (ROS) generation, as well as apoptosis and necrosis [21,22].

Studies have shown that T-2 toxin causes DNA damage [23–25]. Cells are able to use many mechanisms in order to repair their DNA; thus, the integrity of nuclear (nDNA) and mitochondrial DNA (mtDNA) can be maintained. In the absence of damage recognition or repair fails, an accumulation of DNA lesions appears [26]. mtDNA is associated with a sustained 10-fold higher level of damage in comparison to nDNA due to the lack of protective histone proteins in mitochondria [27]. The apparent lack of mtDNA repair mechanisms and also the low fidelity of the mtDNA polymerase lead to a higher mutation rate in the mtDNA compared to the nuclear genome [28]. Moreover, mtDNA is particularly susceptible to mutation due to the production of ROS in mitochondria during respiration, which can cause oxidative lesions in mtDNA [29,30]. mtDNA is more susceptible to damage than nDNA, mainly due to the fact that the entire mitochondrial genome codes expressed genes, whereas the nuclear genome contains a large amount of nontranscribed sequences. Furthermore, in contrast to nDNA, mtDNA is continuously replicated, even in terminally differentiated cells such as cardiomyocytes [31].

In our previous study performed on the human skin fibroblast Hs68 cell line, it was demonstrated that T-2 toxin in a dose and time-dependent manner had cytotoxic effect. The bioluminometry results showed that the relative levels of ATP in the treated cells decreased. Further analysis of the toxin's impact on the apoptosis induction and necrosis processes clearly indicates the necrosis process in treated cells. This paper contains the results of an in vitro human skin fibroblast model study and reveals for the first time that T-2 toxin induces necrosis as an effect of toxicity [32].

Due to the lack of information on the T-2 molecular mechanisms of action on the skin and the effects of this toxin on mitochondria, in vitro studies with a cell line of normal

human fibroblasts Hs68 were conducted in order to explain the effect of this toxin on mitochondria and mtDNA.

2. Results

2.1. Assessment of Mitochondrial Membrane Potential (MMP)

In the first step of our study, T-2 toxin's effect on cell mitochondria's physiological status was determined. The effect of T-2 toxin on a cell line of normal human fibroblasts Hs68 mitochondrial membrane potential was examined. MMP plays a key role in mitochondrial homeostasis through the selective elimination of dysfunctional mitochondria. The treatment of cell line resulted in a dose- and time-dependent changes of tetraethylbenzimidazolylcarbocyanine iodide (JC-1) monomer fluorescence aggregates ratio (Figure 1), which indicated a decrease in the membrane potential in cells treated with T-2 toxin.

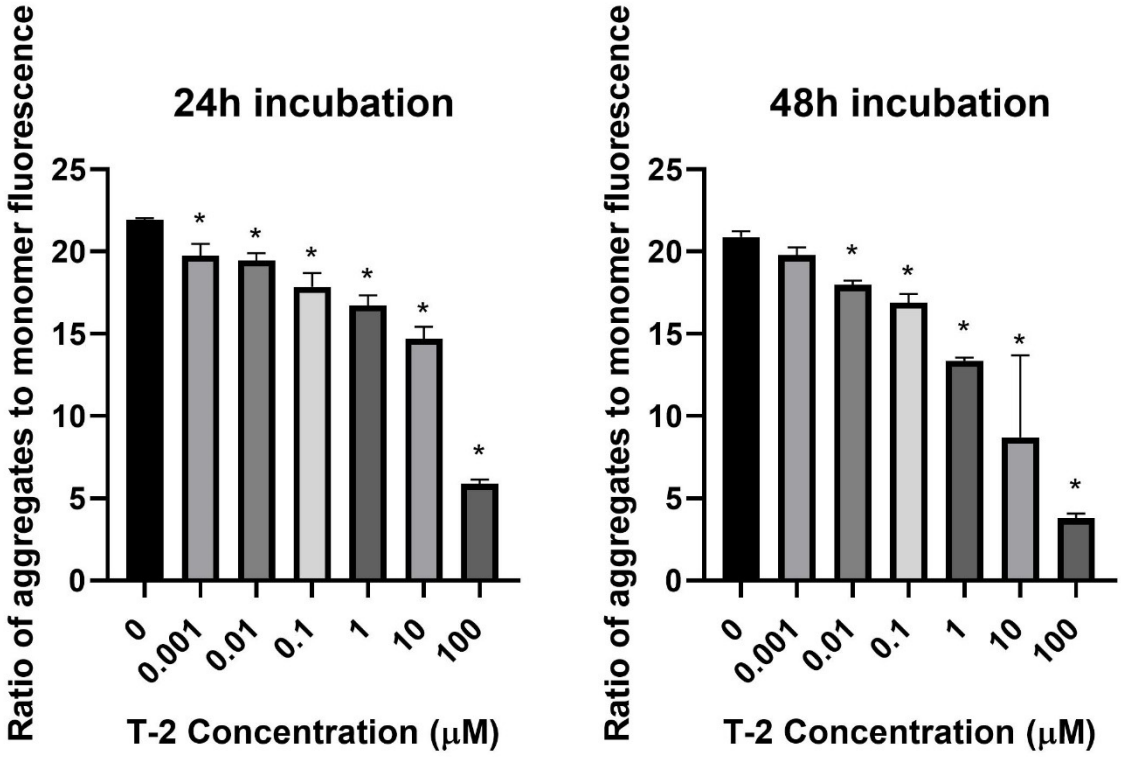

Figure 1. The T-2 toxin effect on the mitochondrial membrane potential of Hs68 cells estimated by the fluorescence dye JC-1 method. The values are presented as means ± SD (n = 6). * $p < 0.5$.

2.2. Assessment of Intracellular Reactive Oxygen Species (ROS) Level

The next step of the study was the assessment of the impact of T-2 on Hs68 mitochondria by an evaluation of the intracellular generation of reactive oxygen species. In order to perform this analysis, the experiments with 2′,7′-dichlorofluorescein diacetate (DCFH-DA) dye, which oxidizes to highly fluorescent 2′,7′-dichlorofluorescein (DCF) in the presence of intracellular ROS, were executed. The incubation of Hs68 cells with T-2 toxin at all tested concentrations showed no impact on the intracellular ROS (Figure 2).

2.3. Mitochondrial DNA (mtDNA) Copy Number Quantification

The next experiments focused on the impact of T-2 toxin on the mitochondrial genome. The potential genotoxicity of T-2 was observed as a change in the mtDNA copy number. According to the cytotoxicity results, three T-2 toxin concentrations were tested: 0.1, 1, and 10 μM. The incubation of the Hs68 cells with T-2 toxin in a dose- and time-dependent manner decreased the number of mtDNA copies in the cells (Figure 3). In the case of the highest tested concentration (10 μM) and a 48 h incubation period, the level decreased by more than 100 times.

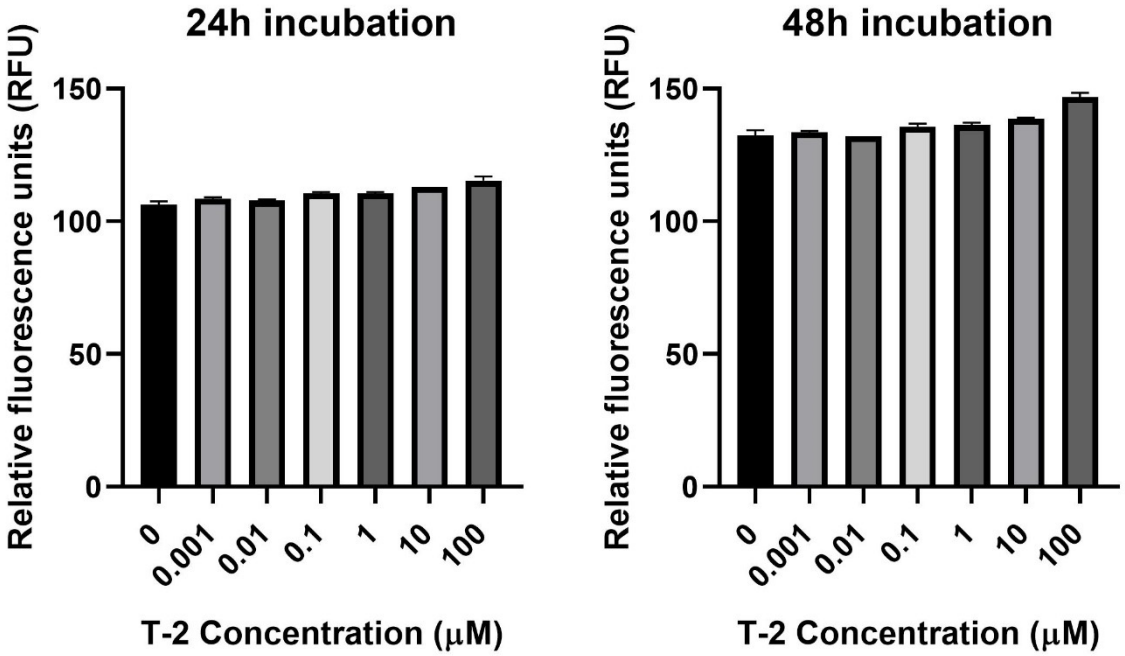

Figure 2. The T-2 toxin's effect on intracellular ROS production in the Hs68 cell line, measured as the DCF fluorescence intensity. The values are presented as means ± SD (n = 6).

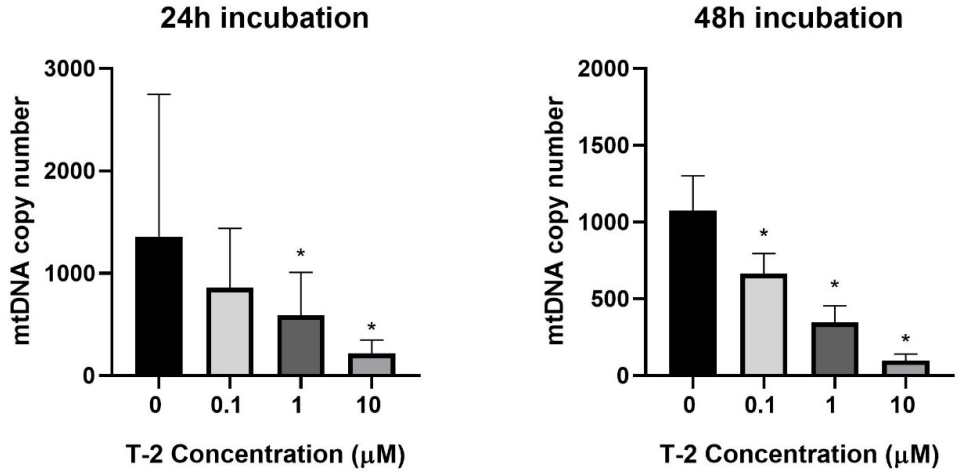

Figure 3. The T-2 toxin's effect on the mitochondrial DNA copy number in the Hs68 cell line, measured by real-time quantitative polymerase chain reaction (rt-qPCR). The values are presented as means ± SD (n = 6). * $p < 0.05$.

2.4. Determination of Mitochondrial DNA Damage

As a complementary study on the determination of T-2 toxin on the mitochondrial genome of Hs68 cells, toxin genotoxicity by measurement of the mtDNA damage was performed. The mtDNA damage, by semi-long-run quantitative real-time polymerase chain reaction (SLR-qRT-PCR) amplification of the DNA isolated from cells exposed to T-2 toxin at concentrations of 0.1, 1, and 10 μM for both 24 and 48 h, was examined. The incubation of Hs68 cells with T-2 toxin in a dose- and time-dependent manner increased the level of mtDNA damage in both tested mtDNA regions—NADH dehydrogenase subunit 1 (ND1) (Figure 4A) and NADH dehydrogenase subunit 5 (ND5) (Figure 4B).

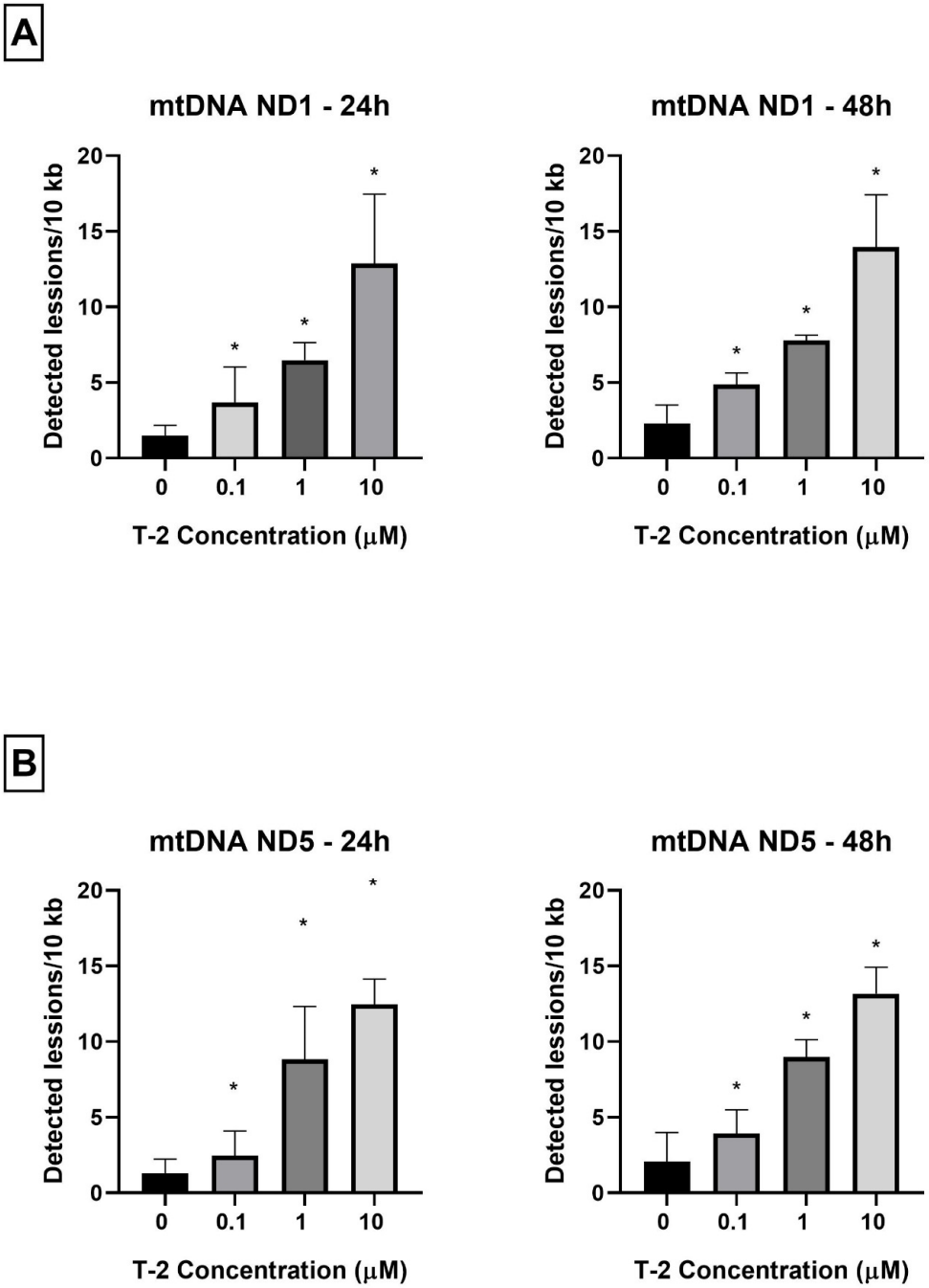

Figure 4. (**A**,**B**) The effect of T-2 toxin on mtDNA lesion frequency per 10 kb DNA in the ND1 and ND5 genes, estimated using SLR-qRT-PCR amplification of the total DNA from the Hs68 cells. The values are presented as means ± SD (n = 6). * $p < 0.05$.

3. Discussion

T-2 toxin has a unique character, which was the main reason behind the initiation of our studies focused on the determination of the molecular mechanism of action of T-2 toxin in in vitro human foreskin fibroblast cell line Hs68. The first paper [32] in the series of our studies showed the necrotic potential of T-2 toxin alongside a strong reduction in ATP production by cells. Consecutively, the aim of this paper was to present the impact of T-2 toxin on mitochondrial physiology and disruption of mitochondrial DNA.

The mitochondrial membrane potential is a driving force behind the transport of ions and proteins, which is crucial for healthy mitochondrial functioning [5]. The decrease in MMP might be an indicator of cell death and a cause of various pathologies [33]. A decrease

in MMP was observed in both necrotic and apoptotic cell deaths. One theory proposes that the ATP level (ATP may be the switch) determines whether cell destruction occurs by necrosis or apoptosis. In this context, necrotic cell death is solely dependent on oxidative phosphorylation for ATP. When the decrease in MMP occurs without ATP depletion, apoptosis can develop. When the decrease in MMP is related to mitochondrial disfunction and ATP depletion, necrotic cell death might occur [34]. This theory is decisively confirmed by our studies. In this study, a strong decrease in the mitochondrial membrane potential in cells treated with T-2 toxin (Figure 1) was demonstrated. In our previous paper [32], using the bioluminometry method, we observed that the treatment of cell line resulted in a dose- and time-dependent decrease in the level of luminescence, which directly corresponds to the ATP level in the sample (see Figure 3 in [32]). The samples were from the same batch of culture used in the current research. In this context, the potential mechanism of necrotic cell death caused by T-2 toxin is dependent on the mitochondrial damage caused by the ATP disturbance in oxidative phosphorylation.

ATP oxidative phosphorylation in mitochondria points to the fact that these organelles are the main cellular consumers of oxygen. The redox enzymes present in mitochondria cause the transfer of single electrons to oxygen and nonenzymatic production of $O_2^{-\bullet}$. Mitochondrial damage and physiological imbalance can cause a disproportion between ROS production and removal, resulting in net ROS production [35]. The results presented in Figure 2 demonstrate that the T-2 toxin at all tested concentrations and times did not change the intracellular ROS level. This observation also confirms the fact that T-2 toxin inhibits ATP oxidative phosphorylation. In a study of the role of mitochondria in T-2-induced apoptosis of human chondrocytes, a decrease in the MMP of chondrocytes following T-2 toxin administration was shown. In addition, the ROS levels, as a mitochondrial apoptotic factor, significantly increased. In addition, caspase-3 and caspase-9 were activated in those chondrocytes [36]. This study shows that T-2 toxin can also decrease the MMP of fibroblast cells, however, with no effect on the ROS level. Our previous study on T-2 toxin's impact on the induction of apoptosis and necrosis processes in a fibroblast cell line showed a lack of caspase-3, which controls the fragmentation of DNA and morphological changes of apoptosis, and caspase-7, which is related to the loss of cellular viability [32]. The lack of changes in the ROS level and the activity of caspase-3/7, which are involved in the apoptosis process, indicate a necrosis process as the impact of T-2 toxin on the fibroblast cells. Additionally, experiments on the same samples using the double-staining flow cytometry method, which were presented in our previous paper [32], demonstrated that the T-2 mycotoxin resulted in both a dose- and time-dependent increase in propidium iodide (PI) fluorescence in cells. At the highest tested concentration of the toxin, 100 μM, the % of PI-stained cells was 79% after 24 h of incubation and 93% after 48 h of incubation.

The next steps of the research presented in this paper focused on molecular damage, which can be caused by the presence of T-2 toxin in mitochondria. mtDNA is crucial for mitochondrial physiological status and function. mtDNA replication is independent from the cell cycle and from nuclear DNA replication. This process is conducted by the encoded polymerase γ, the only DNA polymerase found in mitochondria [37]. A sufficient number of mtDNA copies is necessary to meet their specific requirements for the generation of cellular energy through oxidative phosphorylation [38]. mtDNA is susceptible to reactive species generated from cellular metabolism and to environmental agents, including therapeutic drugs, radiation, and industrial byproducts [39]. The significance of mtDNA in homeostasis is evidenced by the fact that many diseases are caused by mtDNA depletion or mutations [40]. Mitochondrial dysfunctions are associated with numerous human diseases, such as neurodegenerative disorders, neurometabolic diseases, cardiovascular disorders, cancer, or obesity [41]. This study shows that T-2 toxin can cause a significant decline in the number of mtDNA copies (Figure 3). This observation confirmed previous conclusions concerning mitochondrial damage and the disturbance of ATP production induced by T-2. The molecular mechanism of this action is probably linked to mtDNA damage. As a final confirmation of the responsibility of T-2 toxin for mtDNA damage, the analysis of mtDNA

lesions in two genes—ND1 and ND5—was performed. The mitochondrial ND1 gene is translated into the NADH-ubiquinone oxidoreductase chain 1 (ND1) [42], whereas the ND5 gene encodes the NADH-ubiquinone oxidoreductase chain 5 protein [43]. Both of these proteins are subunits of NADH dehydrogenase—the largest of the five complexes of the electron transport chain [44]. The results of our research presented in the current paper demonstrate that the T-2 toxin induced mtDNA damage in both of the tested mtDNA genes—ND1 (Figure 4A) and ND5 (Figure 4B). This observation confirmed the damaging effect of T-2 toxin on mitochondrial function at the molecular level, which can, consequently, lead to the inhibition of ATP production [32] and cell necrosis.

The studies performed by Pace et al. [45] demonstrated that T-2 toxin, in dose-dependent manner, inhibited protein synthesis in isolated rat liver mitochondria. The concentration of toxin, which inhibited 50% of protein synthesis, was approximately 0.05 μM. T-2 toxin was presented as an inducer of mitochondrial dysfunction and an inhibitor of ATP synthesis in cardiomyocytes [46]. Many studies have also demonstrated that T-2 toxin induced MMP loss [36,47–49].

It has been shown that other fungal toxins can also cause mitochondrial and mtDNA damage. A study on ducklings showed that the administration of aflatoxin B_1 (AFB_1) can induce hepatic mitochondrial antioxidant dysfunction. An analysis of the ducklings' liver tissue revealed morphological changes, including fat necrosis, steatosis, and the formation of lymphoid nodules, with infiltrated lymphocytes. AFB_1 exposure induced mitochondrial swelling with increased opening of the liver mitochondrial permeability transition pore. In addition, a sequence analysis of the mtDNA D-loop region indicated that AFB1 induces mtDNA damage. Mutations in the D-loop region interfere with a transcription of the entire mtDNA genome and possibly cause potent alterations in mitochondrial function [50].

In this paper, for the first time, we have demonstrated the molecular mechanism of mitochondrial disfunction induced by T-2 toxin. The damaging of mitochondrial DNA can be responsible for ATP synthesis disruption and can lead to cell death.

4. Materials and Methods

4.1. Reagents

Dimethyl sulfoxide (DMSO) and T-2 toxin from Fusarium sp. (cat. No T4887) were obtained from Sigma-Aldrich Chemical Co. (St. Louis, MO, USA). Dulbecco's modified Eagle medium (DMEM) with 4.5 g/L glucose and L-glutamine, heat-inactivated fetal bovine serum (FBS), penicillin–streptomycin mixture, and PBS (1X) without calcium or magnesium were purchased at Lonza (Basel, Switzerland). The 5,5′,6,6′-tetrachloro-1,1′,3,3′-tetraethylbenzimidazol-carbocyanine iodide (JC-1) probe, Hank's Balanced Salt Solution (HBSS), 2′,7′-dichlorodihydrofluorescein diacetate (H_2DCFDA) probe and JC-1 dye were from Thermo Fisher Scientific (Waltham, MA, USA). All other chemicals were of molecular grade or the highest quality available.

4.2. Cell Culture

In this study, the human foreskin fibroblast cell line Hs68 (ATCC® CRL-1635™), obtained from the American Type Culture Collection (ATCC™, Manassas, VA, USA), was used. The Hs68 cells were cultured in DMEM supplemented with 100 units of potassium penicillin and 100 μg of streptomycin sulphate per 1 mL of culture media, 10% (*v*/*v*) FBS and kept in an incubator with a 5% CO_2 atmosphere at 100% humidity and 37 °C.

4.3. Assessment of Mitochondrial Membrane Potential (MMP)

The MMP was assessed using tetraethylbenzimidazolylcarbocyanine iodide (JC-1) cationic carbocyanine dye, which accumulates in the mitochondrial membrane in a potential-dependent manner. A high potential of the inner mitochondrial membrane leads to the formation of dye aggregates. Depolarization and permeation of the mitochondrial membrane lead to a breakdown of aggregates into monomers emitting green fluorescence with excitation and emission values of 485 and 538 nm, respectively [33]. The cells used for

analysis were seeded into 96-well, black plates with transparent bottoms (Greiner Bio-One, Kremsmünster, Austria) at a density of 1×10^5 cells/well in 50 µL culture medium and allowed to adhere for 12 h. Next, cells were incubated with T-2 toxin in a concentration range of 0.001 to 100 µM for 24 and 48 h. The untreated cells were used as a control. After treatment, cells were preincubated for 30 min with 5 µM JC-1 dye in HBBS in a 5% CO_2 atmosphere at 37 °C. The cells were centrifuged (300× *g* for 10 min at 22 °C) and washed twice with the HBSS. The fluorescence was measured on a Bio-Tek Synergy HT Microplate Reader (Bio-Tek Instruments, Winooski, VT, USA), with filter pairs of 530/590 and 485/538 nm. The results are presented as a ratio of the aggregates to monomer fluorescence.

4.4. Assessment of Intracellular ROS Level

The relative level of intracellular ROS in cells was measured using the 2′,7′-dichlorodihydrofluorescein diacetate (H2DCFDA) dye. The nonpolar, cell-permeable H2DCFDA was diffused into cells and deacetylated by cellular esterase to the polar and membrane impermeable form 2′,7′-dichlorodihydrofluorescein (H2DCF). H2DCF is nonfluorescent, but in the presence of intracellular ROS, it rapidly oxidizes to highly fluorescent 2′,7′-dichlorofluorescein (DCF). The fluorescence intensity is proportional to the ROS levels within the cell cytosol [51]. The cells used for analysis were seeded into 96-well plates at 1×10^5 cells/well in 50 µL culture medium and cultured at 37 °C for 12 h in a 5% CO_2-containing environment. Next, the cells were treated with T-2 toxin in the concentration range 0.001 to 100 µM and incubated for 24 and 48 h. The untreated cells were used as the control. After treatment, the cells were incubated with 5 µM of 2′,7′-dichlorofluorescein diacetate (DCFH-DA) (prepared in Tyrode's Ca2+/Mg2+ free buffer) at 37 °C for 45 min. The fluorescence was measured at a 480 nm excitation wavelength and a 510 nm emission wavelength, using a Bio-Tek Synergy HT Microplate Reader (Bio-Tek Instruments, Winooski, VT, USA), and expressed as the intensity of the DCF fluorescence.

4.5. Isolation of Total Genomic DNA from Cell Lines

To perform the analysis, cells were seeded at 3×10^6 cells per well and left in the incubator for 12 h before the treatment procedures. Then, they were incubated with T-2 toxin (Sigma-Aldrich Chemical Co., St. Louis, MO, USA) in the concentration range 0.1 to 10 µM for 24 and 48 h. The working solutions of the T-2 toxin were made by the direct dilution of the toxin in culture medium. The untreated cells were used as the control. The total genomic DNA (mitochondrial and nuclear) from the cell pellets was isolated using the commercially available EXTRACT ME RNA & DNA KIT (BLIRT S.A., Gdansk, Poland), according to the producer's protocol. The DNA concentrations were determined by spectrophotometric measurement of the absorbance at 260 nm. The purities were calculated by a A260/A280 ratio using the Bio-Tek Synergy HT Microplate Reader (Bio-Tek Instruments, Winooski, VT, USA). The purified DNA was stored at −30 °C until further analysis.

4.6. Mitochondrial DNA Copy Number Quantification

The relative number of copies of human mtDNA using nDNA content as a standard was evaluated by quantitative real-time PCR (qRT-PCR). For quantification, two primer pairs for mtDNA detection (*ND1* and *ND5*) and two primer pairs for nDNA detection (SERPINA1 and SLCO2B1) were selected. All primers were designed with the Primer3 software (http://bioinfo.ut.ee/primer3-0.4.0/ (accessed on 15 July 2021)) and synthesized by Sigma-Aldrich Chemical Co. (St. Louis, MO, USA). Complete nucleotide sequences for each gene were obtained from the ENSEMBL database (https://ensembl.org/ (accessed on 15 July 2021)). The mitochondrial *ND1* (124 bp fragment size) and *ND5* genes (124 bp fragment size) were amplified using the pairs of primers (forward primer 5′-CCTAAAACCCGCCACATCTA-3′ and reverse primer 5′-GCCTAGGTTGAGGTTGACCA-3′; forward primer 5′-AGGCGCTATCACCACTCTGT-3′ and reverse primer 5′-TTGGTTGATGCCGATTGTAA-3′, respectively). The amount of nuclear DNA was determined using the SLCO2B1 (135 bp fragment size) and SERPINA1 (148 bp fragment size) genes as a reference: forward primer 5′-GATCCCAGCCAGTGGACTTA-3′, reverse primer:

5′-CCTGAAGCTGAGGAGACAGG-3′; forward primer 5′-TGCAGCTTCCTCTTCACAGA-3′ and reverse primer 5′-CTCAGCCCCAAGTATCTCCA-3′, respectively. The qRT-PCR was performed using a CFX96 Real-Time PCR Detection System (Bio-Rad Laboratories, Hercules, CA, USA). The qRT-PCR reaction mix was performed in a total volume of 10 µL with 1 × Power SYBR Green PCR Master Mix (Thermo Fisher Scientific, Waltham, MA, USA), 250 nM of each primer, and 1 µL (5 ng) of genomic DNA. The cycling sequence was as follows: enzyme activation at 95 °C for 10 min, then 40 cycles of 3 s denaturation at 95 °C, 30 s annealing at 65 °C, and 15 s extension at 72 °C, with plate reading at this step. The reactions were performed in duplicate and included a negative control (without template DNA). The cycle threshold (Ct) values were computed automatically and then analyzed using CFX Manager™ Software, version 3.1 (Bio-Rad Laboratories, Hercules, CA, USA). The relative nDNA copy number was calculated using the formula $2^{\Delta Ct1}$ and $^{\Delta Ct2}$, where ΔCt1 = Ct for SLCO2B1 − Ct for ND1; ΔCt2 = Ct for SERPINA1 − Ct for ND5. The relative mtDNA copy number was calculated using the formula $2^{\Delta Ct1}$ and $^{\Delta Ct2}$, where ΔCt1 = Ct for SLCO2B1 − Ct for ND1; ΔCt2 = Ct for SERPINA1 − Ct for ND5.

4.7. Determination of Mitochondrial DNA Damage

The assessment of the mtDNA damage was performed using a semi-long-run quantitative RT-PCR (SLR-qRT-PCR) [52]. The levels of DNA lesions in the tested region of the mitochondrial genome were measured using two fragments of different lengths (i.e., short and long fragments) located in the same mitochondrial genomic region. The sequences of all primers used in this study are listed in Table 1. All primers were designed using Primer3 software (http://bioinfo.ut.ee/primer3--0.4.0/ (accessed on 17 July 2021)) and synthesized by Sigma-Aldrich (St. Louis, MO, USA). The complete nucleotide sequences for each gene were taken from the ENSEMBL database (https://ensembl.org/ (accessed on 17 July 2021)).

Table 1. Specifications of the SLR-qRT-PCR primers used for the quantification of mitochondrial DNA damage.

Target Gene Symbol	Forward Primer Sequences (5′→3′)	Reverse Primer Sequence (5′→3′)	Amplicon Length (bp)
ND1 (mitochondrially encoded NADH: ubiquinone oxidoreductase core subunit 1)	Long fragment: ATGGC-CAACCTCCTACTCCT	Long fragment: GATGAGT-GTGCCTGCAAAGA	1214
	Small fragment: CCTAAAAC-CCGCCACATCTA	Small fragment: GCCTAG-GTTGAGGTTGACCA	124
ND5 (mitochondrially encoded NADH: ubiquinone oxidoreductase core subunit 5)	Long fragment: TCCAACT-CATGAGACCCACA	Long fragment: AGGTGAT-GATGGAGGTGGAG	1156
	Small fragment: AGGCGC-TATCACCACTCTGT	Small fragment: TTGGTTGAT-GCCGATTGTAA	124

The SLR-qRT-PCR amplification was performed using a CFX96 Real-Time PCR Detection System (Bio-Rad Laboratories, Hercules, CA, USA). The SLR-qRT-PCR reaction mix was performed in a total volume of 10 µL with 1 × Power SYBR Green PCR Master Mix (Thermo Fisher Scientific, Waltham, MA, USA), 250 nM of each primer, and 5 ng of template DNA. The PCR reaction conditions were enzyme activation at 95 °C for 10 min followed by up to 40 cycles of 15 s denaturation at 95 °C, 30 s annealing at 65 °C, and 15 s extension at 72 °C (for short amplicons) or 45 s at 72 °C (for long amplicons). The Ct values were computed automatically and then analyzed using CFX Manager™ software (version 3.1). The DNA damage was calculated as lesion per 10 kb DNA of each region, by including the size of a particularly long fragment. The following formula was used: lesion per 10 kb DNA = $(1 - 2^{-(\Delta long - \Delta short)}) \times 10{,}000$ (bp)/size of long fragment (bp), where Δlong and Δshort show differences in the Ct value between treated samples and nontreated

cells (control). The DNA isolated from the controls was used as a reference, while the Ct of the large and small mitochondrial fragments was used for the DNA damage quantification.

4.8. Data Analysis

All obtained experimental values were elaborated using Microsoft Excel software (Redmond, WA, USA) and stated as mean values ± standard deviations (SDs). The statistical analysis was performed using StatsDirect statistical software V. 2.7.2. (Cheshire, UK). All results were analyzed according to the normality of the distribution using the Shapiro–Wilk test. The results were examined according to equality of variance via Levene's test. The significance of the differences among the values was analyzed using ANOVA, Tukey's range test (for data with normal distribution and equality of variance), or the Kruskal–Wallis test; $p < 0.05$ was accepted as statistically significant [53,54].

5. Conclusions

We demonstrated for the first time that in an in vitro human skin fibroblast model, T-2 toxin has an influence on the physiological role of the fibroblast mitochondrial Hs68 cell line. Based on our current and previous observations, we conclude that T-2 toxin reduces the mitochondrial membrane potential and inhibits the production of ATP. The T-2 toxin-induced damage to mitochondrial functions is a probable major cause of necrotic death of Hs68 cells. The molecular mechanism of this toxic effect is related to mtDNA damage, leading to the maintenance of its integrity, which is critical for proper organellar function.

Author Contributions: Conceptualization, M.B., M.C., M.N. and E.S.; experiments, E.J.-K., M.B. and E.S.; writing—original draft preparation, E.J.-K. and M.B.; writing—review and editing, M.B., M.N. and T.S.; supervision, M.C. and M.B. All authors have read and agreed to the published version of the manuscript.

Funding: This study was funded by the National Science Centre of Poland, grant: 2020/37/N/NZ9/01678.

Institutional Review Board Statement: Not applicable.

Informed Consent Statement: Not applicable.

Data Availability Statement: Not applicable.

Conflicts of Interest: The authors declare no conflict of interest.

References

1. Osellame, L.D.; Blacker, T.S.; Duchen, M.R. Cellular and molecular mechanisms of mitochondrial function. *Best Pract. Res. Clin. Endocrinol. Metab.* **2012**, *26*, 711–723. [CrossRef]
2. Lin, Y.-T.; Lin, K.-H.; Huang, C.-J.; Wei, A.-C. MitoTox: A comprehensive mitochondrial toxicity database. *BMC Bioinform.* **2021**, *22*, 369. [CrossRef]
3. Gammage, P.A.; Frezza, C. Mitochondrial DNA: The overlooked oncogenome? *BMC Biol.* **2019**, *17*, 53. [CrossRef] [PubMed]
4. Yuan, Y.; Ju, Y.S.; Kim, Y.; Li, J.; Wang, Y.; Yoon, C.J.; Yang, Y.; Martincorena, I.; Creighton, C.J.; Weinstein, J.N.; et al. Comprehensive molecular characterization of mitochondrial genomes in human cancers. *Nat. Genet.* **2020**, *52*, 342–352. [CrossRef] [PubMed]
5. Zorova, L.D.; Popkov, V.A.; Plotnikov, E.Y.; Silachev, D.N.; Pevzner, I.B.; Jankauskas, S.S.; Babenko, V.A.; Zorov, S.D.; Balakireva, A.V.; Juhaszova, M.; et al. Mitochondrial membrane potential. *Anal. Biochem.* **2018**, *552*, 50–59. [CrossRef]
6. Ricci, J.-E.; Muñoz-Pinedo, C.; Fitzgerald, P.; Bailly-Maitre, B.; Perkins, G.A.; Yadava, N.; Scheffler, I.E.; Ellisman, M.H.; Green, D.R. Disruption of Mitochondrial Function during Apoptosis Is Mediated by Caspase Cleavage of the p75 Subunit of Complex I of the Electron Transport Chain. *Cell* **2004**, *117*, 773–786. [CrossRef]
7. Alpert, N.M.; Guehl, N.; Ptaszek, L.; Pelletier-Galarneau, M.; Ruskin, J.; Mansour, M.C.; Wooten, D.; Ma, C.; Takahashi, K.; Zhou, Y.; et al. Quantitative in vivo mapping of myocardial mitochondrial membrane potential. *PLoS ONE* **2018**, *13*, e0190968. [CrossRef] [PubMed]
8. Taanman, J.-W. The mitochondrial genome: Structure, transcription, translation and replication. *Biochim. Biophys. Acta BBA-Bioenergies* **1999**, *1410*, 103–123. [CrossRef]
9. Fernández-Silva, P.; Enriquez, J.A.; Montoya, J. Replication and transcription of mammalian mitochondrial dna. *Exp. Physiol.* **2003**, *88*, 41–56. [CrossRef]
10. Fazzini, F.; Schöpf, B.; Blatzer, M.; Coassin, S.; Hicks, A.A.; Kronenberg, F.; Fendt, L. Plasmid-normalized quantification of relative mitochondrial DNA copy number. *Sci. Rep.* **2018**, *8*, 15347. [CrossRef]

11. Bottje, W. Chapter 4—Mitochondrial physiology. In *Sturkie's Avian Physiology*, 6th ed.; Colin, G., Ed.; Scanes; Academic Press: San Diego, CA, USA, 2015; pp. 39–51.
12. Luo, S.; Valencia, C.A.; Zhang, J.; Lee, N.-C.; Slone, J.; Gui, B.; Wang, X.; Li, Z.; Dell, S.; Brown, J.; et al. Biparental inheritance of mitochondrial DNA in humans. *Proc. Natl. Acad. Sci. USA* **2018**, *115*, 13039–13044. [CrossRef]
13. Nayakwadi, S.; Ramu, R.; Sharma, A.K.; Gupta, V.K.; Rajukumar, K.; Kumar, V.; Shirahatti, P.S.; L., R.; Basalingappa, K.M. Toxicopathological studies on the effects of T-2 mycotoxin and their interaction in juvenile goats. *PLoS ONE* **2020**, *15*, e0229463. [CrossRef] [PubMed]
14. Ji, F.; He, D.; Olaniran, A.O.; Mokoena, M.P.; Xu, J.; Shi, J. Occurrence, toxicity, production and detection of fusarium mycotoxin: A review. *Food Prod. Process. Nutr.* **2019**, *1*, 6. [CrossRef]
15. EFSA Panel on Contaminants in the Food Chain (CONTAM); Knutsen, H.; Barregård, L.; Bignami, M.; Brüschweiler, B.; Ceccatelli, S.; Cottrill, B.; Dinovi, M.; Edler, L.; Grasl-Kraupp, B.; et al. Appropriateness to set a group health based guidance value for T2 and HT2 toxin and its modified forms. *EFSA J.* **2017**, *15*, e04655. [CrossRef] [PubMed]
16. Szabó, R.T.; Kovács-Weber, M.; Balogh, K.M.; Mézes, M.; Kovács, B. Changes of DNA damage effect of T-2 or deoxynivalenol toxins during three weeks exposure in common carp (*Cyprinus carpio* L.) revealed by LORD-Q PCR. *Toxins* **2021**, *13*, 576. [CrossRef] [PubMed]
17. Wu, Q.; Qin, Z.; Kuca, K.; You, L.; Zhao, Y.; Liu, A.; Musilek, K.; Chrienova, Z.; Nepovimova, E.; Oleksak, P.; et al. An update on T-2 toxin and its modified forms: Metabolism, immunotoxicity mechanism, and human exposure assessment. *Arch. Toxicol.* **2020**, *94*, 3645–3669. [CrossRef] [PubMed]
18. Adhikari, M.; Negi, B.; Kaushik, N.; Adhikari, A.; Al-Khedhairy, A.A.; Kaushik, N.K.; Choi, E.H. T-2 mycotoxin: Toxicological effects and decontamination strategies. *Oncotarget* **2017**, *8*, 33933–33952. [CrossRef]
19. Janik, E.; Niemcewicz, M.; Podogrocki, M.; Ceremuga, M.; Stela, M.; Bijak, M. T-2 toxin—The most toxic trichothecene mycotoxin: Metabolism, toxicity, and decontamination strategies. *Molecules* **2021**, *26*, 6868. [CrossRef]
20. Wannemacher, R.W.; Wiener, S.L.; Sidell, F.R.; Takafuji, E.T.; Franz, D.R. Trichothecene mycotoxins. *Med. Asp. Chem. Biol. Warf.* **1997**, *6*, 655–676.
21. Escrivá, L.; Font, G.; Manyes, L. In vivo toxicity studies of fusarium mycotoxins in the last decade: A review. *Food Chem. Toxicol.* **2015**, *78*, 185–206. [CrossRef]
22. Kiš, M.; Vulić, A.; Kudumija, N.; Šarkanj, B.; Tkalec, V.J.; Aladić, K.; Škrivanko, M.; Furmeg, S.; Pleadin, J. A Two-Year Occurrence of *Fusarium* T-2 and HT-2 Toxin in Croatian Cereals Relative of the Regional Weather. *Toxins* **2021**, *13*, 39. [CrossRef] [PubMed]
23. Chaudhari, M.; Jayaraj, R.; Bhaskar, A.S.B.; Lakshmana Rao, P.V. Oxidative stress induction by T-2 toxin causes DNA damage and triggers apoptosis via caspase pathway in human cervical cancer cells. *Toxicology* **2009**, *262*, 153–161. [CrossRef] [PubMed]
24. Frankič, T.; Pajk, T.; Rezar, V.; Levart, A.; Salobir, J. The role of dietary nucleotides in reduction of DNA damage induced by T-2 toxin and deoxynivalenol in chicken leukocytes. *Food Chem. Toxicol.* **2006**, *44*, 1838–1844. [CrossRef] [PubMed]
25. Zhang, Y.F.; Yang, J.Y.; Li, Y.K.; Zhou, W. Toxicity and oxidative stress induced by T-2 toxin in cultured mouse Leydig cells. *Toxicol. Mech. Methods* **2017**, *27*, 100–106. [CrossRef]
26. Chatterjee, N.; Walker, G.C. Mechanisms of DNA damage, repair, and mutagenesis. *Environ. Mol. Mutagen.* **2017**, *58*, 235–263. [CrossRef]
27. Hsu, C.-C.; Lee, H.-C.; Wei, Y.-H. Mitochondrial DNA alterations and mitochondrial dysfunction in the progression of hepatocellular carcinoma. *World J. Gastroenterol.* **2013**, *19*, 8880–8886. [CrossRef]
28. Amorim, A.; Fernandes, T.; Taveira, N. Mitochondrial DNA in human identification: A review. *PeerJ* **2019**, *7*, e7314. [CrossRef]
29. Dannenmann, B.; Lehle, S.; Lorscheid, S.; Huber, S.M.; Essmann, F.; Schulze-Osthoff, K. Simultaneous quantification of DNA damage and mitochondrial copy number by long-run DNA-damage quantification (LORD-Q). *Oncotarget* **2017**, *8*, 112417–112425. [CrossRef]
30. Movassaghi, S.; Jafari, S.; Falahati, K.; Ataei, M.; Sanati, M.H.; Jadali, Z. Quantification of mitochondrial DNA damage and copy number in circulating blood of patients with systemic sclerosis by a qPCR-based assay. *An. Bras. Dermatol.* **2020**, *95*, 314–319. [CrossRef]
31. Mutlu, A.G. Increase in mitochondrial DNA copy number in response to ochratoxin a and methanol-induced mitochondrial DNA damage in drosophila. *Bull. Environ. Contam. Toxicol.* **2012**, *89*, 1129–1132. [CrossRef]
32. Janik-Karpinska, E.; Ceremuga, M.; Wieckowska, M.; Szyposzynska, M.; Niemcewicz, M.; Synowiec, E.; Sliwinski, T.; Bijak, M. Direct T-2 toxicity on human skin—Fibroblast Hs68 cell line—In vitro study. *Int. J. Mol. Sci.* **2022**, *23*, 4929. [CrossRef] [PubMed]
33. Bijak, M.; Synowiec, E.; Sitarek, P.; Sliwiński, T.; Saluk-Bijak, J. Evaluation of the cytotoxicity and genotoxicity of flavonolignans in different cellular models. *Nutrients* **2017**, *9*, 1356. [CrossRef] [PubMed]
34. Lemasters, J.J.; Nieminen, A.-L.; Qian, T.; Trost, L.C.; Elmore, S.P.; Nishimura, Y.; Crowe, R.A.; Cascio, W.E.; Bradham, C.A.; Brenner, D.A.; et al. The mitochondrial permeability transition in cell death: A common mechanism in necrosis, apoptosis and autophagy. *Biochim. Biophys. Acta BBA-Bioenerg.* **1998**, *1366*, 177–196. [CrossRef] [PubMed]
35. Zorov, D.B.; Juhaszova, M.; Sollott, S.J. Mitochondrial reactive oxygen species (ROS) and ROS-induced ROS release. *Physiol. Rev.* **2014**, *94*, 909–950. [CrossRef]
36. Rooney, J.P.; Ryde, I.T.; Sanders, L.H.; Howlett, E.H.; Colton, M.D.; Germ, K.E.; Mayer, G.D.; Greenamyre, J.T.; Meyer, J.N. PCR based determination of mitochondrial DNA copy number in multiple species. *Methods Mol. Biol.* **2015**, *1241*, 23–38. [CrossRef]

37. Spikings, E.C.; Alderson, J.; John, J.C.S. Regulated mitochondrial DNA replication during oocyte maturation is essential for successful porcine embryonic development. *Biol. Reprod.* **2007**, *76*, 327–335. [CrossRef]
38. Cline, S.D. Mitochondrial DNA damage and its consequences for mitochondrial gene expression. *Biochim. Biophys. Acta BBA-Gene Regul. Mech.* **2012**, *1819*, 979–991. [CrossRef] [PubMed]
39. Hershberger, K.A.; Rooney, J.P.; Turner, E.A.; Donoghue, L.J.; Bodhicharla, R.; Maurer, L.L.; Ryde, I.T.; Kim, J.J.; Joglekar, R.; Hibshman, J.D.; et al. Early-life mitochondrial DNA damage results in lifelong deficits in energy production mediated by redox signaling in Caenorhabditis elegans. *Redox Biol.* **2021**, *43*, 102000. [CrossRef]
40. Thangaraj, K.; Khan, N.A.; Govindaraj, P.; Meena, A.K. Mitochondrial disorders: Challenges in diagnosis & treatment. *Indian J. Med. Res.* **2015**, *141*, 13–26. [CrossRef]
41. Kim, H.; Komiyama, T.; Inomoto, C.; Kamiguchi, H.; Kajiwara, H.; Kobayashi, H.; Nakamura, N.; Terachi, T. Mutations in the Mitochondrial ND1 Gene Are Associated with Postoperative Prognosis of Localized Renal Cell Carcinoma. *Int. J. Mol. Sci.* **2016**, *17*, 2049. [CrossRef]
42. Shigenobu, Y.; Yoneda, M.; Kurita, Y.; Ambe, D.; Saitoh, K. Population subdivision of Japanese flounder paralichthys olivaceus in the Pacific coast of Tohoku Japan detected by means of mitochondrial phylogenetic information. *Int. J. Mol. Sci.* **2013**, *14*, 954–963. [CrossRef] [PubMed]
43. Passarella, S.; Schurr, A.; Portincasa, P. Mitochondrial Transport in Glycolysis and Gluconeogenesis: Achievements and Perspectives. *Int. J. Mol. Sci.* **2021**, *22*, 12620. [CrossRef] [PubMed]
44. P Pace, J.G.; Watts, M.R.; Canterbury, W.J. T-2 mycotoxin inhibits mitochondrial protein synthesis. *Toxicon* **1988**, *26*, 77–85. [CrossRef]
45. Ngampongsa, S.; Hanafusa, M.; Ando, K.; Ito, K.; Kuwahara, M.; Yamamoto, Y.; Yamashita, M.; Tsuru, Y.; Tsubone, H. Toxic effects of T-2 toxin and deoxynivalenol on the mitochondrial electron transport system of cardiomyocytes in rats. *J. Toxicol. Sci.* **2013**, *38*, 495–502. [CrossRef]
46. Fatima, Z.; Guo, P.; Huang, D.; Lu, Q.; Wu, Q.; Dai, M.; Cheng, G.; Peng, D.; Tao, Y.; Ayub, M.; et al. The critical role of p16/Rb pathway in the inhibition of GH3 cell cycle induced by T-2 toxin. *Toxicology* **2018**, *400–401*, 28–39. [CrossRef] [PubMed]
47. Wu, J.; Jing, L.; Yuan, H.; Peng, S.-Q. T-2 toxin induces apoptosis in ovarian granulosa cells of rats through reactive oxygen species-mediated mitochondrial pathway. *Toxicol. Lett.* **2011**, *202*, 168–177. [CrossRef]
48. Liu, J.; Wang, L.; Guo, X.; Pang, Q.; Wu, S.; Wu, C.; Xu, P.; Bai, Y. The role of mitochondria in T-2 toxin-induced human chondrocytes apoptosis. *PLoS ONE* **2014**, *9*, e108394. [CrossRef]
49. Dai, C.; Xiao, X.; Sun, F.; Zhang, Y.; Hoyer, D.; Shen, J.; Tang, S.; Velkov, T. T-2 toxin neurotoxicity: Role of oxidative stress and mitochondrial dysfunction. *Arch. Toxicol.* **2019**, *93*, 3041–3056. [CrossRef] [PubMed]
50. Shi, D.; Liao, S.; Guo, S.; Li, H.; Yang, M.; Tang, Z. Protective effects of selenium on aflatoxin B1-induced mitochondrial permeability transition, DNA damage, and histological alterations in duckling liver. *Biol. Trace Elem. Res.* **2015**, *163*, 162–168. [CrossRef]
51. Smiałowski, A.; Bijak, M. Repeated imipramine treatment increases the responsivity of the rat hippocampus to dopamine. An in vitro study. *J. Neural Transm.* **1986**, *66*, 187–196. [CrossRef]
52. Rothfuss, O.; Gasser, T.; Patenge, N. Analysis of differential DNA damage in the mitochondrial genome employing a semi-long run real-time pcr approach. *Nucleic Acids Res.* **2010**, *38*, e24. [CrossRef] [PubMed]
53. Bijak, M.; Saluk, J.; Antosik, A.; Ponczek, M.B.; Zbikowska, H.M.; Borowiecka, M.; Nowak, P. Aronia melanocarpa as a protector against nitration of fibrinogen. *Int. J. Biol. Macromol.* **2013**, *55*, 264–268. [CrossRef] [PubMed]
54. Zbikowska, H.M.; Antosik, A.; Szejk, M.; Bijak, M.; Olejnik, A.K.; Saluk, J.; Nowak, P. Does Quercetin Protect Human Red Blood Cell Membranes against Γ-irradiation? *Redox Rep.* **2014**, *19*, 65–71. [CrossRef] [PubMed]

Article

DNA damage induced by T-2 Mycotoxin in Human Skin Fibroblast Cell Line – Hs68

Edyta Janik-Karpinska[1] (E.J.K.), Michal Ceremuga[2] (M.C.), Marcin Niemcewicz[1] (M.N.), Ewelina Synowiec[3] (E.S.), Tomasz Sliwinski[3] (T.S.) and Michal Bijak[1*] (M.B.)

[1]Biohazard Prevention Centre, Faculty of Biology and Environmental Protection, University of Lodz, Pomorska 141/143, 90-236 Lodz, Poland.
[2]Military Institute of Armament Technology, Prymasa Stefana Wyszyńskiego 7, 05-220 Zielonka, Poland
[3]Laboratory of Medical Genetics, Faculty of Biology and Environmental Protection, University of Lodz, Pomorska 141/143, 90-236 Lodz, Poland.
* Correspondence: The corresponding author: michal.bijak@biol.uni.lodz.pl

Abstract

T-2 mycotoxin is the most potent representative of the trichothecene group A and is produced by various Fusarium species including F. sporotrichioides, F. poae and F. acuminatum. T-2 toxin has been reported to have toxic effects on various tissues and organs and alike humans and animals suffer a variety of pathological conditions after consumption of mycotoxin contaminated food. The T-2 toxin unique feature is dermal toxicity characterized by skin inflammation. In this in vitro study we investigated the molecular mechanism of T-2 toxin induced genotoxicity in human skin fibroblast - Hs68 cell line. For the purpose of investigation, the cells were treated with T-2 toxin in 0.1; 1 and 10 μM concentrations and incubated for 24 h and 48 h. The alkaline comet assay results showed that, T-2 toxin induces DNA alkali-labile sites. The DNA strand breaks in cells and the DNA damage level is correlated with the increasing concentration and time of exposure to T-2 toxin. The evaluation of nuclear DNA damage revealed that exposure to toxin resulted in increasing lesion frequency in Hs68 cells HPRT1 and TP53 genes. Further analysis were focused on mRNA expression changes in two groups of genes: involved in inflammatory and repair process. The level of mRNA increased for all examined inflammatory genes (TNF, INFG, IL1A and IL1B). In the second group of genes related with the repair process, the changes of expression induced by toxin in genes – LIG3 and APEX was observed. The level of mRNA for LIG3 decreased, while for APEX increased. In the case of LIG1, FEN and XRCC1 no changes in mRNA level between the control and T-2 toxin probes were observed. Additional, in silico molecular docking analysis exhibited that T-2 toxin has a strong affinity to interact with the major groove of the DNA double helix. In conclusion, the results of this study indicate that T-2 toxin shows genotoxic effects on Hs68 cells, and the molecular mechanism of this toxic effect is related to nDNA damage.

Keywords: T-2 toxin; skin; Hs68 cell line; genotoxicity; DNA

1. Introduction

Trichothecene mycotoxins are produced mainly by *Fusarium* species and are common contaminants found in various cereals, including wheat, maize, barley, and other agricultural products. Therefore, there is a major health and food safety concern due to their toxicity to both humans and animals [1]. T-2-toxin is the most toxic representative of the trichothecene group A and is produced by different *Fusarium* species such as *F. sporotrichioides*, *F. acuminatum* and *F. poae* It is extremely high chemically stable under various environmental conditions like high temperature and UV light. What is more, the T-2 toxin inactivation during feed production and processing is not always effective. The T-2 toxin lipophilic nature suggests that, it is easily absorbed through the intestines, pulmonary mucosa and skin [2]. Numerous *in vitro* and *in vivo* studies showed that exposure to T-2 toxin can cause various organ damage, including liver [3], kidney [4], intestines [5], brain [6], and reproductive system In addition, unlike most biological toxins, T-2-mycotoxin is characterized by possessing highly irritating effect on the skin [7]. In our previous study [8] performed on human skin fibroblast Hs68 cell line, the T-2 toxin cytotoxic effect was demonstrated . This study clearly indicated that, the T-2 toxin induces necrosis as a toxicity effect in *in vitro* human skin model. A variety of mechanisms of action have been proposed for T-2 toxin. At the molecular level, T-2 toxin inhibits the protein synthesis by binding peptidyl transferase, which is an integral part of the 60S ribosomal subunit. The inhibition of DNA and RNA biosynthesis by T-2 toxin were also observed [9]. T-2 toxin interferes with metabolism of phospholipids membrane, and increases the level of liver lipid peroxides [10]. Studies showed that toxin also inhibits the mitochondrial function, mitochondrial electron transport system and mitochondrial protein synthesis [11]. *In vitro* study also revealed cell membrane disruption and toxic effect of cell division and cell proliferation after T-2 toxin exposure [12].

A number of studies have suggested that T-2 mycotoxin may induce DNA damage and apoptosis. Chaudhari et al. investigated the molecular mechanisms of DNA damage induced by T-2 toxin and apoptosis in human cervical cancer (HeLa) cell line. The obtained results showed increased levels of mitochondrial apoptogenic factors Bax, Bcl-2 and cytochrome-c followed by activation of caspases-3, -7 and -9, leading to DNA fragmentation and apoptosis. Moreover, caspase-independent apoptosis-inducing factor (AIF) pathway also leads to DNA fragmentation and apoptosis in T-2 toxin treated HeLa cells [13]. In different study, the impact of T-2 toxin on reproductive cells using TM3 Leydig cells was investigated. DNA condensation and fragmentation were clearly observed in TM3 Leydig cells treated with T-2 toxin. According to the results, T-2 toxin inhibited cell proliferation and induced cell membrane and DNA damage, which led to increase apoptosis in treated cells [14]. *In vivo* study provided the evidence that T-2 toxin is genotoxic to pig lymphocytes at concentration of 3 mg/kg feed leading to the lymphocyte DNA fragmentation [15]. Similar results were obtained in experiment on chickens, where T-2 toxin caused DNA fragmentation in spleen leukocytes, when added at concentration of 10 mg/kg feed [16]. Different study results indicated dose-dependent impaired performance and DNA fragmentation in spleen leukocytes of broiler chickens induced by T-2 toxin [17]. Szabo et al. analyzed the T-2 toxin genotoxic effect in broiler chicken hepatocytes. The aim of this study was to evaluate the effect of mycotoxin resulted in DNA damage in chicken liver cells. Results showed the potential T-2 toxin DNA damaging effect after 14 days of exposure [18].

Although T-2 toxin has adverse effects on different tissues and organs, its molecular effects and mechanism of action on the skin still remain unknown. The objective of this study was to investigate the T-2 effects resulted in DNA damage in the *in vitro* model using normal human fibroblast Hs68 cell line.

2. Results

2.1. DNA damage – comet assay

The level of DNA damage induced by T-2 toxin in Hs68 cell line was determined using an alkaline version of the comet assay, which measure the amount of DNA alkali-labile sites and strand breaks. Significantly higher DNA damage was noticed after treatment of the Hs68 cells with T-2 toxin ($p < 0.05$) (Figure 1). The increasing DNA damages has been demonstrated as an increasing % of DNA in comet tail and decreasing of % DNA in head. The dose-dependent manner as well as time-dependent manner were observed.

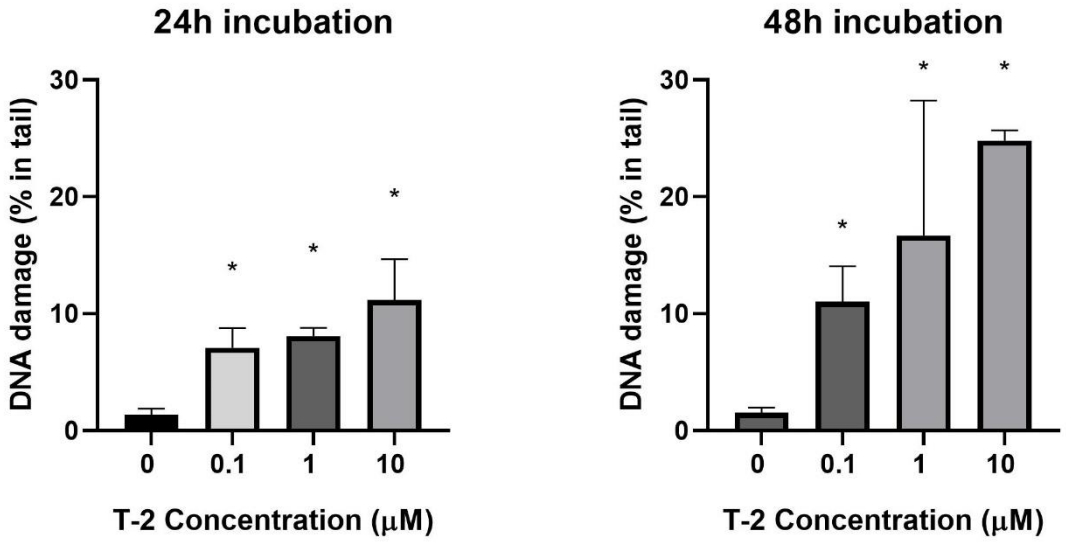

Figure 1. Mean level of DNA strand breaks, alkali-labile sites and oxidative DNA damage induced by T-2 toxin in Hs68 cells. Values present means ± SD (n = 6). * $p < 0.05$.

2.2. Determination of Nuclear DNA Damage—Semi-Long Run qRT-PCR (SLR-qRT-PCR)

As a next evaluation of T-2 toxin genotoxicity, the determination in nDNA damages in the HPRT1 and TP53 regions was performed. The nDNA damage by SLR-qRT-PCR amplification of DNA isolated from cells exposed to T-2 toxin at concentrations of 0.1; 1 and 10 μM in two incubation periods - 24h and 48h were examined. It was observed that treatment of Hs68 cells by T-2 toxin in a dose- and time-dependent manner increased the level of nDNA damage in both tested nDNA regions – hypoxanthine-guanine phosphoribosyltransferase 1 (HPRT1) (Figure 2A) and the tumor suppressor protein p53 (TP53) (Figure 2B). No significant difference in the level of damage was found between evaluated regions. In both tested genes in case of probes treated by T-2 toxin at concentration 10 μM after 48 hours the maximum of calculation possibilities (the highest attempts measurements) were obtained.

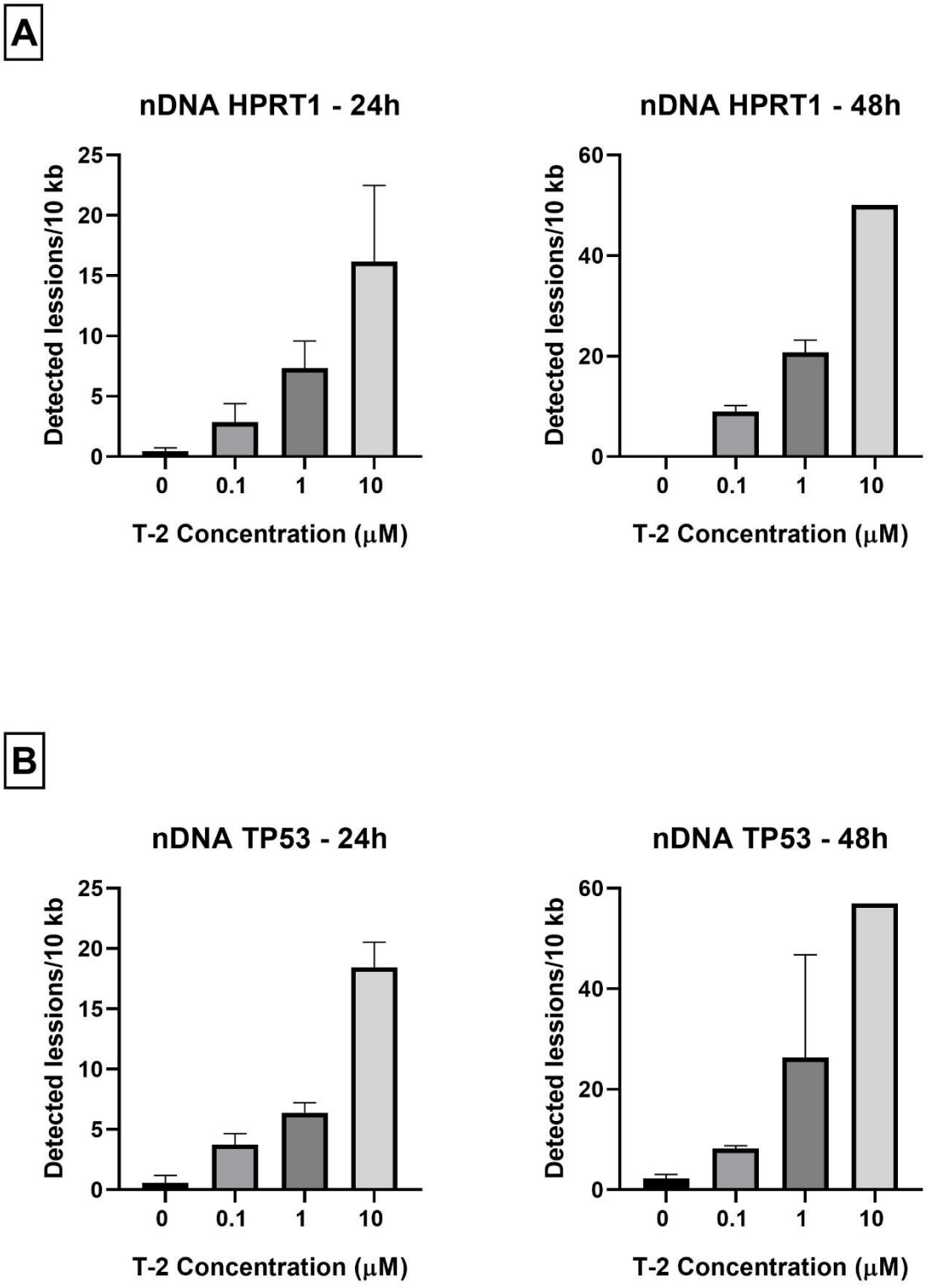

Figure 2 (A, B). The effect of T-2 toxin on nDNA lesion frequency per 10 kb DNA in HPRT1 and TP53 genes, estimated by SLR-qRT-PCR amplification of total DNA from Hs68 cells. Values present means ± SD (n = 6). * $p < 0.05$.

2.3. Analysis of Gene Expression

In order to evaluate the effect of T-2 toxin on expression of important in DNA damages genes, a gene expression analysis at the mRNA level using the Real-Time PCR method were performed. The

evaluation of changes in mRNA expression of two group of genes was executed. First were the inflammatory genes: Tumor Necrosis Factor (TNF), Interferon Gamma (INFG), Interleukin 1 alpha (IL1A) and Interleukin 1 beta (IL1B). The second group was related with DNA repair process – DNA LIGASE 1 (LIG1), DNA LIGASE 3 (LIG3), Flap Structure-Specific Endonuclease (FEN), X-Ray Repair Cross Complementing 1 (XRCC1) and Apurinic/Apyrimidinic Endodeoxyribonuclease (APEX). The results presented on Figure 3A-D demonstrate that T-2 toxin in a dose- and time-dependent manner increased the level of mRNA for TNF, INFG, IL1A and IL1B. In case of INFG gene it was detected in probes without T-2 toxin and probes treated by T-2 toxin at the lowest concentration (0,1 μM) however the mRNA was detected in probes treated by T-2 toxin at the lowest concentration of 1 and 10 μM in both incubation periods – 24 h and 48 h (Figure 3B).

In the next group of genes (Figure 4A-E) the changes of expression induced by T-2 toxin in two of them – LIG3 and APEX was observed. The level of mRNA for LIG3 decreasing in a dose-dependent manner (Figure 4B), while for APEX increasing of mRNA level (Figure 4E). In the case of LIG1 (Figure 4A), FEN (Figure 4C) and XRCC1 (Figure 4D) the were no changes in mRNA level between the control and T-2 toxin probes.

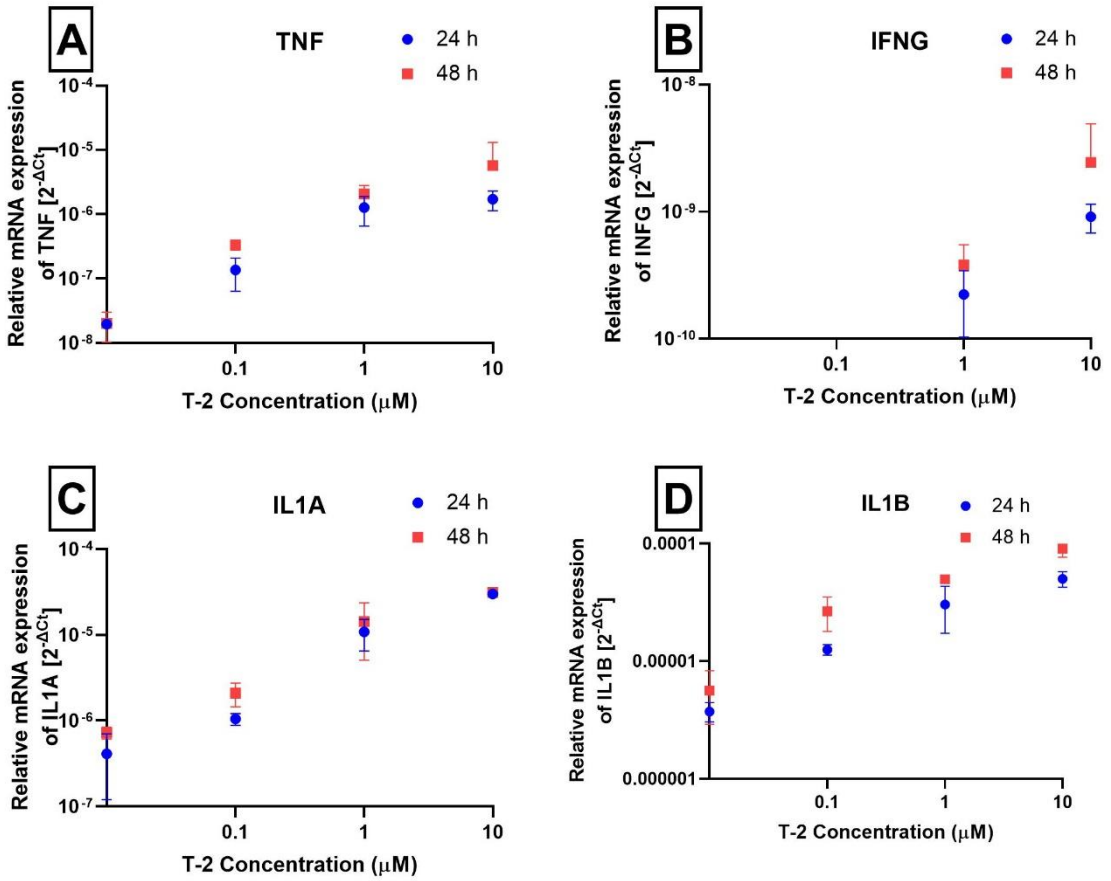

Figure 3. The effect of T-2 toxin on the expression of INF (A), IFNG (B), IL1 (C) and IL1B (D) genes (measured at the mRNA level). The results are expressed as a mean of $2^{-\Delta Ct}$ (according to the reference gene - 18S rRNA) ± SD, n=6.

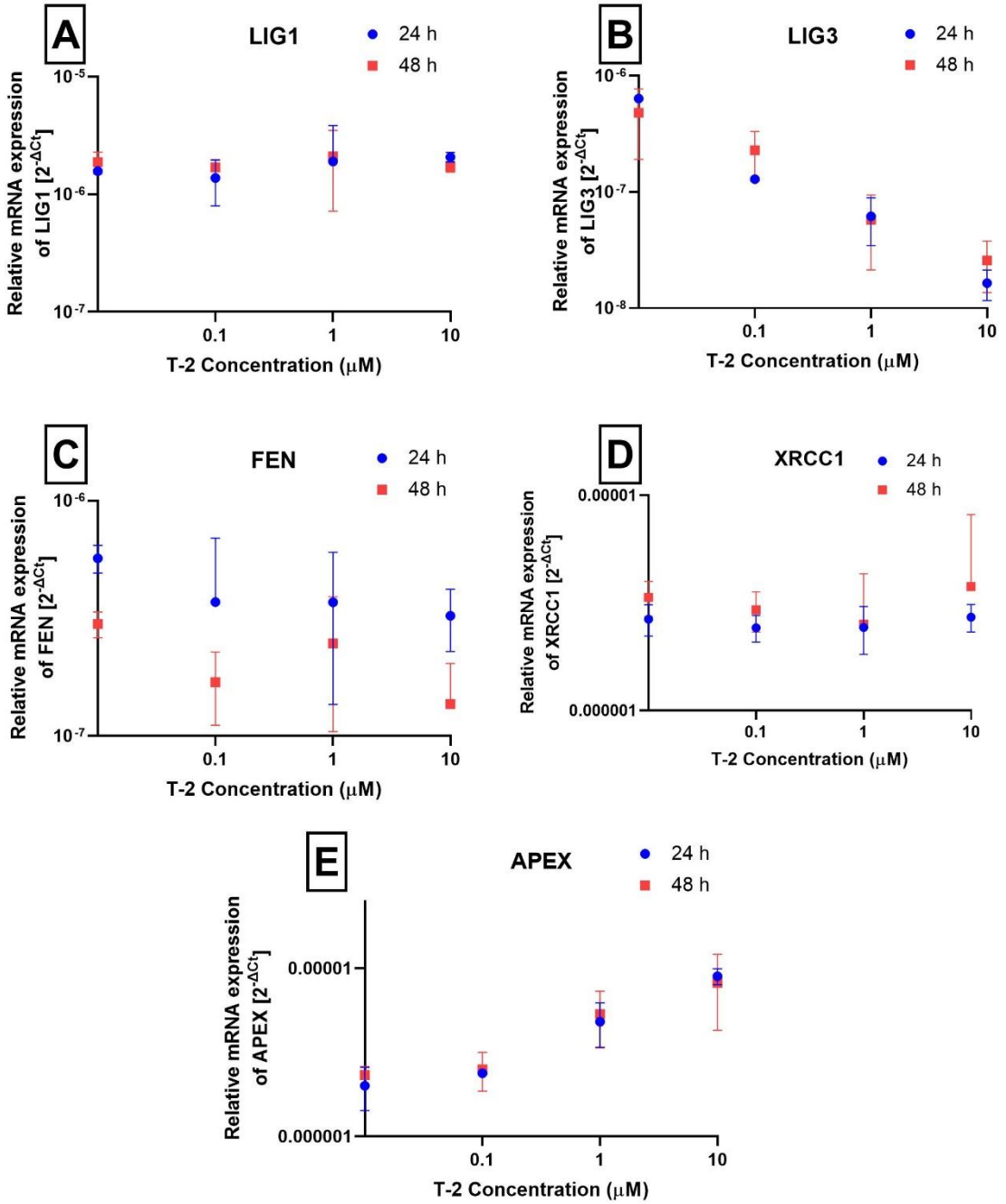

Figure 4. The effect of T-2 toxin on the expression of LIG1 (A), LIG3 (B), FEN (C) XRCC1 (D) and APEX (E) genes (measured at the mRNA level). The results are expressed as a mean of $2^{-\Delta Ct}$ (according to the reference gene - 18S rRNA) ± SD, n=6.

2.4. In silico molecular docking

In our *in silico* study, computer-generated models of interaction DNA structure and T-2 toxin was created. Due to the availability of only small DNA fragments in the databases of 3D structures, 3 different structures were docked – 1BDZ [19], 3AAF [20] and 6O3T [21]. For each of these structure T-2 toxin showed a very strong affinity and generated structural conformer thermodynamically favorably attached to the Eukaryotic DNA structures. The Table 2 shows the numerical values of the obtained affinities of T-2 toxin for the individual DNA structures.

Table 2. The affinity of T-2 toxin to DNA structures. Results (affinity in kcal/mol) were obtained during analysis with Autodock Vina 1.0 algorithm [15].

Generated conformer	1BDZ structure (affinity in kcal/mol)	3AAF structure (affinity in kcal/mol)	6O3T structure (affinity in kcal/mol)
1	-6.0	-5.0	-6.0
2	-5.7	-4.9	-5.7
3	-5.6	-4.7	-5.7
4	-5.4	-4.7	-5.1
5	-5.4	-4.6	-5.0
6	-5.3	-4.4	-5.0
7	-5.3	-4.3	-4.8
8	-5.2	-4.2	-4.8
9	-5.2	-4.2	-4.8

As a reference point for the obtained affinity values for the T-2, the reference compound toxic to the DNA structure were performed. For these analyses, sulfur mustard was selected, which possess the ability to attach to DNA molecules (the so-called alkylating compound). The obtained affinity values for sulfur mustard (numbers given below in table 3) are much lower (oscillating around -2 kcal/mol) than those of T-2 toxin.

Table 3. The affinity of sulfur mustard to DNA structures. Results (affinity in kcal/mol) were obtained during analysis with Autodock Vina 1.0 algorithm [15].

Generated conformer	1BDZ structure (affinity in kcal/mol)	3AAF structure (affinity in kcal/mol)	6O3T structure (affinity in kcal/mol)
1	-2.5	-2.1	-2.3
2	-2.3	-2.0	-2.1
3	-2.3	-2.0	-2.1
4	-2.0	-1.9	-2.0
5	-1.9	-1.9	-2.0
6	-1.9	-1.9	-1.9
7	-1.9	-1.8	-1.9

8	-1.9	-1.8	-1.9
9	-1.9	-1.7	-1.8

Detailed analysis of the mycotoxin binding site within the DNA molecule shows that mycotoxin T-2 has a strong affinity to interact with the major groove of the DNA double helix. On the example of the DNA structure - 1BDZ, it was observed that all conformers were joined within this site in double-stranded DNA. An example of such interaction is presented in Figure 5.

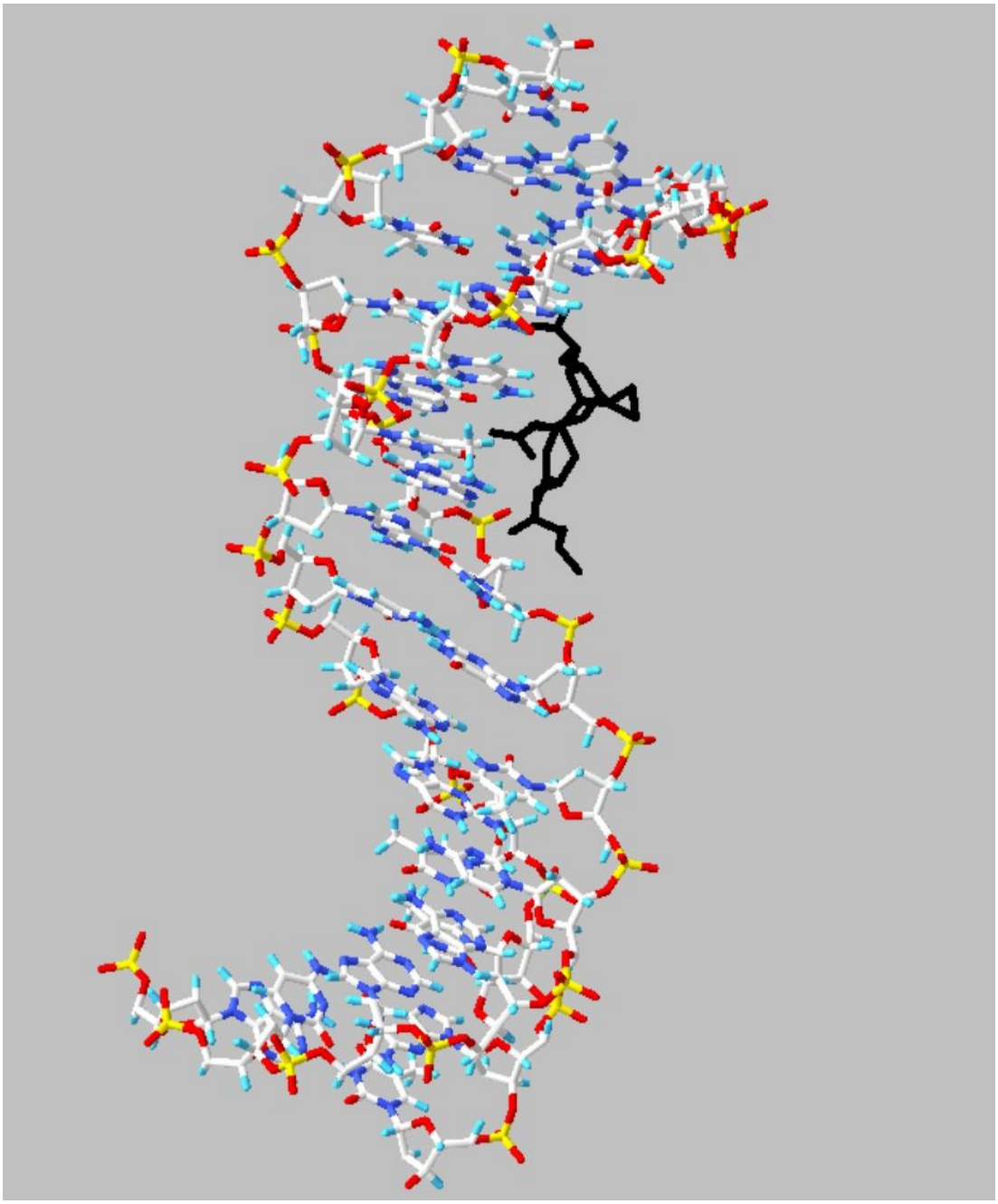

Figure 5. 3D structures of the DNA - T-2 toxin binding site. The DNA fragment crystal structure (PDB: 1 BDZ) was taken from the RCSB PDB databank (http://www.rcsb.org/). 3D ligand structure was obtained from the PubChem website (http://pubchem.ncbi.nlm.nih.gov/). Autodock Vina 1.0 together with Autodock Tools v 1.5.6rc1 software

was used for docking. Visualization of the docking results (conformation with the highest affinity), was rendered using Swiss-PdbViewer.

3. Discussion

The T-2 toxin possess harmful toxic effects on humans and animals [12,22]. Although various studies have examined DNA damage in different *in vitro* and *in vivo* models [3,13,23,24], no reports have focused on this effects of T-2 toxin on human skin. Herein, we report that T-2 toxin induces nuclear DNA damages in human Hs68 cell lines.

DNA is the basic unit of inheritance and a template for the processes of replication and transcription, making the maintenance of genetic stability crucial for viability. It is also an intrinsically reactive molecule and is highly susceptible to chemical modifications by various endogenous and exogenous (environmental) agents [25]. DNA damage is a common phenomenon for every cell during its lifetime and is defined as a change in the chemical structure of genomic DNA. Most of the endogenous DNA damage arises from the chemically active DNA involved in oxidative and hydrolytic reactions with reactive oxygen species (ROS) and water, respectively, that are naturally present within cells [26]. Cells may also accumulate somatic genome changes due to the errors during DNA replication in the form of base small insertions or deletions (indels), substitutions, and gross chromosomal rearrangements. DNA damaging events caused by endogenous agents generally occur much more frequently than damage caused by exogenous agents [27]. The source of exogenous DNA damage are ionizing radiation (IR), ultraviolet (UV), and various chemical agents [28]. IR is a type of high-energy radiation which is able to release electrons from atoms and molecules generating ions that can break covalent bonds. IR directly affects DNA structure by inducing DNA breaks, in particular DNA double-strand breaks (DSBs). The secondary effect is ROS generation that oxidize lipids and proteins and also induce several DNA damages such as generation of a basic sites and single strand breaks (SSBs). Taking together, these changes induce mitotic failure and cell death [29]. UV is a form of non-ionizing radiation that is emitted by the sun and different artificial sources like tanning beds, some halogen, fluorescent, and incandescent lights or mercury vapor lighting [30]. UV radiation causes DNA damage indirectly by producing ROS, and directly by covalent modification of neighboring pyrimidines. Two major UV-induced DNA lesions are cyclobutane pyrimidine dimers, and 6-4 photoproduct that is characterized by the formation of a covalent bond between two adjacent pyrimidine bases: C6 of the 5'-base and C4 of the 3'-base. DNA damage induced by UV radiation causes genetic alterations resulting in mutagenesis and cancer formation [31]. Another exogenous DNA damage is caused by alkylating agents. Major sources of external alkylating agents include industrial processing, tobacco smoke, chemotherapeutic agents and dietary components. The cytotoxic effect of alkylating agents is mainly due to the alkylation of DNA bases that can interfere essential DNA processes like DNA replication and/or transcription [32]. Alkylating agents react with the nitrogen's (N) ring and extracyclic oxygen (O) atoms of DNA bases to form a variety of covalent adducts ranging from simple methyl groups to complex alkyl additions. DNA damage generated by these agents depends on its specific chemical reactivity (S_N1-type or S_N2-type nucleophilic substitution), number of reactive sites in the alkylating agent (monofunctional or bifunctional), the type of alkyl group addition and the DNA substrate (single-stranded or double-stranded) [33]. Monofunctional agents contain one active chemical moiety to modify a single site in DNA, while bifunctional agents contain two reactive groups that can bond to separate DNA bases, forming interstrand crosslinks. S_N2-alkylating agents mainly target ring nitrogen atoms in DNA bases, whereas S_N1-alkylating agents can modify these nitrogen and the extracyclic oxygen groups. Depending on the nature of the nucleophile and of the alkylating agent, preferential sites of alkylation in DNA can be distinguished. Generally, base alkylation mainly occurs on position guanine N7 and O6, adenine N1 and N3, and cytosine N3. Most of the monofunctional methylating agents induce the formation of N7-methylguanine (7meG) as the dominant methylation adduct, which

accounts for 60–80% of all alkylation changes in DNA. 7meG does not have any cytotoxic and mutagenic properties but it is prone to spontaneous depurination forming apurinic (AP) site that is toxic and mutagenic. Monofunctional methylating agents can also generate N3-methyladenine (3meA) as the other N-methylation product, which accounts for 10–20% of all methyl adducts. The 3meA is highly cytotoxic, as it can block most DNA polymerases and thus inhibit synthesis of DNA [32,34]. Among the DNA oxygen atoms , the O6 position of guanine is primary site of methylation by S_N1-type agents for generating O6-methylguanine (O6meG). Induction of O6meG lesions is of crucial biological importance as O6meG can easy mispair with thymine during DNA replication to cause many of the cytotoxic and mutagenic effects [34]. Sulfur and nitrogen mustards are highly reactive bifunctional alkylating agents. These compounds react readily with N7-guanine and, to a lesser extent, with N3-adenine and N7-adenine forming N-monoadducts. Then, these monoadducts can react with another base to form guanine–guanine (G–G) and guanine–adenine (G–A) inter-strand crosslinks [35].

This study is continuation of our *in vitro* research focused on T-2 mechanism of action on human skin model. In our previous study [8] we demonstrated the necrosis potential of T-2 toxin with strong reduction of ATP production by cells. We also determined the impact of T-2 toxin on mitochondria physiology and disruption of mitochondrial DNA (mtDNA) [36]. This study focuses on the nDNA damage of the human normal fibroblast cell line – Hs68 as a results of exposure to T-2 toxin.

The comet assay (single cell gel electrophoresis) is a method for measuring DNA damage in eukaryotic cells. There are two types of comet assay. Neutral comet assay is used to detect DNA double strand breaks (DSBs). Alkaline version of comet assay is the most widely used and is appropriate for smaller amounts of DNA damage, including DNA single strand breaks (SSBs) and DSBs, SSBs associated with incomplete excision repair sites, alkali-labile sites and DNA-DNA or DNA-protein cross-linking. Both versions allow visualization of fragmented DNA, and provide a simple way to quantify DNA damage [37]. Comet assay is considered as a sensitive method for *in vitro* and *in vivo* genetic toxicological studies and is also suitable for various research areas, like molecular biology [38], environmental monitoring [39] and medicine [40]. In various studies genotoxic effect of T-2 toxin was measured by comet assay. In Szabo et al. [18] study, comet assay was used to investigate the DNA damaging effects of T-2 and HT-2 mycotoxins in the liver of broiler chickens. Results showed that comet assay was successfully adapted to chicken hepatocytes, and the DNA damage was determined by a decrease of the DNA % in the comet tail in the experimental groups. Each toxin-treated group differed significantly from the control group, indicating that this assay can be useful for the evaluation of primary DNA damage caused by T-2/HT-2 mycotoxins. In different study, the rate of DNA damage caused by T-2 toxin in healthy porcine mononuclear cells was assessed. As T-2 toxin concentration increased, the frequency of intact lymphocytes decreased from 50.2% (0.1 μM) to 36.3% (1.0 μM) within the first 24 h. It was concluded that a dose- and time-dependent DNA damaging effect of T-2 toxin could be demonstrated using peripheral blood mononuclear cells from porcine by alkaline comet assay [41]. However, this is the first study in which the normal human fibroblast cell line - Hs68 exposed to T-2 toxin was used in comet assay to detect the time and concentration dependent DNA damaging effects. Using this technique, we evaluated the rate of DNA damage caused by T-2 toxin in increasing concentrations after 24 h and 48 h incubation. Our results showed that T-2 toxin induces DNA alkali-labile sites and strand breaks in Hs68 cell line. The level of DNA damage in cells is correlated with the level and time of T-2 toxin exposure. These results confirm that T-2 toxin is toxic to fibroblast cells, and this toxicity includes DNA damage.

The HPRT1 (hypoxanthine-guanine phosphoribosyltransferase) gene is believed to be a housekeeping gene and is the most frequently analyzed in DNA damage studies. The protein encoded by this gene is an enzyme transferase which plays a crucial role in the generation of purine nucleotides through the purine salvage pathway. HPRT1 enzyme recycles nucleotides to supply for DNA and RNA synthesis in vital and actively dividing cells, explaining the great presence of HPRT1 in most tissues It

is considered that HPRT1 functions in multiple housekeeping roles, including cell cycle and proliferation mechanisms, DNA replication and repair or RNA metabolism [42]. TP53 gene encodes a TP53 protein containing transcriptional activation, DNA binding, and oligomerization domains. The TP53 protein provides substantial functions in the cellular response to various stresses and ensures the maintenance of genome integrity. It responds to diverse cellular stresses to regulate expression of target genes, hence inducing DNA repair, cell cycle arrest, apoptosis or metabolic adaptations [43]. Both of these genes play an essential role in cell function. In this study, we evaluated the effect of T-2 toxin on nDNA lesion frequency in HPRT1 and TP53 genes from Hs68 cells. According to the results, T-2 toxin increases DNA lesions in evaluated regions in a dose- and time-dependent manner. It confirms that T-2 toxin has toxic effect to fibroblast skin cells, and this effect includes nDNA lesions.

A number of cytokines, especially Interleukin 1 (IL1) and tumor necrosis factor (TNF), play a significant role in the initiating of inflammatory process. They are secreted by different cells including macrophages, monocytes and adipocytes. Together with various cytokines and growth factors such as Interleukin 8 (IL8) and the granulocyte-macrophage colony-stimulating factor (GM-CSF), induce gene expression and protein synthesis. Thus mediating the onset and development of inflammation process. IL1A and IL1B, which belong to the group of cytokines, which are elements of innate and adaptive immunity, acting as mediators of inflammation. Interleukins are classified as proteins and are mainly synthesized by leukocytes, although they can also be produced by non-immune cells such as endothelial cells in response to inflammation. Despite the significant similarities of both interleukins in structure, biological activity, and the same type of receptor, the key difference between both ILs is the place where they interact with other cells. IL1A associates with the cell membrane of the cells in which it is produced, from where it affects the cells in the immediate vicinity, while IL1B, synthesized in the form of pro-interleukin, which requires caspase 1 to activate, is secreted into the blood, acting systemically [44]. The level of gene expression of both ILs, and thus the activity of cytokines, is low in the case of good health, and increases under the influence of inflammation. The increase in gene expression of both ILs suggests that T-2 toxin induces inflammation in Hs68 cells. A particularly significant increase in expression is observed in the IL1B gene, which may indicate that the inflammation induction associated with cell DNA damage, resulting in the cell's necrotic pathway, may affect other, distant cells in the context of the entire organism.

The APEX gene is responsible for encoding the major human endonuclease AP sites resulting in DNA damage. In the case of DNA replication containing AP sites, random insertion of a nucleotide may occur during the synthesis of a new strand of DNA. To eliminate replication errors that could result in mutation, cells have developed a system to identify and repair AP sites. AP endonuclease leads to cleavage of the phosphodiester backbone from the 5' end towards the AP site, initiating base excision repair (BER) [26]. The APEX protein is ubiquitous in the organism, but variable levels have been found in various types of cancer, like hepatocellular carcinomas, breast carcinomas, rhabdomyosarcomas or gastric carcinomas. According to the Kim et al. [45] study results on the expression of APEX as a potential diagnostic biomarker of clear cell renal cell carcinoma and hepatobiliary carcinomas suggest active extracellular secretion of APEX from cancer cells, activated stromal and inflammatory cells. Thus, it can be seen that APEX gene expression increases with the level of DNA damage. LIG3 encodes a protein functioning in DNA replication and repair pathways, including nucleotide excision repair, base excision repair and single-strand break repair. LIG3 is also involved in the repair of DNA double-strand breaks when nonhomologous end joining (NHEJ) activity is impaired. The LIG3 gene is ubiquitously expressed at low levels in almost all human tissues and cells [46]. Treatment of Hs68 cells with T-2 toxin at appropriate concentrations resulted in an increase in APEX genes expression, which indicates an increase in cell's DNA damage caused also by the appearance of AP sites. Decrease in LIG3 gene expression can be a result of substantial cells damage and as a consequence impairment of DNA repair mechanisms.

The molecular dockings performed in our study were subjected to confirm or deny the potential interaction between T-2 toxin and small fragments of double-stranded DNA molecules: 1BDZ [19], 3AAF [20] and 6O3T [21]. Docking software computes the best conformation and placement of chemical compounds ligands in a 3D structure of biomolecule. For our study, we used the AutoDock Vina program, which combines some of the advantages of knowledge-based potentials and empirical scoring functions. It extracts empirical information from both the conformational preferences of the receptor-ligand complex and from experimental affinity measurements [15]. The results of in silico analysis clearly demonstrated interaction of T-2 toxin with DNA structure. To make the assessment of the affinity energy of mycotoxins for DNA even more illustrative, a comparison to sulfur mustard was performed. The second docking of the same fragments of the DNA structure to sulfur mustard, equally toxic to DNA, was executed. The affinity results of dockings are presented in Table 1 and 2 and confirmed that T-2 toxin has a very strong affinity for DNA structures. After analyzing the results of the affinity of the reference compound to DNA structures and comparing them with the binding energy of the tested toxin to DNA, it can be stated that the affinity of T-2 toxin to the DNA chain is at least twice as high as that of toxic sulfur mustard.

4. Conclusions

We demonstrated for the first time that in *in vitro* human skin fibroblast model, T-2 toxin shows genotoxic properties. Results presented in this study showed that T-2 toxin exposure causes DNA fragmentation, decrease the expression of repair process gene and increase the expression of inflammatory genes. Moreover, *in silico* analysis exhibited that T-2 toxin has a strong affinity to interact with the major groove of the DNA double helix. The molecular mechanism of this toxic effect is related to nDNA damage, leading to the impaired cellular function and cell loss.

5. Materials and methods

5.1. Reagents

Dimethyl sulfoxide (DMSO), T-2 Toxin from *Fusarium* sp. (cat. No T4887) DAPI (4',6-diamidino-2-phenylindole), low and normal melting point agarose were obtained from the Sigma-Aldrich Chemical Co. (St. Louis, MO, USA). Penicillin-Streptomycin mixture, Dulbecco's Modified Eagle Medium (DMEM) with 4.5 g/L Glucose and with L-Glutamine, fetal bovine serum (FBS) heat inactivated, PBS (1X) without calcium or magnesium were purchased in Lonza (Basel, Switzerland). High-Capacity cDNA Reverse Transcription Kit, TaqMan probes and Universal Master Mix were obtained from Life Technologies (Grand Island, NY, USA). All other chemicals were reagent grade or the highest-quality available.

5.2. Cell Culture and Treatment

The human foreskin fibroblast line Hs68 (ATCC® CRL-1635™) was obtained from the American Type Culture Collection (ATCC™, Manassas, VA, USA). Hs68 cells were cultured in DMEM supplemented with 100 units of potassium penicillin and 100 µg of streptomycin sulphate per 1 mL of culture media and 10% (v/v) FBS. Cultures were maintained at 37 °C in a humidified atmosphere with 5% CO_2. To perform analysis cells were seeded at 3×10^6 cells and left in incubator for 12h before treatment procedures. Next the cell samples were incubated with T-2 toxin with a concentration range of 0.1 to 10 µM for 24h and 48h. The working solutions of T-2 toxin were made by direct dilution of toxin in culture medium. The untreated cells were used as control.

5.3. DNA Damage – comet assay

DNA damage in Hs68 cell line was estimated by the alkaline version (pH > 13) of the comet assay [47]. A freshly prepared suspension of cells in 0.75% low melting point agarose dissolved in phosphate buffered saline was cast on a microscope slides precoated with 0.5% normal melting agarose and then covered with a cover glass, and placed on a cold plate for 10 min. Next, cover glass was removed, and cells were lysed for 1 h at 4 °C in a buffer consisting of 2.5 M NaCl, 100 mM EDTA, 1% Triton X-100, 10 mM Tris, pH 10. Then, DNA was allowed to unwind for 20 min in electrophoretic solution consisting of 300 mM NaOH, 1 mM EDTA. Electrophoresis was conducted for 20 min at electric field strength 0.73 V/cm (30 mA) in a buffer of pH > 13 (300 mM NaOH and 1 mM EDTA). After electrophoresis, slides were washed twice with deionized water and left to dry out. For analysis, samples were stained for at least 60 min with 2 μg/ml DAPI and covered with cover slips. Then the comet pictures were captured at 200× magnification in an Eclipse fluorescence microscope (Nikon, Tokyo, Japan) with COHU 4910 video camera (Cohu, Inc., San Diego, CA, USA) equipped with a UV filter block consist of an excitation filter (359 nm) and barrier filter (461 nm) and connected to image analysis system, Lucia-Comet v. 4.51 (Laboratory Imaging, Prague, Czech Republic). For each sample, 50 comets were randomly selected, and the comet's tail DNA was measured. Two parallel tests with aliquots of the same sample of cells were performed for a total of 100 cells. Each experiment was repeated twice. Percentage of DNA in the tail (% tail DNA) was analyzed. The mean value of the % tail DNA in sample was taken as an index of DNA damage.

5.4. Isolation of Total Genomic DNA from Cell Lines

Total genomic DNA (mitochondrial and nuclear) from the cell pellets was isolated by using the commercially available EXTRACT ME RNA & DNA KIT (BLIRT S.A., Gdansk, Poland), according to the producer's protocol. DNA concentrations were determined by spectrophotometric measurement of the absorbance at 260 nm. The purities were calculated by a A260/A280 ratio using the Bio-Tek Synergy HT Microplate Reader (Bio-Tek Instruments, Winooski, VT, USA). The purified DNA was stored at −30 °C until further analysis.

5.5. Determination of Nuclear DNA Damage—Semi-Long Run qRT-PCR (SLR-qRT-PCR)

The assessment of nuclear DNA (nDNA) damage was performed using the semi-long run quantitative RT-PCR (SLR-qRT-PCR). The levels of the DNA lesions in the tested region of the nuclear genome were measured using two fragments of different lengths, i.e., small and long fragments, located in the same nuclear genomic region. The sequence of all primers used in this study are listed in Table 1. All primers were designed using the Primer3 software (http://bioinfo.ut.ee/primer3-0.4.0/) and synthesized by Sigma-Aldrich (St. Louis, MO, USA). Complete nucleotide sequences for each gene were taken from the ENSEMBL database (https://ensembl.org/).

Table 1. SLR-qRT-PCR primers used for quantification of nuclear DNA damage.

Target gene symbol	Forward primer sequences (5′→3′)	Reverse primer sequence (5'→3')	Amplicon length (bp)
TP53 (tumor protein p53)	Long fragment: GGGTGTAGATGATGGGGATG	Long fragment: AACTGCGGAATGAAACAACC	1172
	Small fragment: AAGCTGCTAAGGTCCCACAA	Small fragment: GGAAAGATCGCTCCAGGAA	56

HPRT1 (hypoxanthine phosphoribosyltransferase 1)	Long fragment: AGGGCAAAGGATGTGTTACG	Long fragment: AGTGGTTTCTGGTGCGACTT	1018
	Small fragment: TGCTGACCTGCTGGATTACA	Small fragment: TCTACAGTCATAGGAATGGATCTATCA	69

SLR-qRT-PCR amplification was performed using a CFX96 Real-Time PCR Detection System (Bio-Rad Laboratories, Hercules, CA, USA). The SLR-qRT-PCR reaction mix in a total volume of 10 µL included 1 × Power SYBR Green PCR Master Mix (Thermo Fisher Scientific, Waltham, MA, USA), 250 nM of each primer and 5 ng of template DNA. The PCR reaction conditions were as follows: enzyme activation at 95 °C for 10 min followed by up to 40 cycles of 15 s denaturation at 95 °C, 30 s annealing at 65 °C, and 15 s extension at 72 °C (for short amplicons) or 45 s at 72 °C (for long amplicons). The Ct values were computed automatically and subsequently analyzed using the CFX Manager™ Software (version 3.1). DNA damage was calculated as lesion per 10 kb DNA of each region, by including the size of the particular long fragment. The following formula was used: lesion per 10 kb DNA = (1 − 2−(Δlong − Δshort)) × 10,000 (bp)/size of long fragment (bp), where Δlong and Δshort show differences in Ct value between treated samples and non-treated cells (control). DNA isolated from controls was used as the reference while the Ct of large and small nuclear fragments was used for DNA damage quantification.

5.6. Gene expression analysis using Real-Time PCR

Total RNA from the cell pellets was extracted by using EXTRACT ME RNA & DNA KIT (BLIRT S.A., Poland), according to the manufacturer's protocol. RNA purity and concentration were determined by comparing the absorbances at 260 and 280 nm using the Bio-Tek Synergy HT Microplate Reader (Bio-Tek Instruments, Winooski, VT, USA). RNA was stored at −30 °C until further analysis. cDNA was synthesized from total RNA using the High-Capacity cDNA Reverse Transcription Kit. A sample of 2 µg of total RNA was used as a template in a total volume of 10 µL. Gene expression were analyzed by TaqMan probe-based real-time PCR assay. Reactions were carried out in a thermal cycler CFX96™ Real-Time PCR Detection System (BIO-RAD Laboratories, Hercules, CA, USA). The thermal cycling conditions were as follows: 10 min of polymerase activation at 95 °C, followed by 40 cycles of 30 s denaturation at 95 °C and 60 s annealing/extension at 60 °C. Each sample was run in triplicate. The cycle threshold (Ct) values were calculated automatically by CFX96™ Real-Time PCR Detection System software (BIO-RAD). Relative expressions of the studied genes were calculated using the equation 2-ΔCt, where ΔCt = Ct target gene – Ct18S rRNA.

5.7. In silico molecular docking

The T-2 toxin ligand dockings to the DNA structure were calculated *in silico* with Autodock Vina 1.0, an algorithm released by Scripps Research Institute [15] (http://vina.scripps.edu/), in accordance with the previously used procedure [16-18]. The coordinates and PDB format structure of the DNA structures were taken from the website of the RSCB Protein Data Bank (http://www.rcsb.org). The three-dimensional chemical structures were downloaded from PubChem (http://pubchem.ncbi.nlm.nih.gov/) and converted to pdb files using Avogadro 1.1.0, an open-source molecular builder and visualization tool (http://avogadro.openmolecules.net/) [20]. DNA fragment preparation for the docking procedure was performed in a Swiss-PdbViewer (http://spdbv.vital-it.ch/). The non-bonded atoms presented in the crystal structure were removed. The DNA structure was adapted in Auto Dock Tools v 1.5.6rc1 (http://autodock.scripps.edu) [21] and the missing hydrogen atoms, Gasteiger charges [22] as well as Kollman [23] united atom charges were calculated and assigned.

The DNA structure file was prepared in .pdbqt format, which is pdb plus ''q'' charges and the ''t'' AutoDock type. The binding points were computed and the binding affinity of the ligand to the DNA structure counted in kcal/mol. Analysis and visualization of the three-dimensional structures of the DNA with the bound ligand was performed with the Python Molecular Viewer of Auto Dock Tools v 1.5.6rc1 (http://autodock.scripps.edu) [21], and Swiss-PdbViewer (http://spdbv.vital-it.ch/) [24].

5.8. Data analysis

All obtained experimental values were elaborated using Microsoft Excel software (Redmond, WA, USA) and stated as mean values ± standard deviations (SD). The statistical analysis procedures were made using StatsDirect statistical software V. 2.7.2. (Cheshire, UK). All data were analyzed using the Shapiro-Wilk test for normality normal distribution. The results were examined according to equality of variance *via* Levene's test. The significance of the differences among the values was analyzed using ANOVA: Tukey's range test (for data with normal distribution and significant equality of variance) or the Kruskal-Wallis test; $p<0.05$ was accepted as statistically significant [48,49].

Author Contributions

Conceptualization, M.B., MC, M.N., and E.S.; experiments, E.J., M.B., E.S. writing – original draft preparation, E.J. and M.B.; writing – review and editing, M.B., M.N. and T.S.; supervision, M.C. and M.B. All authors have read and agreed to the published version of the manuscript.

Funding

This study was funded by the National Science Centre of Poland grant (2020/37/N/NZ9/01678).

Institutional Review Board Statement

Not applicable.

Informed Consent Statement

Not applicable.

Data Availability Statement

Not applicable.

Acknowledgments

Not applicable.

Conflicts of Interest

The authors declare no conflict of interest.

References

1. Grovey, J.F. The trichothecenes and their biosynthesis. *Progress in the Chemistry of Organic Natural Products* **2007**, 63-130.
2. Chaudhary, M.; Bhaskar, A.S.B.; Rao, P.V.L. Differential effects of route of T-2 toxin exposure on hepatic oxidative damage in mice. *Environmental Toxicology* **2015**, *30*, 64-73, doi:https://doi.org/10.1002/tox.21895.
3. Nayakwadi, S.; Ramith, R.; Anil, K.S.; Vivek, K.G.; K., R.; Vijay, K.; S., S.P.; Rashmi, L.; M., B.K. Toxicopathological studies on the effects of T-2 mycotoxin and their interaction in juvenile goats. *PLoS One* **2020**, *15*, e0229463-e0229463.
4. Rahman, S.; Sharma, A.K.; Singh, N.; Prawez, S. T-2 toxin induced nephrotoxicity in Wistar rats. *Indian Journal of Veterinary Pathology* **2016**, *40*, 320, doi:10.5958/0973-970x.2016.00074.2.
5. Lin, R.; Sun, Y.; Ye, W.; Zheng, T.; Wen, J.; Deng, Y. T-2 toxin inhibits the production of mucin via activating the IRE1/XBP1 pathway. *Toxicology* **2019**, *424*, 152230, doi:https://doi.org/10.1016/j.tox.2019.06.001.

6. Weidner, M.; Lenczyk, M.; Schwerdt, G.; Gekle, M.; Humpf, H.-U. Neurotoxic Potential and Cellular Uptake of T-2 Toxin in Human Astrocytes in Primary Culture. *Chemical Research in Toxicology* **2013**, *26*, 347-355, doi:10.1021/tx3004664.
7. Bhavanishankar, T.N.; Ramesh, H.P.; Shantha, T. Dermal toxicity of Fusarium toxins in combinations. *Archives of Toxicology* **1988**, *61*, 241-244, doi:10.1007/BF00316641.
8. Janik-Karpinska, E.; Ceremuga, M.; Wieckowska, M.; Szyposzynska, M.; Niemcewicz, M.; Synowiec, E.; Sliwinski, T.; Bijak, M. Direct T-2 Toxicity on Human Skin-Fibroblast Hs68 Cell Line-In Vitro Study. *Int J Mol Sci* **2022**, *23*, doi:10.3390/ijms23094929.
9. Zhuang, Z.; Yang, D.; Huang, Y.; Wang, S. Study on the apoptosis mechanism induced by T-2 toxin. *PloS one* **2013**, *8*, e83105-e83105, doi:10.1371/journal.pone.0083105.
10. Rizzo, A.F.; Atroshi, F.; Ahotupa, M.; Sankari, S.; Elovaara, E. Protective Effect of Antioxidants against Free Radical-Mediated Lipid Peroxidation Induced by DON or T-2 Toxin. *Journal of Veterinary Medicine Series A* **1994**, *41*, 81-90, doi:https://doi.org/10.1111/j.1439-0442.1994.tb00070.x.
11. Liu, J.; Wang, L.; Guo, X.; Pang, Q.; Wu, S.; Wu, C.; Xu, P.; Bai, Y. The role of mitochondria in T-2 toxin-induced human chondrocytes apoptosis. *PLoS One* **2014**, *9*, e108394.
12. Zhang, Y.; Han, J.; Zhu, C.-C.; Tang, F.; Cui, X.-S.; Kim, N.-H.; Sun, S.-C. Exposure to HT-2 toxin causes oxidative stress induced apoptosis/autophagy in porcine oocytes. *Scientific Reports* **2016**, *6*, 33904, doi:10.1038/srep33904.
13. Chaudhari, M.; Jayaraj, R.; Bhaskar, A.S.B.; Lakshmana Rao, P.V. Oxidative stress induction by T-2 toxin causes DNA damage and triggers apoptosis via caspase pathway in human cervical cancer cells. *Toxicology* **2009**, *262*, 153-161, doi:https://doi.org/10.1016/j.tox.2009.06.002.
14. Yuan, Z.; Matias, F.B.; Yi, J.-e.; Wu, J. T-2 toxin-induced cytotoxicity and damage on TM3 Leydig cells. *Comparative Biochemistry and Physiology Part C: Toxicology & Pharmacology* **2016**, *181-182*, 47-54, doi:https://doi.org/10.1016/j.cbpc.2015.12.005.
15. Frankič, T.; Salobir, J.; Rezar, V. The effect of vitamin E supplementation on reduction of lymphocyte DNA damage induced by T-2 toxin and deoxynivalenol in weaned pigs. *Animal Feed Science and Technology* **2008**, *141*, 274-286, doi:https://doi.org/10.1016/j.anifeedsci.2007.06.012.
16. Frankič, T.; Pajk, T.; Rezar, V.; Levart, A.; Salobir, J. The role of dietary nucleotides in reduction of DNA damage induced by T-2 toxin and deoxynivalenol in chicken leukocytes. *Food and Chemical Toxicology* **2006**, *44*, 1838-1844, doi:https://doi.org/10.1016/j.fct.2006.06.002.
17. Rezar, V.; Frankič, T.; Narat, M.; Levart, A.; Salobir, J. Dose-Dependent Effects of T-2 Toxin on Performance, Lipid Peroxidation, and Genotoxicity in Broiler Chickens. *Poultry Science* **2007**, *86*, 1155-1160, doi:https://doi.org/10.1093/ps/86.6.1155.
18. Szabó, R.T.; Kovács-Weber, M.; Erdélyi, M.; Balogh, K.; Fazekas, N.; Horváth, Á.; Mézes, M.; Kovács, B. Comet assay study of the genotoxic effect of T-2 and HT-2 toxins in chicken hepatocytes. *Biologia Futura* **2019**, *70*, 330-335, doi:10.1556/019.70.2019.37.
19. Radha, P.K.; Patel, P.K.; Hosur, R.V. NMR structure of the extended Myb cognate sequence and modeling studies on specific DNA-Myb complexes. *Biochemistry* **1998**, *37*, 9952-9963, doi:10.1021/bi9806753.
20. Kitano, K.; Kim, S.Y.; Hakoshima, T. Structural basis for DNA strand separation by the unconventional winged-helix domain of RecQ helicase WRN. *Structure* **2010**, *18*, 177-187, doi:10.1016/j.str.2009.12.011.
21. Li, S.; Pradhan, L.; Ashur, S.; Joshi, A.; Nam, H.J. Crystal Structure of FOXC2 in Complex with DNA Target. *ACS Omega* **2019**, *4*, 10906-10914, doi:10.1021/acsomega.9b00756.
22. Gholampour Azizi, I.; Azarmi, M.; Danesh Pouya, N.; Rouhi, S. T-2 toxin Analysis in Poultry and Cattle Feedstuff. *Jundishapur J Nat Pharm Prod* **2014**, *9*, e13734-e13734, doi:10.17795/jjnpp-13734.
23. Yin, H.; Han, S.; Chen, Y.; Wang, Y.; Li, D.; Zhu, Q. T-2 Toxin Induces Oxidative Stress, Apoptosis and Cytoprotective Autophagy in Chicken Hepatocytes. *Toxins* **2020**, *12*, doi:10.3390/toxins12020090.
24. Lei, Y.; Guanghui, Z.; Xi, W.; Yingting, W.; Xialu, L.; Fangfang, Y.; Goldring, M.B.; Xiong, G.; Lammi, M.J. Cellular responses to T-2 toxin and/or deoxynivalenol that induce cartilage damage are not specific to chondrocytes. *Scientific Reports* **2017**, *7*, 2231, doi:10.1038/s41598-017-02568-5.
25. Branzei, D.; Foiani, M. The DNA damage response during DNA replication. *Current Opinion in Cell Biology* **2005**, *17*, 568-575, doi:https://doi.org/10.1016/j.ceb.2005.09.003.
26. Chatterjee, N.; C., W.G. Mechanisms of DNA damage, repair, and mutagenesis. *Environ Mol Mutagen* **2017**, *58*, 235-263.
27. Saini, N.; Giacobone, C.K.; Klimczak, L.J.; Papas, B.N.; Burkholder, A.B.; Li, J.-L.; Fargo, D.C.; Bai, R.; Gerrish, K.; Innes, C.L.; et al. UV-exposure, endogenous DNA damage, and DNA replication errors

shape the spectra of genome changes in human skin. *PLOS Genetics* **2021**, *17*, e1009302, doi:10.1371/journal.pgen.1009302.
28. Friedberg, E.C.; McDaniel, L.D.; Schultz, R.A. The role of endogenous and exogenous DNA damage and mutagenesis. *Current Opinion in Genetics & Development* **2004**, *14*, 5-10, doi:https://doi.org/10.1016/j.gde.2003.11.001.
29. Borrego-Soto, G.; Ortiz-López, R.; Rojas-Martínez, A. Ionizing radiation-induced DNA injury and damage detection in patients with breast cancer. *Genetics and molecular biology* **2015**, *38*, 420-432, doi:10.1590/S1415-475738420150019.
30. Greinert, R.; de Vries, E.; Erdmann, F.; Espina, C.; Auvinen, A.; Kesminiene, A.; Schüz, J. European Code against Cancer 4th Edition: Ultraviolet radiation and cancer. *Cancer Epidemiology* **2015**, *39*, S75-S83, doi:https://doi.org/10.1016/j.canep.2014.12.014.
31. Yu, S.-L.; Lee, S.-K. Ultraviolet radiation: DNA damage, repair, and human disorders. *Molecular & Cellular Toxicology* **2017**, *13*, 21-28, doi:10.1007/s13273-017-0002-0.
32. Chatterjee, N.; Walker, G.C. Mechanisms of DNA damage, repair, and mutagenesis. *Environmental and molecular mutagenesis* **2017**, *58*, 235-263, doi:10.1002/em.22087.
33. Puyo, S.; Montaudon, D.; Pourquier, P. From old alkylating agents to new minor groove binders. *Critical Reviews in Oncology/Hematology* **2014**, *89*, 43-61, doi:https://doi.org/10.1016/j.critrevonc.2013.07.006.
34. Fu, D.; Calvo, J.A.; Samson, L.D. Balancing repair and tolerance of DNA damage caused by alkylating agents. *Nature Reviews Cancer* **2012**, *12*, 104-120, doi:10.1038/nrc3185.
35. Kehe, K.; Schrettl, V.; Thiermann, H.; Steinritz, D. Modified immunoslotblot assay to detect hemi and sulfur mustard DNA adducts. *Chemico-Biological Interactions* **2013**, *206*, 523-528, doi:https://doi.org/10.1016/j.cbi.2013.08.001.
36. Janik-Karpinska, E.; Ceremuga, M.; Niemcewicz, M.; Synowiec, E.; Sliwiński, T.; Bijak, M. Mitochondrial Damage Induced by T-2 Mycotoxin on Human Skin—Fibroblast Hs68 Cell Line. *Molecules* **2023**, *28*, doi:10.3390/molecules28052408.
37. Cordelli, E.; Bignami, M.; Pacchierotti, F. Comet assay: a versatile but complex tool in genotoxicity testing. *Toxicology Research* **2021**, *10*, 68-78, doi:10.1093/toxres/tfaa093.
38. Copp, M.E.; Chubinskaya, S.; Bracey, D.N.; Shine, J.; Sessions, G.; Loeser, R.F.; Diekman, B.O. Comet assay for quantification of the increased DNA damage burden in primary human chondrocytes with aging and osteoarthritis. *Aging Cell* **2022**, *21*, e13698.
39. Costa, P.M.; Pinto, M.; Vicente, A.M.; Gonçalves, C.; Rodrigo, A.P.; Louro, H.; Costa, M.H.; Caeiro, S.; Silva, M.J. An integrative assessment to determine the genotoxic hazard of estuarine sediments: combining cell and whole-organism responses. *Frontiers in Genetics* **2014**, *5*, 437.
40. Islam, J.; Kabir, Y. Measurement of DNA damage in bladder cancer patients by alkaline comet assay. *Ann Urol Oncol* **2019**, *2*, 64-70.
41. Horvatovich, K.; Hafner, D.; Bodnár, Z.; Berta, G.; Hancz, C.; Dutton, M.; Kovács, M. Dose-related genotoxic effect of T-2 toxin measured by comet assay using peripheral blood mononuclear cells of healthy pigs. *Acta Veterinaria Hungarica* **2013**, *61*, 175-186.
42. Kang, T.H.; Park, Y.; Bader, J.S.; Friedmann, T. The housekeeping gene hypoxanthine guanine phosphoribosyltransferase (HPRT) regulates multiple developmental and metabolic pathways of murine embryonic stem cell neuronal differentiation. *PLoS One* **2013**, *8*, e74967.
43. Aubrey, B.J.; Strasser, A.; Kelly, G.L. Tumor-suppressor functions of the TP53 pathway. *Cold Spring Harbor perspectives in medicine* **2016**, *6*, a026062.
44. Miller, T.; Tokarz-Deptuła, B.; Deptuła, W. Cytokiny z rodziny interleukiny 1. *Postepy Mikrobiologii* **2011**, *50*, 217-221.
45. Kim, J.-M.; Yeo, M.-K.; Lim, J.S.; Song, I.-S.; Chun, K.; Kim, K.-H. APEX1 Expression as a Potential Diagnostic Biomarker of Clear Cell Renal Cell Carcinoma and Hepatobiliary Carcinomas. *Journal of Clinical Medicine* **2019**, *8*, doi:10.3390/jcm8081151.
46. Tomkinson, A.E.; Sallmyr, A. Structure and function of the DNA ligases encoded by the mammalian LIG3 gene. *Gene* **2013**, *531*, 150-157, doi:https://doi.org/10.1016/j.gene.2013.08.061.
47. Pu, X.; Wang, Z.; Klaunig, J.E. Alkaline Comet Assay for Assessing DNA Damage in Individual Cells. *Curr Protoc Toxicol* **2015**, *65*, 3.12.11-13.12.11, doi:10.1002/0471140856.tx0312s65.
48. Bijak, M.; Saluk, J.; Antosik, A.; Ponczek, M.B.; Żbikowska, H.M.; Borowiecka, M.; Nowak, P. Aronia melanocarpa as a protector against nitration of fibrinogen. *International Journal of Biological Macromolecules* **2013**, *55*, 264-268, doi:https://doi.org/10.1016/j.ijbiomac.2013.01.019.

49. Zbikowska, H.M.; Antosik, A.; Szejk, M.; Bijak, M.; Olejnik, A.K.; Saluk, J.; Nowak, P. Does quercetin protect human red blood cell membranes against γ-irradiation? *Redox Report* **2014**, *19*, 65-71, doi:10.1179/1351000213Y.0000000074.

mgr Edyta Janik-Karpińska
Centrum Zapobiegania Zagrożeniom Biologicznym
Wydział Biologii i Ochrony Środowiska
Uniwersytet Łódzki

Łódź, 21.05.2023 r.

Oświadczenie o udziale w publikacjach

Oświadczam, że w pracy **Janik-Karpinska E**, Ceremuga M, Niemcewicz M, Synowiec E, Sliwinski T, Bijak M. *DNA damage induced by T-2 Mycotoxin in Human Skin Fibroblast Cell Line – Hs68.* Toxins 2023 (w trakcie recenzji) mój udział wynosił 50% i obejmował opracowanie koncepcji pracy przeglądowej, przygotowanie manuskryptu oraz rycin i tabel.

Oświadczam, że w pracy **Janik-Karpinska E**, Ceremuga M, Niemcewicz M, Synowiec E, Sliwinski T, Bijak M. *Mitochondrial Damage Induced by T-2 Mycotoxin on Human Skin- Fibroblast Hs68 Cell Line*. Molecules 2023, 28(5), 2408; doi.org/10.3390/molecules28052408 mój udział wynosił 50% i obejmował realizację części doświadczalnej, opracowanie wyników i ich interpretację oraz przygotowanie manuskryptu.

Oświadczam, że w pracy **Janik-Karpinska E**, Ceremuga M, Wieckowska M, Szyposzynska M, Niemcewicz M, Synowiec E, Sliwinski T, Bijak M. *Direct T-2 Toxicity on Human Skin-Fibroblast Hs68 Cell Line-In Vitro Study*. International Journal of Molecular Sciences 2022, 23(9), 4929; doi:10.3390/ijms23094929 mój udział wynosił 50% i obejmował realizację części doświadczalnej, opracowanie wyników i ich interpretację oraz przygotowanie manuskryptu.

Oświadczam, że w pracy **Janik E**, Niemcewicz M, Podogrocki M, Ceremuga M, Stela M, Bijak M. *T-2 Toxin-The Most Toxic Trichothecene Mycotoxin: Metabolism, Toxicity, and Decontamination Strategies.* Molecules 2021, 26(22), 6868; doi:10.3390/molecules26226868 mój udział wynosił 50% i obejmował opracowanie koncepcji pracy przeglądowej, przygotowanie manuskryptu oraz rycin i tabel.

Edyta Janik-Karpińska

dr hab. Michał Bijak prof. UŁ
Centrum Zapobiegania Zagrożeniom Biologicznym
Wydział Biologii i Ochrony Środowiska
Uniwersytet Łódzki

Łódź, 23.05.2023 r.

Oświadczenie o udziale w publikacjach

Oświadczam, że w pracy:
Janik-Karpinska E, Ceremuga M, Niemcewicz M, Synowiec E, Sliwinski T, **Bijak M**. *DNA damage induced by T-2 Mycotoxin in Human Skin Fibroblast Cell Line – Hs68.* Toxins 2023 (w trakcie recenzji) mój udział wynosił 20% i obejmował współudział w opracowaniu koncepcji pracy oraz w wykonywaniu eksperymentów, merytoryczne konsultacje oraz pomoc w redakcji i korekcie tekstu.

Oświadczam, że w pracy:
Janik-Karpinska E, Ceremuga M, Niemcewicz M, Synowiec E, Sliwinski T, **Bijak M**. *Mitochondrial Damage Induced by T-2 Mycotoxin on Human Skin- Fibroblast Hs68 Cell Line*. Molecules 2023, 28(5), 2408; doi.org/10.3390/molecules28052408 mój udział wynosił 20% i obejmował współudział w opracowaniu koncepcji pracy oraz w wykonywaniu eksperymentów, merytoryczne konsultacje oraz pomoc w redakcji i korekcie tekstu.

Oświadczam, że w pracy:
Janik-Karpinska E, Ceremuga M, Wieckowska M, Szyposzynska M, Niemcewicz M, Synowiec E, Sliwinski T, **Bijak M**. *Direct T-2 Toxicity on Human Skin-Fibroblast Hs68 Cell Line-In Vitro Study*. International Journal of Molecular Sciences 2022, 23(9), 4929; doi:10.3390/ijms23094929 mój udział wynosił 15% i obejmował współudział w opracowaniu koncepcji pracy, merytoryczne konsultacje oraz pomoc w redakcji i korekcie tekstu.

Oświadczam, że w pracy:
Janik E, Niemcewicz M, Podogrocki M, Ceremuga M, Stela M, **Bijak M**. *T-2 Toxin-The Most Toxic Trichothecene Mycotoxin: Metabolism, Toxicity, and Decontamination Strategies.* Molecules 2021, 26(22), 6868; doi:10.3390/molecules26226868 mój udział wynosił 20% i obejmował pomoc merytoryczną w opracowaniu koncepcji pracy przeglądowej oraz pomoc w redakcji i korekcie tekstu.

płk dr inż. Michał Ceremuga
Wojskowy Instytut Techniki
Pancernej i Samochodowej

Sulejówek, 23.05.2023 r.

Oświadczenie o udziale w publikacjach

Oświadczam, że w pracy Janik-Karpinska E, **Ceremuga M**, Niemcewicz M, Synowiec E, Sliwinski T, Bijak M. *DNA damage induced by T-2 Mycotoxin in Human Skin Fibroblast Cell Line – Hs68.* Toxins 2023 (w trakcie recenzji) mój udział wynosił 7,5% i obejmował współudział w opracowaniu koncepcji pracy oraz merytoryczne konsultacje.

Oświadczam, że w pracy Janik-Karpinska E, **Ceremuga M**, Niemcewicz M, Synowiec E, Sliwinski T, Bijak M. *Mitochondrial Damage Induced by T-2 Mycotoxin on Human Skin-Fibroblast Hs68 Cell Line*. Molecules 2023, 28(5), 2408; doi.org/10.3390/molecules28052408 mój udział wynosił 7,5% i obejmował współudział w opracowaniu koncepcji pracy oraz merytoryczne konsultacje.

Oświadczam, że w pracy Janik-Karpinska E, **Ceremuga M**, Wieckowska M, Szyposzynska M, Niemcewicz M, Synowiec E, Sliwinski T, Bijak M. *Direct T-2 Toxicity on Human Skin-Fibroblast Hs68 Cell Line-In Vitro Study*. International Journal of Molecular Sciences 2022, 23(9), 4929; doi:10.3390/ijms23094929 mój udział wynosił 5% i obejmował współudział w opracowaniu koncepcji pracy oraz merytoryczne konsultacje.

Oświadczam, że w pracy Janik E, Niemcewicz M, Podogrocki M, **Ceremuga M**, Stela M, Bijak M. T-2 *Toxin-The Most Toxic Trichothecene Mycotoxin: Metabolism, Toxicity, and Decontamination Strategies.* Molecules 2021, 26(22), 6868; doi:10.3390/molecules26226868 mój udział wynosił 5% i obejmował pomoc merytoryczną w opracowaniu koncepcji pracy przeglądowej.

dr Marcin Niemcewicz
Centrum Zapobiegania Zagrożeniom Biologicznym
Wydział Biologii i Ochrony Środowiska
Uniwersytet Łódzki

Łódź, 23.05.2023 r.

Oświadczenie o udziale w publikacjach

Oświadczam, że w pracy Janik-Karpinska E, Ceremuga M, **Niemcewicz M**, Synowiec E, Sliwinski T, Bijak M. *DNA damage induced by T-2 Mycotoxin in Human Skin Fibroblast Cell Line – Hs68.* Toxins 2023 (w trakcie recenzji) mój udział wynosił 7,5% i obejmował współudział w opracowaniu koncepcji pracy oraz pomoc w redakcji i korekcie tekstu.

Oświadczam, że w pracy Janik-Karpinska E, Ceremuga M, **Niemcewicz M**, Synowiec E, Sliwinski T, Bijak M. *Mitochondrial Damage Induced by T-2 Mycotoxin on Human Skin-Fibroblast Hs68 Cell Line*. Molecules 2023, 28(5), 2408; doi.org/10.3390/molecules28052408 mój udział wynosił 7,5% i obejmował współudział w opracowaniu koncepcji pracy oraz pomoc w redakcji i korekcie tekstu.

Oświadczam, że w pracy Janik-Karpinska E, Ceremuga M, Wieckowska M, Szyposzynska M, **Niemcewicz M**, Synowiec E, Sliwinski T, Bijak M. *Direct T-2 Toxicity on Human Skin-Fibroblast Hs68 Cell Line-In Vitro Study*. International Journal of Molecular Sciences 2022, 23(9), 4929; doi:10.3390/ijms23094929 mój udział wynosił 5% i obejmował współudział w opracowaniu koncepcji pracy oraz pomoc w redakcji i korekcie tekstu.

Oświadczam, że w pracy Janik E, **Niemcewicz M**, Podogrocki M, Ceremuga M, Stela M, Bijak M. *T-2 Toxin-The Most Toxic Trichothecene Mycotoxin: Metabolism, Toxicity, and Decontamination Strategies.* Molecules 2021, 26(22), 6868; doi:10.3390/molecules26226868 mój udział wynosił 10% i obejmował pomoc merytoryczną w opracowaniu koncepcji pracy przeglądowej, pomoc w przygotowaniu manuskryptu oraz redakcji i korekcie tekstu.

dr Ewelina Synowiec
Pracownia Genetyki Medycznej
Wydział Biologii i Ochrony Środowiska
Uniwersytet Łódzki

Łódź, 22.05.2023 r.

Oświadczenie o udziale w publikacjach

Oświadczam, że w pracy Janik-Karpinska E, Ceremuga M, Niemcewicz M, **Synowiec E**, Sliwinski T, Bijak M. *DNA damage induced by T-2 Mycotoxin in Human Skin Fibroblast Cell Line – Hs68.* Toxins 2023 (w trakcie recenzji) mój udział wynosił 10% i obejmował współudział w tworzeniu koncepcji pracy oraz w wykonywaniu eksperymentów.

Oświadczam, że w pracy Janik-Karpinska E, Ceremuga M, Niemcewicz M, **Synowiec E**, Sliwinski T, Bijak M. *Mitochondrial Damage Induced by T-2 Mycotoxin on Human Skin- Fibroblast Hs68 Cell Line*. Molecules 2023, 28(5), 2408; doi.org/10.3390/molecules28052408 mój udział wynosił 10% i obejmował współudział w tworzeniu koncepcji pracy oraz w wykonywaniu eksperymentów.

Oświadczam, że w pracy Janik-Karpinska E, Ceremuga M, Wieckowska M, Szyposzynska M, Niemcewicz M, **Synowiec E**, Sliwinski T, Bijak M. *Direct T-2 Toxicity on Human Skin-Fibroblast Hs68 Cell Line-In Vitro Study*. International Journal of Molecular Sciences 2022, 23(9), 4929; doi:10.3390/ijms23094929 mój udział wynosił 10% i obejmował współudział w tworzeniu koncepcji pracy oraz w wykonywaniu eksperymentów.

Ewelina Synowiec

prof. dr hab. Tomasz Śliwiński
Pracownia Genetyki Medycznej
Wydział Biologii i Ochrony Środowiska
Uniwersytet Łódzki

Łódź, 24.05.2023 r.

Oświadczenie o udziale w publikacjach

Oświadczam, że w pracy Janik-Karpinska E, Ceremuga M, Niemcewicz M, Synowiec E, **Sliwinski T**, Bijak M. *DNA damage induced by T-2 Mycotoxin in Human Skin Fibroblast Cell Line – Hs68.* Toxins 2023 (w trakcie recenzji) mój udział wynosił 5% i obejmował pomoc w redakcji i korekcie tekstu.

Oświadczam, że w pracy Janik-Karpinska E, Ceremuga M, Niemcewicz M, Synowiec E, **Sliwinski T**, Bijak M. *Mitochondrial Damage Induced by T-2 Mycotoxin on Human Skin- Fibroblast Hs68 Cell Line.* Molecules 2023, 28(5), 2408; doi.org/10.3390/molecules28052408 mój udział wynosił 5% i obejmował pomoc w redakcji i korekcie tekstu.

Oświadczam, że w pracy Janik-Karpinska E, Ceremuga M, Wieckowska M, Szyposzynska M, Niemcewicz M, Synowiec E, **Sliwinski T**, Bijak M. *Direct T-2 Toxicity on Human Skin-Fibroblast Hs68 Cell Line-In Vitro Study.* International Journal of Molecular Sciences 2022, 23(9), 4929; doi:10.3390/ijms23094929 mój udział wynosił 5% i obejmował pomoc w redakcji i korekcie tekstu.

mgr inż. Maksymilian Stela
Centrum Zapobiegania Zagrożeniom Biologicznym
Wydział Biologii i Ochrony Środowiska
Uniwersytet Łódzki

Łódź, 23.05.2023 r.

Oświadczenie o udziale w publikacjach

Oświadczam, że w pracy Janik E, Niemcewicz M, Podogrocki M, Ceremuga M, **Stela M**, Bijak M. *T-2 Toxin-The Most Toxic Trichothecene Mycotoxin: Metabolism, Toxicity, and Decontamination Strategies.* Molecules 2021, 26(22), 6868; doi:10.3390/molecules26226868 mój udział wynosił 10% i obejmował pomoc merytoryczną w opracowaniu koncepcji pracy przeglądowej oraz pomoc w redakcji i korekcie tekstu.

Stela

dr Monika Szyposzyńska
Zakład Rozpoznania i Likwidacji Skażeń
Wojskowy Instytut Chemii i Radiometrii

Warszawa, 23.05.2023 r.

Oświadczenie o udziale w publikacjach

Oświadczam, że w pracy Janik-Karpinska E, Ceremuga M, Wieckowska M, **Szyposzynska M**, Niemcewicz M, Synowiec E, Sliwinski T, Bijak M. *Direct T-2 Toxicity on Human Skin-Fibroblast Hs68 Cell Line-In Vitro Study*. International Journal of Molecular Sciences 2022, 23(9), 4929; doi:10.3390/ijms23094929 mój udział wynosił 5% i obejmował pomoc w wykonywaniu eksperymentów.

Szyposzyńska

mgr Magdalena Więckowska
Centrum Zapobiegania Zagrożeniom Biologicznym
Wydział Biologii i Ochrony Środowiska
Uniwersytet Łódzki

Łódź, 15.05.2023 r.

Oświadczenie o udziale w publikacjach

Oświadczam, że w pracy Janik-Karpinska E, Ceremuga M, **Wieckowska M**, Szyposzynska M, Niemcewicz M, Synowiec E, Sliwinski T, Bijak M. *Direct T-2 Toxicity on Human Skin-Fibroblast Hs68 Cell Line-In Vitro Study*. International Journal of Molecular Sciences 2022, 23(9), 4929; doi:10.3390/ijms23094929 mój udział wynosił 5% i obejmował pomoc w wykonywaniu eksperymentów.

Magdalena Więckowska

mgr Marcin Podogrocki
Centrum Zapobiegania Zagrożeniom Biologicznym
Wydział Biologii i Ochrony Środowiska
Uniwersytet Łódzki

Łódź, 05.05.2023 r.

Oświadczenie o udziale w publikacjach

Oświadczam, że w pracy Janik E, Niemcewicz M, **Podogrocki M**, Ceremuga M, Stela M, Bijak M. T-2 *Toxin-The Most Toxic Trichothecene Mycotoxin: Metabolism, Toxicity, and Decontamination Strategies.* Molecules 2021, 26(22), 6868; doi:10.3390/molecules26226868 mój udział wynosił 5% i obejmował pomoc w przygotowaniu manuskryptu.